POLITECNICO DI MILANO
DEPARTMENT OF CHEMISTRY, MATERIALS AND CHEMICAL ENGINEERING
Doctoral program in Chemical Engineering and Industrial Chemistry
XXXI cycle


Final dissertation
Chiara Pennetta


Synthesis, characterization and biological evaluation of aminoglycoside-conjugates for cell transfection.



Advisor
Prof. Alessandro Volonterio

Coordinator of the Doctoral Course
Prof. Alessio Frassoldati

Tutor
Prof. Giulia Luisa Bozzano

# Abstract

Gene delivery aims to introduce genetic materials into cells by using vectors for therapeutic purposes. The development of efficient and safe methods for delivery of exogenous nucleic acids into cells, is still a challenging task. Gene transfer by means of non-viral vectors has attracted great interest because non-viral vectors are easy to synthesize, stable, and relatively safe. In this context, cationic lipids and polymers are promising candidates for designing alternative vectors. Cationic lipids and polymers are able to spontaneously complex the genetic material and promote its uptake into cells. However, their clinical application is still hampered by their low transfection efficiency.

Aminoglycosides, which are a class of polyaminosugars with inherent antimicrobial properties, are known to bind to nucleic acids, thus providing a favorable scaffold for the synthesis of non-viral vectors.

During my PhD project I have explored the synthesis and the transfection potential of novel classes of non-viral gene delivery vectors based on the use of aminoglycosides as polar head. Aminoglycosides were tethered to different structures to obtain non-viral vectors:

– A library of cationic lipids was obtained by exploring a triazine core with different lipophilic moieties in combination with neomycin and paromomycin (chapter II),

– Calix[4]arene, a macrocyclic scaffold already employed in the synthesis of vectors with high transfection efficiency, was also explored in combination with neamine, neomycin and paromomycin (chapter III),

– PAMAM, dendrimeric, well-defined structure that allows for an easy functionalization, was conjugated with neomycin (chapter IV).

All the conjugates were synthesized and characterized through different techniques. Their biological properties as transfectants were also investigated.

The growth of antimicrobial resistance represents a worldwide emergency that need to be urgently addressed. A promising strategy to overcome this threat to human health consists in the improvement of the effect of already existing antibiotics. During my research project, I have also tried to enhance aminoglycoside antibacterial activity by synthesizing a library of aminoglycoside-antimicrobial peptide conjugates.

# List of publications

## Papers published in international peer-reviewed journals

Bono, N.; Pennetta, C.; Sganappa, A.; Giupponi E.; Sansone, F.; Volonterio, A.; Candiani G.; *Design and synthesis of biologically active cationic amphiphiles built on the calix[4]arene scaffold*; Int. J. Pharm. 549, 436–445 (2018)

Bono, N.; Pennetta, C.; Bellucci, M.C.; Sganappa, A.; Malloggi, C.; Tedeschi, G.; Candiani, G.; Volonterio, A.; *Role of Generation on Successful DNA Delivery of PAMAM-(Guanidino)Neomycin Conjugates,* submitted to ACS Omega.

## Abstract in conferences

**Pennetta, C**; Bono., N.; Viani F.; Candiani G.; Volonterio A.
*XXXVIII Convegno Nazionale della Divisione di Chimica Organica della Società Chimica Italiana* (9-13 september 2018, Milan) Poster: Amphiphilic Aminoglycosides-based vectors for cell transfection: synthesis and biological validation.

**Pennetta, C.**; Bono, N.; Viani F.; Candiani G.; Volonterio A.
*7th EuCheMS Chemistry congress,* (26-30 August 2018, Liverpool, UK) Poster: Synthesis and biological evaluation of aminoglycosides-based vectors.

**Pennetta, C.;** Volonterio,A.
*XXVI International congress of the Italian Chemical Society* (10-14 September, Paestum (SA)), Oral presentation: Amino and guanidinoglycosides-based vectors for cell transfection.

**Pennetta, C.**; Volonterio, A,
*7th International Symposium on Advance in Synthetic and Medicinal Chemistry,* (27-31 August 2017, Vienna, Austria), Poster: Amino and guanidinoglycosides-based vectors for cell transfection.

**Pennetta C.**; Volonterio A.
*'XXXI International School of Organic Synthesis Attilio Corbella',* (*06*-2016, Gargnano (BS)), Poster: Amino- and Guanidinoglycosides as non-viral vectors for cell transfection'.

# List of abbreviations

| | |
|---|---|
| AAC | Acetyltransferases |
| AG | Aminoglycoside |
| AMP | Adenosine Monophosphate |
| ANT | Nucleotidyltransferases |
| APH | Phosphotransferases |
| Boc | Tert-butoxycarbonyl |
| CDI | Carbonyldiimidazole |
| CL | Cationic Lipid |
| $D_H$ | Hydrodynamic diameters |
| DCM | Dichloromethane |
| $dH_2O$ | Deionized Water |
| DLS | Dynamic Light Scattering |
| DMEM | Dulbecco's Modified Eagle's medium |
| DMSO | Dimethyl sulfoxide |
| DNA | DeoxyriboNucleic Acid |
| DOPE | 1,2-Dioleoyl-*sn*-glycero-3-phosphoethanolamine |
| DOS | Deoxystreptamine |
| DOTAP | N-[1-(2,3-Dioleoyloxy)propyl]-N,N,N-trimethylammoniummethyl-sulfate |
| DOTMA | 1,2-di-O-octadecenyl-3-trimethylammonium propane |
| FBS | Fetal Bovine Serum |
| FCC | Flash Column Chromatography |
| GNeo | Guanidino Neomycin |
| HMW | High Molecular Weight |
| HPLC | High Performance Liquid Chromatography |
| MALDI | Matrix-Assisted Laser Desorption/Ionization |
| MBA | N,N′-Methylenebis(acrylamide) |
| MDR | MultiDrug-Resistant |
| MIC | Minimum Inhibitory Concentration |
| NA | Nucleic Acid |
| Neo | Neomycin |
| NMR | Nuclear Magnetic Resonence |
| PAMAM | Polyamidoamine |
| PBS | Phosphate Buffered Saline |
| PEI | Polyethylenimine |
| RLU | Relative Light Unit |

| | |
|---|---|
| RNA | RiboNucleic Acid |
| r.t | Room Temperature |
| RNA | RiboNucleic Acid |
| TBSOTf | Tert-butyldimethylsilyl trifluoromethanesulfonate |
| TBTA | Tris(benzyltriazolylmethyl)amine |
| TFA | Trifluoroacetic Acid |
| TPS | 2,4,6-Triisopropylbenzenesulphonyl |
| VCC | Vacuum Liquid Chromatography |

# Table of Contents

# Thesis outline

This PhD thesis is divided into three major sections referred to as *Parts.*

In Part I *aminoglycosides'* chemical structure, reactivity and mode of action as antibiotics are discussed.

The results of the experimental work carried out during my PhD project are reported in *Part II* and *Part III.* Each part is introduced by a more specific contextualization of the experimental work.

More in detail, in *Part II* the use of aminoglycosides for the synthesis of non-viral vectors is discussed. This section is divided into four chapters. In Chapter I an introduction on gene delivery and the state of the art in the use of aminoglycosides in cell transfection are presented. In Chapters II-IV the synthesis and biological validation of gene delivery vectors carried out during my PhD project is illustrated. In particular, Chapter II discusses the synthesis of aminoglycosides-based cationic lipids, Chapter III focused on the synthesis of aminoglycosides-calix[4]arene conjugates and chapter IV describes aminoglycoside-PAMAM conjugates.

*Part III* describes the work carried out during my 6 months period abroad in the lab of Natural Products and Peptides in the Department of Drug Design and Pharmacology, University of Copenhagen, under the supervision of Prof. Henrik Franzyk. This part is focused on the synthesis and the study of the antibacterial properties of aminoglycoside-antimicrobial peptide conjugates (Chapter VI).

In the last chapter general conclusions are drawn.

Part I:

General Introduction on

Aminoglycosides

# Aminoglycosides

Aminoglycosides (AGs) are highly potent, broad-spectrum antibiotics used in the treatment of serious infections.[1,2] This class of molecules can be natural or semi-synthetic and it is produced by Actinomycetes.[3]

The first AG, streptomycin (Fig. 1a), was isolated in 1943 by Waksman[4] and coworkers from *Streptomyces griseus* by screening heavily manured soils. This was the first effective drug against tuberculosis and its discovery paved the way for findings new antibiotics from natural sources in the next two decades. In the following years other AGs were isolated: neomycin[5] (Neo) (Fig. 1b) has been identified in 1949 by Waksman, whilst gentamicin[6] (Fig. 1c) has been isolated in 1963 by Weinstein's group from *Micromonospora*.

The development of antibacterial resistance due to prolonged administration of the drugs drove the search for new compounds with improved activity. In this sense, the structures of the natural molecules were exploited to develop semi-synthetic variants of the antibiotics to enhance their antibacterial potency and reduce their toxicity. Amikacin[7] (Fig. 1d), for example, was introduced in 1971 as an antibiotic active against AGs-resistant strains. This is a derivative of kanamycin A, obtained through acetylation with the L(-)-γ-amino-α-hydroxybutyryl side chain at the C-1 amino group of the deoxystreptamine (DOS) moiety.
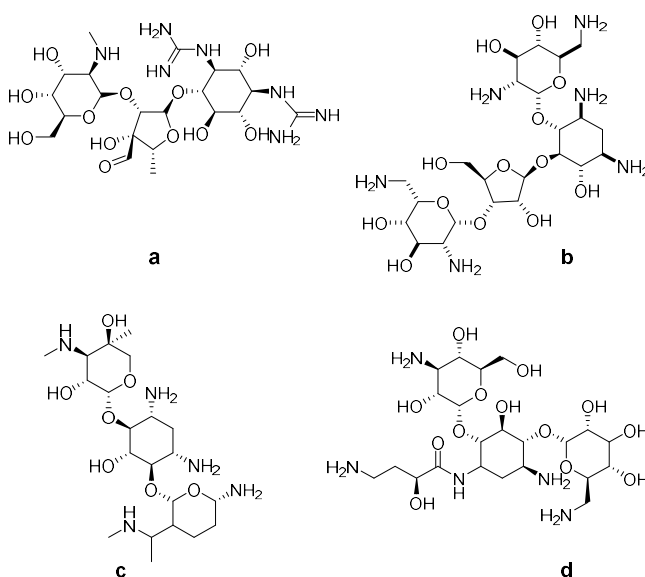


***Fig. 1 Examples of AG structures:*** *Natural AGs: a) streptomycin b) neomycin c) gentamicin and semi-synthetic AGs: d) amikacin.*

AGs are known to be ototoxic and nephrotoxic. It seems that the generation of free radicals within the ear damage neurons ad sensory cell leading to a permanent hearing loss.[8] The second main adverse effect of AGs is nephrotoxicity that is usually reversible and it is due to morphological and functional alterations.[9] Despite these side effects AGs are still a valuable tool employed against severe infections, such as, intra-abdominal infections or urinary tract infections, and are used in septicemia.

Different AGs may have different spectrum of activity however, their bactericidal effect is in general due to the interaction with the ribosomal RNA. AGs can also bind to eukaryotic ribosomes to a lesser extent. This property has been further investigated, and the use of AGs could be extended to antifungal[10], antiprotozoal[11] and genetic regulating[12] agents. Their universal affinity for nucleic acid[13,14] has been exploited in gene delivery.[15,16]

## Structure and reactivity of AGs

AGs are basic, highly hydrophilic molecules, and can be considered polycationic species since they are positively charged at physiological pH. AGs have a common structural core consisting of an aminocyclitol ring saturated with amine and hydroxyl groups and connected to various amino sugars through glycosidic bonds. In most cases, the core unit consists of a 2-deoxystreptamine (DOS) (Fig. 2a) that can be substituted with other amino sugars in position 4,6, such as in tobramycin (Fig. 2b) or 4,5 as in neomycin (Fig. 2c). The central aminocyclitol is referred to as ring II (Fig. 2 in blue) and it is unnumbered, the ring in position 4 is primed and would be ring I (Fig. 2 in red), that one in position 5 or 6 is considered ring III (Fig. 2 green) and it is doubly primed. Ring III can have additional rings, for example in neomycin, that can be referred to as ring IV (Fig. 2 light blue) and it is triply primed.
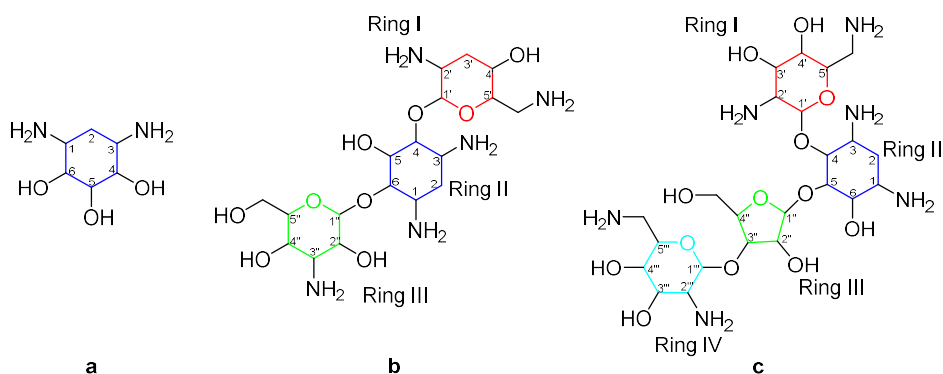


**Fig. 2 Examples of AG structures:** *a) 2-deoxystreptamine, the most diffuse core of AGs b) 4,6 DOS disubstituted AG: tobramycin c) 4,5 DOS disubstituted AG: neomycin.*

The structural complexity of AGs has hampered their total synthesis; nevertheless, natural AG structures can be modified in several ways by exploiting the presence of the hydroxyl and amine groups to obtain the next generation of AGs. Improved biological and therapeutic properties with respect to their parent structure can be obtained, including higher antimicrobial activity, better selectivity and lowered toxicity. Various synthetic approaches have been used.[17] Hereby some examples of the reactivity of neomycin and paromomycin are discussed.

Neomycin has a unique primary and less sterically hindered hydroxyl group in position 5'' (Fig. 3 in blue) that can be exploited as site for chemical modifications. In general, in the first step all the amines are protected by using a proper protecting group (Boc, Cbz). Then the primary hydroxyl group can selectively react with highly bulky reagents, such as tosyl chloride or, to further reduce the probability of obtaining a di-substituted-AG, with 2,4,6 triisopropylbenzenelsulphonyl chloride (TPSCl). The obtained intermediate (Fig. 3a) can be used to introduce within the molecule different functional groups.
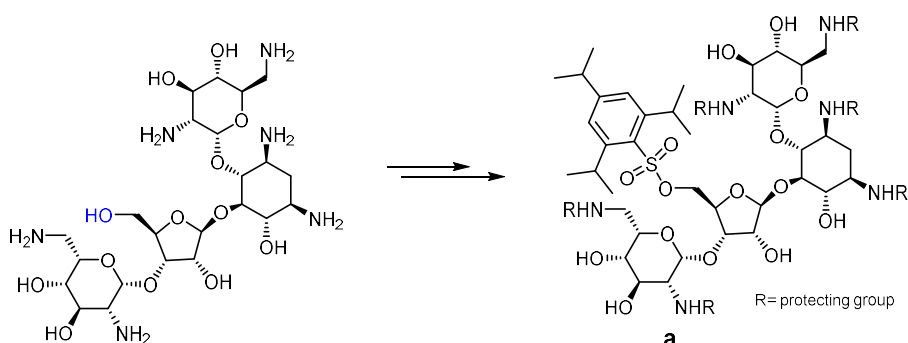


**Fig. 3 Neomycin reactivity:** *After protection of all the amines with a proper protecting group, the unique primary hydroxyl group (blue) on the furanose ring can selectively react with TPSCl leading to the mono-substituted derivative **a**.*

The synthesis of dimeric neomycin, active as ribozyme inhibitor, was reported by Tor and co-workers.[18] They displaced the tosyl-group with 2-mercaptoethyl ether which thiol group was then exploited to obtain the final dimer (Fig. 4).
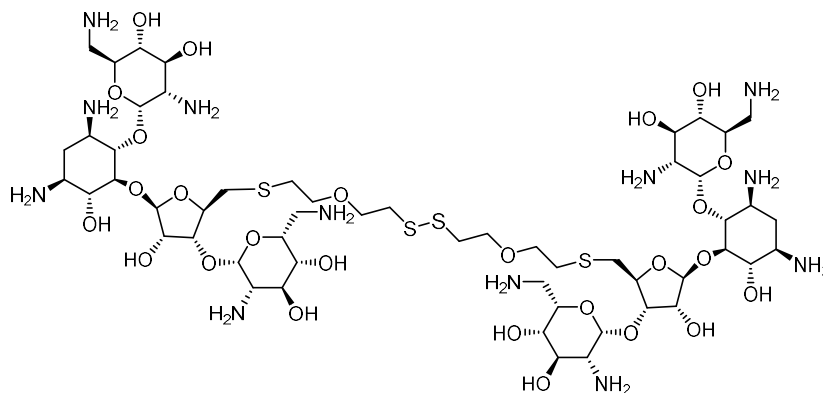
**Fig. 4 Neomycin reactivity II:** *Dimeric neomycin produced by Tor and coworkers. (Michael, K. et al.; Bioorg. Med. Chem.; 1999).*

In others works the bulky group has been displaced by using $NaN_3$, thus introducing an azido group (Fig. 5a) which fate depends on the subsequent reactions. This group can be reduced to an amine through a Staudinger reaction resulting in a product (Fig. 5b) with strong RNA-binding properties.[19] The azido group has been also used for copper catalyzed click chemistry with an alkyne function to obtain AGs coupled to different groups (Fig. 5c) such as dipeptides[20] or different alkyl chains.[21] These compounds exhibited enhanced antibacterial activity against resistant strains.

Cellular uptake of a fully guanidinylated version of neomycin (GNeo) (Fig. 6) has been intensely investigated by the group of Prof. Tor.[22–24] This derivative successfully translocate into cells facilitating the entering of high molecular weight biomacromolecules.[25] GNeo was obtained by exploiting Boc-protected triflylguanidine as guanidylating agent.[26]
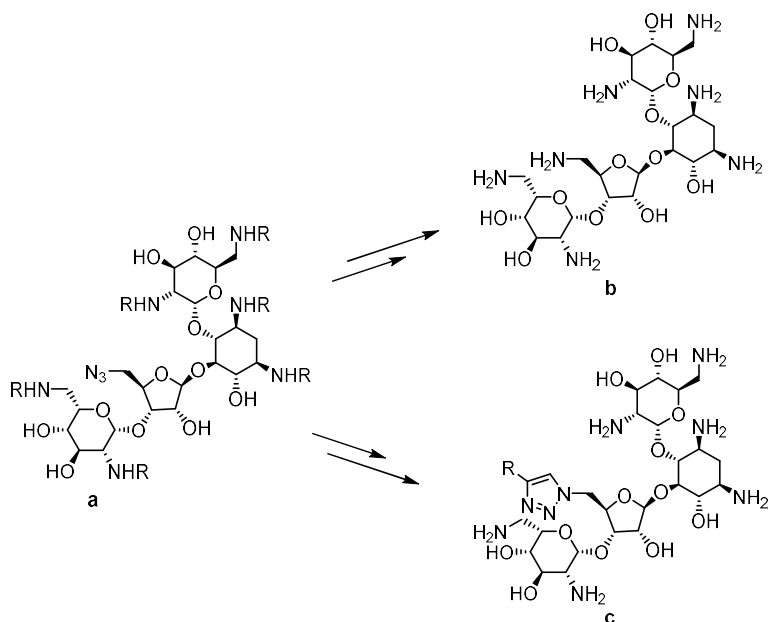
**Fig. 5 Neomycin reactivity III:** *After treating Ts- or TPS-neomycin with NaN₃ derivative **a** is obtained. This intermediate can be further used for Staudinger reaction leading to derivative **b** or for click chemistry with a terminal alkyne derivative to obtain compound **c**.*
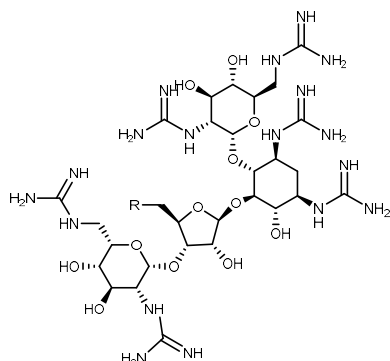


**Fig. 6 Neomycin reactivity IV:** *Guanidino-neomycin is a molecular transporter exhaustively investigated by Tor and coworkers. (Sarrazin et al.; Mol. Ther.; 2010, Luedtke et al.; J. Am. Chem. Soc. 2000).*

A different approach should be used in order to functionalize paromomycin, due to the presence of two primary hydroxyl groups that do not allow their selective functionalization. On one hand, it is possible to exploit the single amino-methylene group (Fig. 7 blue) on ring IV. This site has been used to couple paromomycin with

different lipophilic moieties through amides or carbamates groups (Fig. 7a) to obtain amphiphilic molecules suitable for cell transfection.[27]
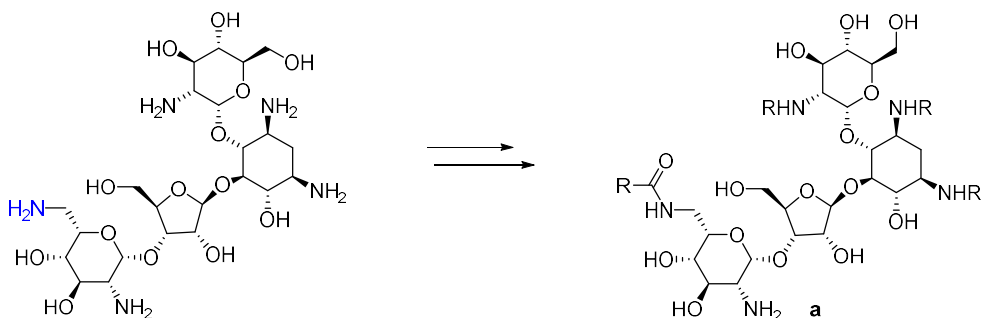


***Fig. 7 Paromomycin reactivity:*** *Paromomycin has a single amino-methylene group that can be exploited as reactive site. This group was coupled to different amphiphilic molecule to obtain vectors for cell transfection.*

In order to obtain O-derivatives it is necessary to protect the hydroxyl groups on ring III (Fig. 8-9 in red) as cyclic acetals or ketals. At this point, after protection of the primary hydroxyl group on the furanose ring by using tert-butyldimethylsilyl trifluoromethanesulfonate (TBSOTf) (Fig. 8a), the hydroxyl group in position 2'' can be used as reactive site. Hanessian[28] and coworkers followed this strategy to develop a series of aminoethyl ethers (Fig. 8b) with enhanced bactericidal activity against *S. aureus.*
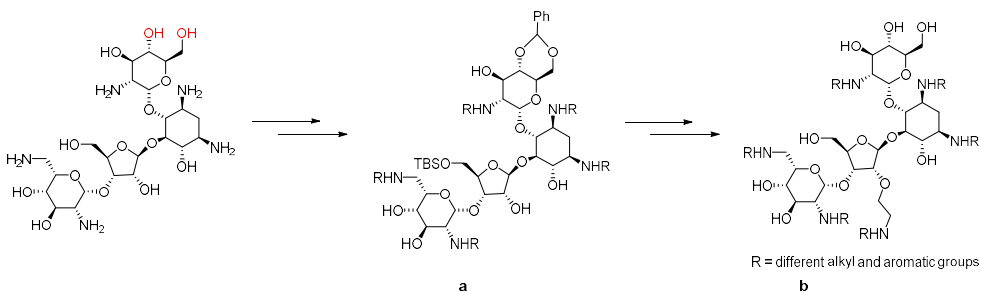


***Fig. 8. Paromomycin reactivity II:*** *Functionalization of paromomycin to obtain O-derivatives with enhanced antibacterial activity. After protection of the two hydroxyl groups on ring I as acetal and the protection of the hydroxyl group in position 5'' with TBSOTf (**a**), position 2''(**b**) can be used as reactive site.*

The hydroxyl group in position 5'' can also be functionalized. In order to do that Kenneth *et al*[29] protected the primary alcohol on ring I as ketal and then selectively activated with a bulky group the hydroxyl group on the furanose ring (Fig. 9a). They finally obtained a conformationally restrained paromomycin (Fig. 9b) used to elucidate the interaction with RNA.
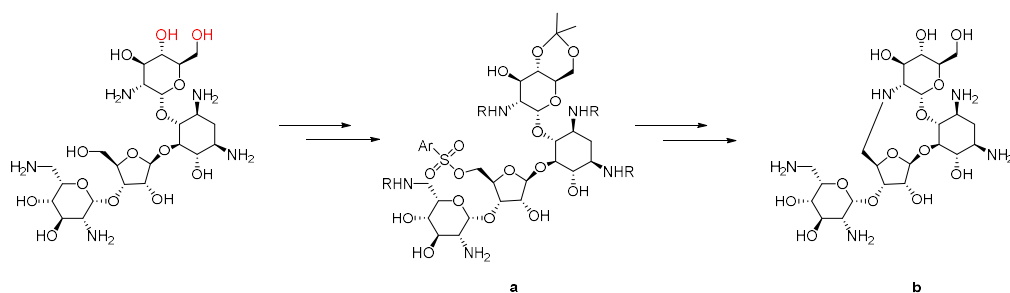
**Fig. 9 Reactivity of paromomycin III:** *Synthesis of a conformationally constrained paromomycin exploiting the primary alcohol on the furanose ring as reactive site.*

## Antibiotic mode of action and resistance

AGs are active against aerobic Gram-negative bacteria (*Escherichia coli*[30], *Pseudomonas aeruginosa*[2]) and some Gram-positive pathogens (*Staphylococcus*[31]). They can also be employed in combination with other antibiotics.[32,33] Despite their nephrotoxicity and ototoxicity, they are still clinically valuable tools against septicemia, peritonitis, endocarditis or skin infections.

Their bactericidal activity is due in most cases to the interaction of the antibiotic with the 16S RNA of the 30S subunit of the ribosome which is responsible of the translation of the genetic material. The final outcome of this interaction is the inhibition of the protein synthesis. At first, AGs electrostatically interact with the negatively charged outer membrane of Gram-negative bacteria through a non-energy dependent process; they diffuse through porin channels and enter the periplasmic space. Their subsequent transport across the cytoplasmic membrane requires metabolic energy from the electron transport system in an oxygen-dependent fashion. Anaerobic bacteria are intrinsically resistant to AGs as they are unable to carry out oxygen- or nitrate-dependent electron transport, thus they fail to transport AGs.[34] Once in the cytosol, different AGs can bind to different sites of rRNA depending on their structures and complementarity with the rRNA. The processes and the mechanism involved in the interaction between the AGs and the ribosome have been widely studied and elucidated through high resolution NMR analysis and X-ray crystallographic structures.[35] The primary binding site of neo and its analogues is the A-site on the 16S rRNA (Fig. 10).[36] Ring I and II are essential for binding the rRNA in a pocket where it adopts a L-shaped conformation.[37] This complex is further stabilized by ring III and IV's additional interactions. The interaction between the AG and the rRNA interferes with the translation process promoting the synthesis of aberrant

proteins that once inserted into the cell membrane led to an altered permeability that finally cause cell death.[3]
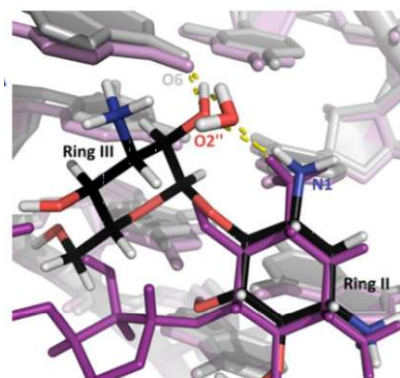


**Fig. 10 2-DOS AGs binding to the 16S RNA model:** *Neomycin (purple) and kanamycin A (coloured by atom name) interaction with RNA (pink and grey).*[38]

The overuse and misuse of AGs accelerate the development of resistance mechanisms[39] in different bacteria strains. Acquired resistance can be ascribed to a reduced affinity for its target by modification of the ribosome or the AG itself. In alternative, bacteria can develop mechanisms to reduce the concentration of the drugs inside the cell, such as efflux pumps.

The most clinically relevant cause of resistance to this class of antibiotics is the enzymatic modification of AG molecules (Fig. 11), which reduces the affinity for the target because of steric or electronical reasons. The enzymes catalyzing a regioselective modification of the AGs can be divided into three classes, namely acetyltransferases (AAC), nucleotidyltransferases (ANT) and phosphotransferases (APH). AACs acetylate one of the amino groups meanwhile ANT and APH produce O-derivatives transferring an AMP (Adenosine Monophosphate) group and a phosphate respectively. These enzymes are named according to the site of modification in the molecule (for example AAC(6') modifies the group in position 6'). This problem has been approached either by producing semi synthetic AGs, unaffected by enzymatic modification, or by designing molecules that interfere with the enzymatic mechanism.[40]
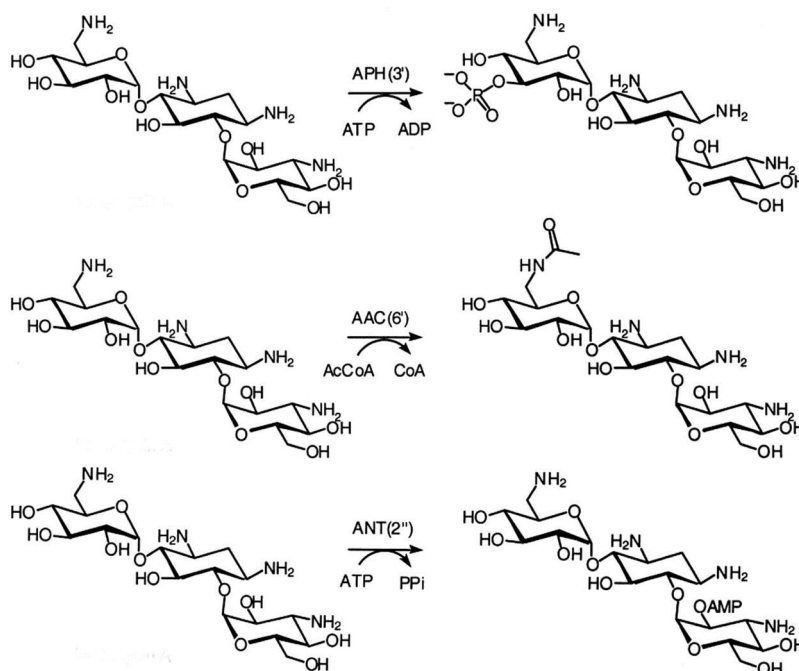
***Fig. 11 Mechanism of resistance against AGs:*** *the enzymatic modification of a specific position hampers the interaction with the rRNA. The enzymes that catalyze the modification can be divided into three classes: phosphotransferases (APH), acetyltransferases (AAC) and nucleotidyltransferases (ANT).*

Another mechanism that confers high resistance is recently rising concerns; the 16s RNA is protected through post transcriptional methylation[41] by means of methylases. Such methylases are produced by AG-producing bacteria themselves and are located on plasmids. Plasmids are highly mobile, thus they easily spread to other strains and carry on the methylase genes. Fortunately, this method of resistance has still a low prevalence, but such strains have to be carefully controlled. In fact, in 2003 it was also found in a clinical isolated *P. aeruginosa.*[42]

A third mechanism of resistance is the structural alteration of rRNA. This altered rRNA retains its biological function, but its interaction with the AG is impaired, thus conferring AG resistance to the bacterium. These random rRNA modifications are extremely rare. However, they were found to be clinically relevant for streptomycin resistance in *M. tubercolosis*.[43]

# References

1.      Zimelis, V. M., Jackson, G. G. Activity of Aminoglycoside Antibiotics against Pseudomonas aeruginosa: Specificity and Site of Calcium and Magnesium Antagonism. *J. Infect. Dis.* **127,** 663–669 (1973).

2.      Ratjen, F., Brockhaus, F., Angyalosi, G. Aminoglycoside therapy against Pseudomonas aeruginosa in cystic fibrosis: A review. *J. Cyst. Fibros.* **8,** 361–369 (2009).

3.      Jana, S., Deb, J.K. Molecular understanding of aminoglycoside action and resistance. *Appl. Microbiol. Biot.* **70,** 140–150 (2006).

4.      Schatz, A., Bugle, E., Waksman, S.A. Streptomycin, a Substance Exhibiting Antibiotic Activity Against Gram-Positive and Gram-Negative Bacteria. *Exp. Biol. Med.* **55,** 66–69 (1944).

5.      Waksman, S.A., Lechesralier, H.A. Neomycin, a New Antibiotic Active against Streptomycin-Resistant Bacteria, Including Tuberculosis Organisms. *Science* **109,** 305–307 (1949).

6.      Weinstein, M.J. Gentamicin, a New Antibiotic Complex from Micromonospora. *J. Med. Chem.* **6,** 463–464 (1963).

7.      Kawaguchi, H., Naito, T., Nakagawa, S., Fujisawa, K.-I. BB-K8, A New semisynthetic aminoglycoside antibiotic. *J. Antibiot. 12, 695-708, (1972)*

8.      Selimoglu, E. Aminoglycoside-Induced Ototoxicity. *Curr. Pharm. Design* **13,** 119–126 (2007).

9.      Mingeot-Leclercq, M.-P., Glupczynski, Y., Tulkens, M. Aminoglycosides : Activity and Resistance. *Antimicrob. Agents Chem.* **43,** 727–737 (1999).

10.     Lee, H.B. *et al.* Activity of some aminoglycoside antibiotics against true fungi, Phytophthora and Pythium species. *J. Appl. Microbiol.* **99,** 836–843 (2005).

11.     Sundar, S., Chakravarty, J. Paromomycin in the treatment of leishmaniasis. *Expert Opin. Inv. Drug* **17,** 787–794 (2008).

12.     Zingman, L.V., Park, S., Olson, T.M., Alekseev, A.E., Terzic, A. Aminoglycoside-induced Translational Read-through in Disease: Overcoming Nonsense Mutations by Pharmacogenetic Therapy. *Clin. Pharmacol. Ther.* **81,** 99–103 (2007).

13.     Arya, D. P. *et al.* Neomycin binding to watson-hoogsteen (W-H) DNA triplex groove: A model. *J. Am. Chem. Soc.* **125,** 3733–3744 (2003).

14.     Wang, H., Tor, Y. Electrostatic interactions in RNA aminoglycosides binding.

*J. Am. Chem. Soc.* **119,** 8734–8735 (1997).

15. Ghilardi, A. *et al.* Synthesis of multifunctional PAMAM-aminoglycoside conjugates with enhanced transfection efficiency. *Bioconjugate Chem.* **24,** 1928–1936 (2013).

16. Iwata, R. *et al.* Synthesis and properties of vitamin e analog-conjugated neomycin for delivery of RNAi drugs to liver cells. *Bioorg. Med. Chem. Lett.* **25,** 815–819 (2015).

17. Bera, S., Mondal, D., Palit, S. Schweizer, F. Structural modifications of the neomycin class of aminoglycosides. *MedChemComm,* **7,** 1499–1534 (2016).

18. Michael, K., Wang, H., Tor, Y. Enhanced RNA binding of dimerized aminoglycosides. *Bioorgan. Med. Chem.* **7,** 1361–1371 (1999).

19. Wang, H. Tor, Y. RNA–Aminoglycoside Interactions: Design, Synthesis, and Binding of "Amino-aminoglycosides" to RNA. *Angew. Chem. Int. Ed.* **37,** 109–111 (1998).

20. Bera, S., Zhanel, G.G., Schweizer, F. Evaluation of amphiphilic aminoglycoside–peptide triazole conjugates as antibacterial agents. *Bioorg. Med. Chem. Lett.* **20,** 3031–3035 (2010).

21. Zhang, J. *et al.* Surprising Alteration of Antibacterial Activity of 5″-Modified Neomycin against Resistant Bacteria. *J. Med. Chem.* **51,** 7563–7573 (2008).

22. Sarrazin, S., Wilson, B., Sly, W.S., Tor, Y., Esko, J.D. Guanidinylated neomycin mediates heparan sulfate-dependent transport of active enzymes to lysosomes. *Mol. Ther.* **18,** 1268–1274 (2010).

23. Luedtke, N.W., Baker, T.J., Goodman, M., Tor, Y. Guanidinoglycosides: A Novel Family of RNA Ligands. *J. Am. Chem. Soc.* **122**, 12035-12036, (2000).

24. Dix, A. V. *et al.* Cooperative, Heparan Sulfate-Dependent Cellular Uptake of Dimeric Guanidinoglycosides. *ChemBioChem* **11,** 2302–2310 (2010).

25. Luedtke, N.W., Carmichael, P., Tor, Y. Cellular Uptake of Aminoglycosides, Guanidinoglycosides, and Poly-arginine. *J. Am. Chem. Soc* **125,** 12374-12375 (2003).

26. Wexselblatt, E., Esko, J.D., Tor, Y. On Guanidinium and Cellular Uptake. *J. Org. Chem.* **79,** 6766–6774 (2014).

27. Mével, M. *et al.* Paromomycin and neomycin B derived cationic lipids: Synthesis and transfection studies. *J. Control. Release* **158,** 461–469 (2012).

28. Hanessian S., *et al.* Structure-Based Design, Synthesis, and A-Site rRNA Cocrystal Complexes of Functionally Novel Aminoglycoside Antibiotics. *Bioorgan. Med. Chem.* **20**, 7097-7101 (2007).

29.     Blount, K.F., Zhao F., Hermann, T., Tor, Y. Conformational Constraint as a Means for Understanding RNA-Aminoglycoside Specificity. *J. Am. Chem. Soc.* **127,** 9818-9829, (2005).

30.     Levison, M. E., Knight, R., Kaye, D. In vitro evaluation of tobramycin, a new aminoglycoside antibiotic. *Antimicrob. Agents Chem.* **1,** 381–4 (1972).

31.     Walkty, A. *et al.* In Vitro Activity of Plazomicin against Gram-Negative and Gram-Positive Clinical Isolates Obtained from Patients in Canadian Hospitals as Part of the CANWARD Study, 2011-2012. *Antimicrob. Agents Chem.* **58,** 2554–2563 (2014).

32.     Cebrero-Cangueiro, T. *et al.* In vitro Activity of Pentamidine Alone and in Combination With Aminoglycosides, Tigecycline, Rifampicin, and Doripenem Against Clinical Strains of Carbapenemase-Producing and/or Colistin-Resistant Enterobacteriaceae. *Front. Cell. Infect. Microbiol.* **8,** 1–7 (2018).

33.     Yadav, R. *et al.* Aminoglycoside concentrations required for synergy with carbapenems against Pseudomonas aeruginosa determined via mechanistic studies and modeling. *Antimicrob. Agents Chemother.* **61,** 1–16 (2017).

34.     Bryan, L.E., Kowand, S.K. Van Den Elzen, H.M. Mechanism of aminoglycoside antibiotic resistance in anaerobic bacteria: Clostridium perfringens and Bacteroides fragilis. *Antimicrob. Agents Chemother.* **15,** 7–13 (1979).

35.     Vicens, Q., Westhof, E. Crystal structure of paromomycin docked into the eubacterial ribosomal decoding A site. *Structure,* **9,** 647–58 (2001).

36.     Moazed, D., Noller, H. F. Interaction of antibiotics with functional sites in 16S ribosomal RNA. *Nature* **327,** 389–394 (1987).

37.     Kotra, L. P., Haddad, J. Mobashery, S. Aminoglycosides : Perspectives on Mechanisms of Action and Resistance and Strategies to Counter Resistance *Antimicrob. Agents Chemother.* **44,** 3249–3256 (2000).

38.     Trylska, J., Kulik, M. Interactions of aminoglycoside antibiotics with rRNA. *Biochem. Soc. Trans.* **44,** 987–93 (2016).

39.     Magnet, S., Blanchard, J. S. Molecular insights into aminoglycoside action and resistance. *Chem. Rev.* **105,** 477–497 (2005).

40.     Shi, K., Caldwell, S.J., Fong, D.H. Berghuis, A. M. Prospects for circumventing aminoglycoside kinase mediated antibiotic resistance. *Front. Cell. Infect. Microbiol.* **3,** 1-17 (2013).

41.     Doi, Y., Arakawa, Y., 16S Ribosomal RNA Methylation: Emerging Resistance Mechanism against Aminoglycosides. *Clin. Infect. Dis.* **45,** 88–94 (2007).

42.     Yokoyama, K. *et al.* Acquisition of 16S rRNA methylase gene in Pseudomonas

aeruginosa. *Lancet* **362,** 1888–1893 (2003).

43.     Alangaden, G. J. *et al.* Mechanism of Resistance to Amikacin and Kanamycin in Mycobacterium tuberculosis. *Antimicrob. Agents Chemother.* **42,** 19295-1297 (1998).

# Part II: Aminoglycoside-conjugates as non-viral vectors for cell transfection

# Chapter I: Introduction to gene delivery

## 1.1 Gene therapy

Gene therapy is a promising strategy of treatment for acquired and genetic diseases that consists in the introduction of exogenous nucleic acids (NAs) into cells.[1] DNA encoding for a missing or defective gene or RNA are transferred into cells to introduce the expression of therapeutic proteins or to silence malignant proteins. After its breakthrough in 1989[2], almost 3000 clinical trials have been approved, 115 of which were conducted in 2018.[3] The largest part of the developed treatment was aimed to defeat cancerous cells (66%) followed by monogenic diseases (11.4%).[4]

## 1.2 Gene delivery

The direct administration of naked NAs into cells is rather ineffective because of their short half-life in biological environments; this is due to their fast clearance by the mononuclear phagocyte system and to their rapid degradation by nucleases.[1] Moreover, NAs being hydrophilic and anionic, they are not able to cross the negatively charged cell membrane. All these factors have a negative effect on gene expression. Therefore, the development of effective delivery systems is necessary in order to transport genetic materials into the target cell, thus achieving a successful therapy. Gene delivery systems can be classified in physical methods and vector-based methods.

### 1.2.1 Physical methods

Physical methods consist in the application of physical-mechanical stimuli to form transient pores on the cell membrane to directly insert the NAs into the cytoplasm and the nucleus.[5] There is a number of physical stimuli that can be employed to promote gene delivery.

The most direct method to introduce DNA into cells is microinjection, that employs a glass needle or a micropipette to inject the DNA into the cell nucleus.[5]

Other physical methods exploit electric fields, ultrasound and magnetic fields that are used in electroporation[6], sonoporation[7] or magnetofection[8], respectively.

Although physical techniques can bypass some of the barriers that compromise an efficient therapeutic effect, they are expensive and not suitable for *in vivo* application.[5]

## 1.2.2 Vector-mediated transfection

Gene delivery mediated by vectors exploits carriers that can simultaneously protect and transport the genetic material into the cells. The most employed vectors are viruses[9,10] or synthetic vectors, such as positively charged compounds.[11,12] Only few examples of negatively charged vectors have been reported,[13] however the latter will not be object of further discussion.

### 1.2.2.1 Viral vectors

Wild type viruses can efficiently transfer genetic material into mammalian cells and exploit the host cell replication process, which makes them an excellent basis for the development of gene carriers.[14] Genetically engineered viruses are derived from wild type viruses to reduce their harmfulness. The gene that causes the disease is replaced with the desired gene in such a way that their ability to insert their own genome into the host's genome is still retained.[15] Several viruses are currently investigated to provide transient or permanent transgene expression, such as adenoviruses[16] or retroviruses.[17] Viral vectors are currently the most efficient way to deliver genes into cells. However, there are some drawbacks[18] related to their use, such as the activation of the immune response or their low carrying capacity, that encourage the development of alternative vectors.

### 1.2.2.2 Non-viral vectors

Non-viral vectors have emerged as promising alternative to viral vectors as they can be produced on a large scale with high reproducibility and acceptable costs.[19,20] Moreover, they are a safer alternative to viral system showing little or no immune response.[21] Non-viral vectors can be divided in two main categories according to their chemical structures: cationic lipid and cationic polymers.[22] These molecules are able to bind and complex the negatively charged NAs by means of electrostatic interactions, resulting in positively charged nano- or micro- scaled assemblies, named lipoplexes in the case of lipids and polyplexes in the case of polymers. These complexes can be prepared at different N/P ratio. This value represents the ratio of moles of the amine groups of cationic lipids or polymers to those of the phosphate ones of NA. It was reported that the N/P ratio affect the binding degree of the vectors with the NAs, thus having an impact on the transfection efficiency.[23]

Cationic complexes can interact with the cellular membrane promoting the uptake of the desired gene by the cell through various endocytic pathways. After internalization, the complexes are held into the endosomes. The endosome has to release the vector-NA complex into the cytosol. This process is referred to as endosomal escape and it is an essential step to achieve an efficient gene expression. In the final step,

the NA has to be released by the vector very close to the nuclear membrane to achieve gene transcription.[24,25] Each step of the cellular pathway affects the transfection process and represent a barrier to gene delivery (Fig. 12).
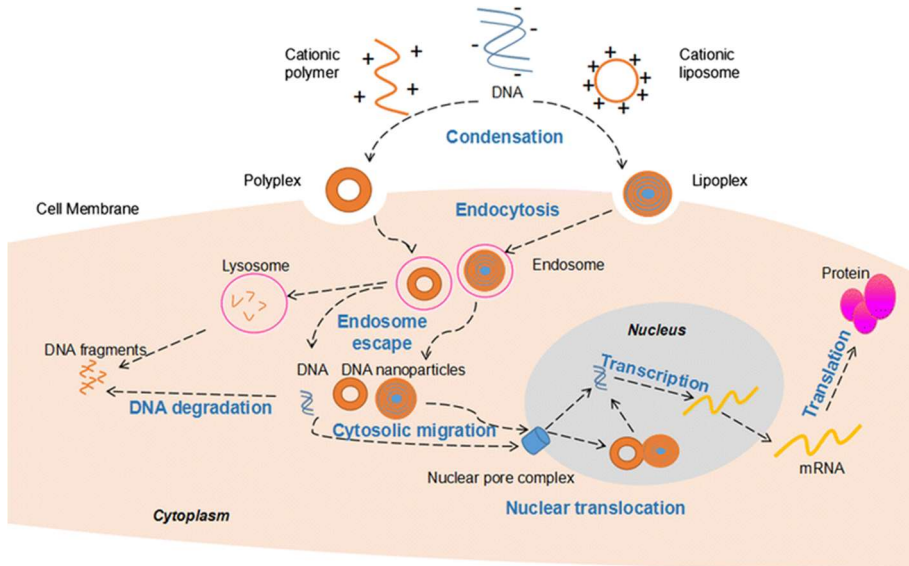


*Fig. 12 Cellular pathway of poly- and lipoplexes: After complexation of the NA by cationic lipids or polymers, the complexes cross the cellular membrane and enter the cell through various endocytic pathways. After internalization the complexes have to be released from the endosome to achieve an efficient gene expression. (Wu, P. et al. Non-viral gene delivery systems for tissue repair and regeneration. J. Transl. Med. 16, 29 (2018)).*

While significant progresses have been made in the development of efficient non-viral vectors, there is still a long way to go before achieving their widespread clinical use[26] due to their still low delivery efficiency. In order to achieve a more effective gene delivery, it is necessary to rationally design novel chemicals while considering the mechanisms involved in the transfection process.

***Cationic lipids (CLs):*** In 1987 Felgner and coworkers[2] developed a transfection protocol by using N-[1-(2,3-dioleyloxy)propyl]-N,N,N,-trimethylammonium chloride (DOTMA) (Fig. 13, upper) liposomes as vector. Since then, many other cationic lipidic structures have been synthesized and used for delivery purposes, such as 1,2-bis(oleoyloxy)-3-(trimethylammonium) propane (DOTAP) (Fig. 13, lower ).[27]
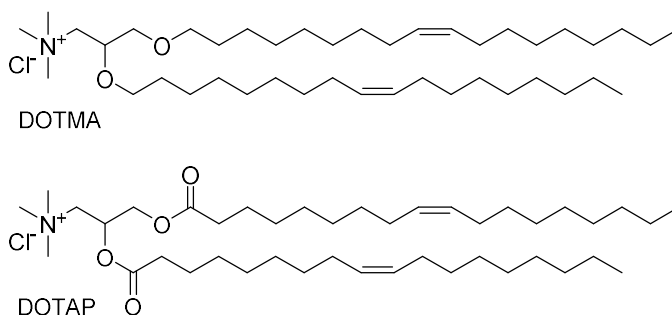
**Fig. 13 Cationic lipids:** *Two examples of the structure of cationic lipids employed in gene delivery: DOTMA and DOTAP.*

CLs are very attractive tools for gene delivery because they can be easily synthesized, and because their properties can be easily tuned by modifying their chemical structure.

CLs are amphiphilic molecules composed of three domains: a hydrophobic group, the positively charged head and a linker connecting these two parts (Fig.14). Each component confers specific properties to the entire molecule, thus affecting its transfection activity.[12]

- The lipidic domain is usually composed of alkyl chains or a steroid moiety. The number, unsaturation and length of the lipidic chain has been found to affect transfection efficiency.[28] Many studies have been carried out to determine the ideal length of the chain in order to improve CL's carrying efficiency. In general, lengths between $C_{10}$ and $C_{18}$ are considered the most favourable.[29]

- The linker, that is responsible for the vector's chemical stability and biodegradability, can be constituted by different functional groups: ethers,[30,31] esters[32,33] or carbamates.[34,35]

- The positively charged group is generally represented by amines with different degrees of substitutions. Primary, secondary, tertiary amines and quaternary ammonium are frequently encountered.[32,36,37] Moreover, the hydrophilic headgroup can be also constituted by guanidinium[38,39] or heterocyclic groups.[40]
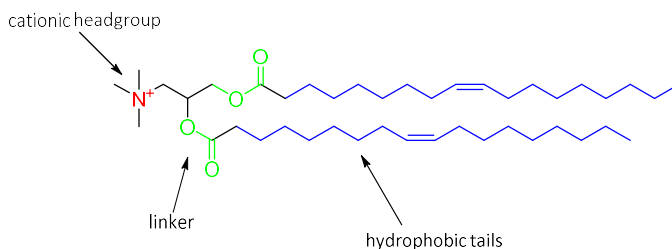
***Fig. 14 Structure of a cationic lipid:*** *CLs are composed of three domains, a polar head (red), a linker (green) and a lipid moiety (blue).*

Despite numerous cationic lipid vectors with a wide range of structures have been synthesized, an effective non-viral vector is yet to be developed. Therefore, the research for novel and effective carriers is still an active area.

***Cationic Polymers:*** Cationic polymers were introduced as a novel delivery system by Wu and coworkers.[41] Many polymers are currently employed as gene vectors, such poly(ethylenimine) (PEI)[42,43] both in its branched or linear form (bPEI and lPEI, respectively), chitosan[44,45] and PAMAM[46,47] (Fig. 15). Cationic polymers offer a high degree of molecular diversity. In fact, their structures can be modified to tune their physico-chemical properties (molecular weight, polydispersity or surface charge) and achieve an improved delivery efficiency.[48]
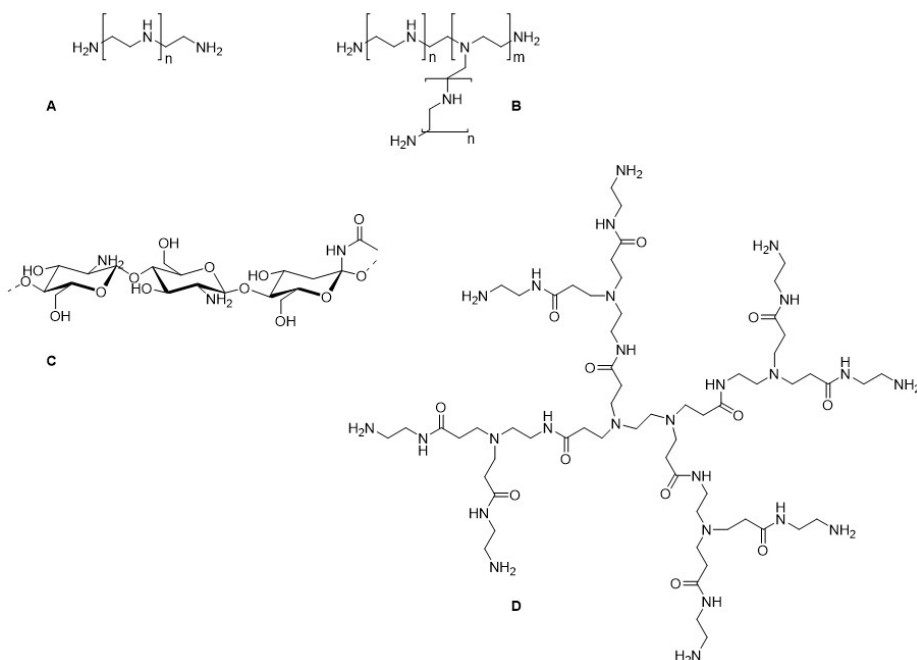


***Fig. 15 Cationic polymer****: Examples of structures of cationic polymers used as non-viral vectors: a) lPEI, b)bPEI, c) chitosan, d) PAMAM.*

Polymeric gene delivery systems usually possess protonable amines. Once into the lysosomes, where the pH decreases owing to the endosomal proton pump, the amines undergo changes in their protonation state preventing acidification of endocytic vesicles. These 'proton sponge polymers' cause the transport of additional protons together with their counterions. The subsequent increase in the ion concentration ultimately causes osmotic swelling of the endosome. This is followed by the rupture of the endosomal membrane and the release of the polyplexes into the cytosol.[49]

# 1.3 AG-conjugates as gene carriers for *in vitro* cell transfection

As already mentioned, AGs are able to interact and electrostatically bind a variety of RNA[50,51] and DNA.[52,53] Their structural variety and valency make them very interesting cationic moieties for synthesizing gene vectors.

### 1.3.1 Cationic Lipids based on aminoglycosides

AGs have been employed as polar head in the synthesis of CLs to develop non-viral vectors with remarkably high gene delivery efficiencies both *in vitro* and *in vivo*. AGs appeared for the first time as constituent of the polar head in CLs in 2002, when Belmont *et al*.[54] coupled kanamycin by means of carbamoyl bond with a cholesterol moiety (KanaChol) (Fig 16a) exploiting the less hindered amine in position 6'. A few years later, in 2005, Napoli *et al*[55] confirmed that the transfection efficiency of DOTAP can be enhanced in the presence of the AG. In the same year Sainlos *et al*[56] investigated the possibility to synthesize amphiphilic derivatives based on kanamycin. Their study aimed to enhance the transfection efficiency of KanaChol by changing the linker's length. They discovered that the introduction of a longer linker (compared to KanaChol) (Fig 16b) can improve transfection efficiency up to 10-folds. On the other hand, they explored the effect of other lipophilic moieties such as distearyl (Fig 16c) and dioleyl chains to elucidate some structure-activity relationship (SAR). These derivatives spontaneously formed vesicles and efficiently mediated gene transfection. Additional effort from Lehn's group[57] accounted for the application of AG based amphiphilic carriers for the delivery of siRNA. Neomycin, kanamycin, tobramycin and paromomycin were linked to a dioleyl moiety by means of a succinyl spacer.
A further study on the use of AG-derivatives for gene silencing was conducted from Zhang *et al* [58] in 2013. A library of AGs derivatives was constructed where all the amines of neomycin, amikacin, paromomycin, ribostamycin, kanamycin, hygromycin

geneticin and gentamycin were functionalized with lipidic chains with a length between 10 and 16 carbons. $C_{11}$ and $C_{12}$ derivatives proved to be the more efficient in a preliminary *in vitro* screening and successfully underwent *in vivo* examination in a mice model. Based on the previous observations, in 2009, Le Gall *et al.*[59] studied 12 neamine derivatives obtaining new SAR insights. One or two neamine molecules were conjugated to various lipophilic chains of different lengths. Each compound was used alone or in formulation with DOPE. The most efficient compounds bore a neamine core and two long lipophilic chains (Fig. 16d). Considering these promising results, more derivatives with neomycin and paromomycin were synthesized.[60] Neomycin B (Fig 16f) and paromomycin (Fig 16e) were equipped on one hand with a cholesterol moiety and on the other with a dioleyl chain. A dimeric paromomycin derivative was also prepared. The derivatives underwent *in vitro* gene delivery and paromomycin with oleyl moiety (DOSP) proved to be particularly efficient, reaching high value of transfection efficiency with low toxicity, whereas no beneficial effects were observed when using the dimer. This study was further expanded to tobramycin[61], which was equipped with different linkers and lipophilic chains. The highest transfection efficiency was reached when a hydrolysable ester was inserted in the linker (Fig 16g). The importance of supramolecular assemblies in the delivery of NAs was finally assessed by Colombani *et al* [62] that elucidate how the organization of the lipid bilayer influences the delivery system. They studied the transfection efficiency of two paromomycin derivatives with an amide and a phosphoramide linker that were used in various combination with two imidazole-based helper lipids bearing analogue functionalities. Neomycin has been also conjugated with small dehydropeptides[63], thus obtaining high efficiency while retaining antibacterial activity, and with Vitamin E analogues.[64]

Even though the combination of AGs with various lipophilic moieties has been intensely studied with some interesting results, we are still far from their effective application in clinics. Therefore, this field still needs to be studied and implemented.
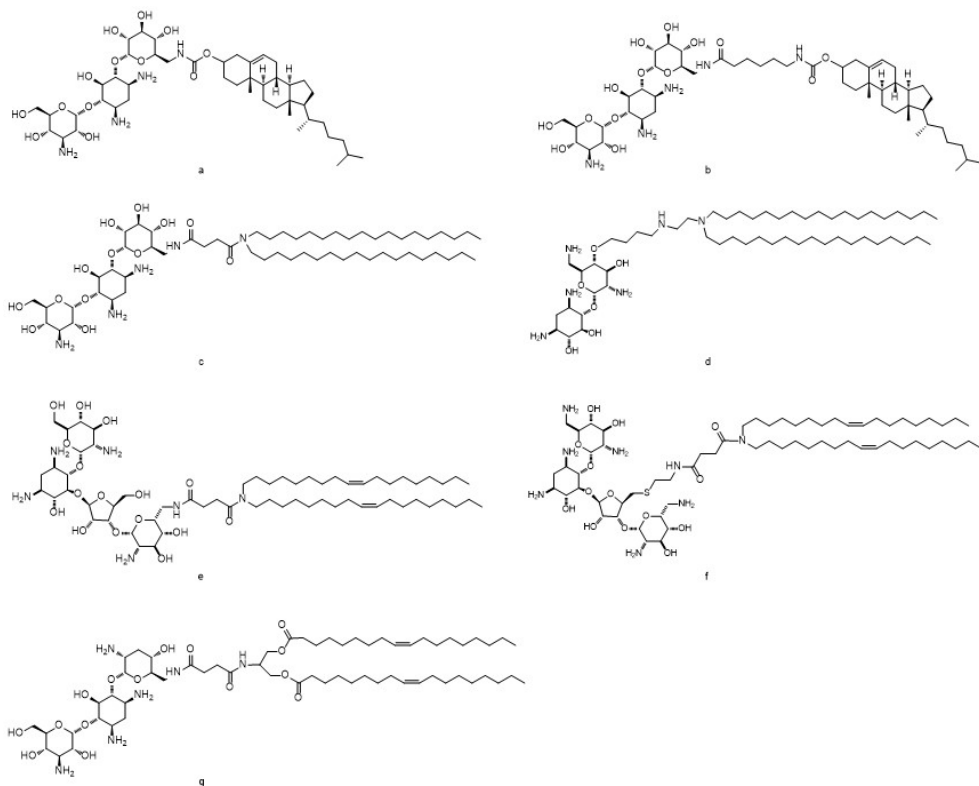
**Fig. 16 AG-based cationic lipids:** *Examples of AGs-lipid derivatives developed in Lehn's group during the last decade. a) and b) kanamycin coupled with a cholesterol moiety c) kanamycin and d) neamine in combination with two stearyl chains e) paromomyin, f) neomycin and g) tobramycin with two oleyl chains.*

## 1.3.2 Aminoglycosides in cationic polymers

AGs have also been included in the backbone of polymers to develop structures with higher transfection efficiency and lower cytotoxicity.

In 2011, Chen *et al.* synthesized hyperbranched glycoconjugates through a Michael-addition polymerization between kanamycin[65] or gentamycin[66] and N,N'-methylenebisacrylamide (MBA) that were able to mediate efficient gene delivery with low cytotoxicity. To shed light on the features that could promote an efficient delivery, a cheminformatic model has been developed to predict the value of transgene expression for a set of AG-based polymers[67] and lipopolymers[68] integrating combinatorial synthesis with cheminformatic (QSAR model). In a later study[69], it was discovered that the transfection efficiency of these AG-based polymers can be enhanced by introducing a glycidyltrimethylammonium chloride group.

AG-PEG polymers were successfully used to load and deliver doxorubicin, an anticancer drug, to cytoplasm and in the nucleus.[70]

Huang *et al.*[71] prepared a series of reduction-responsive hyperbranched disulfide-containing polymers with antibacterial activity based on neomycin, gentamycin and tobramycin that were able to transfect cells with negligible toxicity. Targeted gene delivery of a gentamicin- and neomycin-functionalized bPEI was achieved by Oroojalian[72] by exploiting megalin receptors. Megalin is a 600-kDa transmembrane protein belonging to the LDL-receptor family that mediates retention of drugs, including aminoglycosides. Our group has recently developed AG-G4PAMAM conjugates with neamine (Fig. 17), neomycin and paromomycin, that display good transfection efficacy also in the presence of serum.[46]



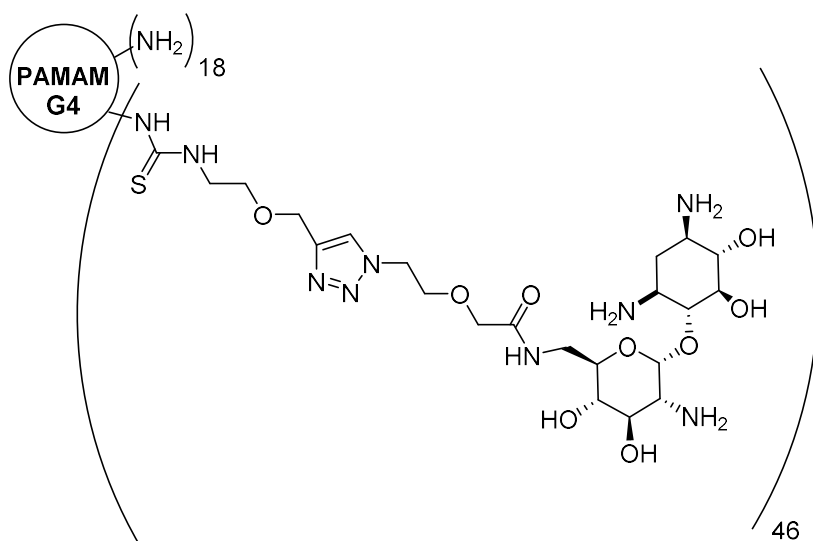***Fig. 17: AGs-Cationic polymers****: Neamine G4-PAMAM derivative synthesized and used for gene delivery by our group.*

Despite AGs have largely proven to be suitable scaffolds in the synthesis of gene delivery carriers, the ideal vector has yet to be developed. The following chapters describe the effort that has been made during my PhD project to develop effective non-viral vectors based on AGs.

# 1.4 References

1. Pezzoli, D., Candiani, G. Non-viral gene delivery strategies for gene therapy: A 'ménage à trois' among nucleic acids, materials, and the biological environment: *J. Nanoparticle Res.* **15,** 1-27 (2013).

2. Felgner, P. L. *et al.* Lipofection: a highly efficient, lipid-mediated DNA-transfection procedure. *Proc. Natl. Acad. Sci. U.S.A.* **84,** 7413–7417 (1987).

3. Available at: http://www.abedia.com/wiley/years.php (Accessed 22nd October 2018).

4. Gene Therapy Clinical Trials Worldwide. Available at: http://www.abedia.com/wiley/indications.php. (Accessed: 22nd October 2018)

5. Mehier-Humbert, S., Guy, R. H. Physical methods for gene transfer: Improving the kinetics of gene delivery into cells. *Adv. Drug Deliv. Rev.* **57,** 733–753 (2005).

6. Somiari, S. *et al.* Theory and in Vivo Application of Electroporative Gene Delivery. *Mol. Ther.* **2,** 178–187 (2000).

7. Unger, E.C., Hersh, E., Vannan, M., McCreery, T. Gene Delivery Using Ultrasound Contrast Agents. *Echocardiography* **18,** 355–361 (2001).

8. Scherer, F. *et al.* Magnetofection: enhancing and targeting gene delivery by magnetic force in vitro and in vivo. *Gene Ther.* **9,** 102–109 (2002).

9. Breakefield, X.O., DeLuca, N.A. Herpes simplex virus for gene delivery to neurons. *New Biol.* **3,** 203–18 (1991).

10. Mulligan, R. *et al.* The basic science of gene therapy. *Science* **260,** 926–932 (1993).

11. Eliyahu, H., Barenholz, Y., Domb, A. J. Polymers for DNA delivery. *Molecules* **10,** 34–64 (2005).

12. Chesnoy, S., Huang, L. Structure and Function of Lipid-DNA Complexes for Gene Delivery. *Annu. Rev. Biophys. Biomol. Struct.* **29,** 27–47 (2000).

13. Srinivasan, C., Burgess, D.J. Optimization and characterization of anionic lipoplexes for gene delivery. *J. Control. Release* **136,** 62–70 (2009).

14. Warnock, J.N., Daigre, C., Al-Rubeai, M. Introduction to Viral Vectors. in *Methods in molecular biology (Clifton, N.J.)* **737,** 1–25 (2011).

15. Thomas, C.E., Ehrhardt, A., Kay, M.A. Progress and problems with the use of viral vectors for gene therapy. *Nat. Rev. Genet.* **4,** 346–358 (2003).

16. Lee, C.S. *et al.* Adenovirus-Mediated Gene Delivery: Potential Applications for Gene and Cell-Based Therapies in the New Era of Personalized Medicine. *Genes Dis.* **4,** 43–63 (2017).

17. Deregowski, V., Canalis, E., Gene Delivery by Retroviruses. in *Methods in*

*molecular biology (Clifton, N.J.)* **455,** 157–162 (2008).

18.  Somia, N., Verma, I.M., Gene therapy: trials and tribulations. *Nat. Rev. Genet.* **1,** 91–99 (2000).

19.  Liu, F., Huang, L. Development of non-viral vectors for systemic gene delivery. *J. Control. Release* **78,** 259–266 (2002).

20.  Yin, H. *et al.* Non-viral vectors for gene-based therapy. *Nat. Rev. Genet.* **15,** 541–555 (2014).

21.  Thomas, M. Klibanov, A.M. Non-viral gene therapy: polycation-mediated DNA delivery. *Appl. Microbiol. Biotechnol.* **62,** 27–34 (2003).

22.  Mintzer A.M., Simanek E.E. Nonviral Vectors for Gene Delivery. *Chem. Rev.* **109,** 259-302 (2009).

23.  Zhao, Q.Q. *et al.* N/P ratio significantly influences the transfection efficiency and cytotoxicity of a polyethylenimine/chitosan/DNA complex. *Biol. Pharm. Bull.* **32,** 706–710 (2009).

24.  Khalil, I.A., Kogure, K., Akita, H., Harashima, H. Uptake pathways and subsequent intracellular trafficking in nonviral gene delivery. *Pharmacol. Rev.* **58,** 32–45 (2006).

25.  Pichon, C., Billiet, L., Midoux, P. Chemical vectors for gene delivery: uptake and intracellular trafficking. *Curr. Opin. Biotechnol.* **21,** 640–645 (2010).

26.  Yin, H. *et al.* Non-viral vectors for gene-based therapy. *Nat. Rev. Genet.* **15,** 541–555 (2014).

27.  Felgner, J., Martin, M., Tsai, Y., Felgner, P.L. Cationic lipid-mediated transfection in mammalian cells: "Lipofection". *J. Tissue Cult. Meth* **15,** 63–68 (1993).

28.  Heyes, J.A., Niculescu-Duvaz, D., Cooper, R. G., Springer, C.J. Synthesis of novel cationic lipids: Effect of structural modification on the efficiency of gene transfer. *J. Med. Chem.* **45,** 99–114 (2002).

29.  Zhi, D. *et al.* Transfection Efficiency of Cationic Lipids with Different Hydrophobic Domains in Gene Delivery. *Bioconjugate Chem.* **21,** 563–577 (2010).

30.  Bhattacharya S.; Dileep, P.V. Cationic Oxyethylene Lipids. Synthesis, Aggregation, and Transfection Properties. *Bioconjugate Chem.* **15,** 508–519 (2004).

31.  Bennett, M.J. *et al.* Cationic Lipid-Mediated Gene Delivery to Murine Lung: Correlation of Lipid Hydration with in Vivo Transfection Activity. *J. Med. Chem.* **40,** 4069–4078 (1997).

32.  Falsini, S., Ristori, S., Lipoplexes from Non-viral Cationic Vectors: DOTAP-DOPE Liposomes and Gemini Micelles. *Methods in Molecular Biology,* **1445,** 33–43 (2016).

33.  Narang, A.S., Thoma L., Miller, D.D., Mahato R.I. Cationic Lipids with Increased DNA Binding Affinity for Nonviral Gene Transfer in Dividing and Nondividing Cells. *Boconjugate Chem.* **16**, 156-168 (2004).

34.  Zhao, Y.N. *et al.* Novel gemini cationic lipids with carbamate groups for gene delivery. *J. Mater. Chem. B* **2**, 2920–2928 (2014).

35.  Gao, X., Huang, L. A novel cationic liposome reagent for efficient transfection of mammalian cells. *Biochem. Biophys. Res. Commun.* **179,** 280–285 (1991).

36.  Felgner, P. L. *et al.* Lipofection: a highly efficient, lipid-mediated DNA-transfection procedure. *Proc. Natl. Acad. Sci. U. S. A.* **84,** 7413–7417 (1987).

37.  Wasungu, L., Hoekstra, D. Cationic lipids, lipoplexes and intracellular delivery of genes. *J. Control. Release* **116,** 255–264 (2006).

38.  Geihe, E.I. *et al.* Designed guanidinium-rich amphipathic oligocarbonate molecular transporters complex, deliver and release siRNA in cells. *Proc. Natl. Acad. Sci.* U.S.A. **109,** 13171–13176 (2012).

39.  Aissaoui, A. *et al.* Progress in Gene Delivery by Cationic Lipids : Guanidinium-Cholesterol-Based Systems as an Example. *Curr. Drug Targets* **3,** 1-16 (2002).

40.  Zhi, D. *et al.* The Headgroup Evolution of Cationic Lipids for Gene Delivery. *Bioconjugate Chem.* **24,** 487–519 (2013).

41.  Wu, G. Y., Wu, C.H. Receptor-mediated in vitro gene transformation by a soluble DNA carrier system. *J. Biol. Chem.* **262,** 4429–32 (1987).

42.  Godbey, W.T., Wu, K.K., Mikos, A.G. Poly(ethylenimine) and its role in gene delivery. *J. Control. Release* **60,** 149–160 (1999).

43.  Lungwitz, U., Breunig, M., Blunk, T., Göpferich, A. Polyethylenimine-based non-viral gene delivery systems. *Eur. J. Pharm. Biopharm.* **60,** 247–266 (2005).

44.  Venkatesh, S., Smith, T.J. Chitosan-Mediated Transfection of HeLa Cells. *Pharm. Dev. Technol.* **2,** 417–418 (1997).

45.  Erbacher, P., Zou, S., Bettinger, T., Steffan, A. Remy, J. Chitosan-Based Vector/DNA Complexes for Gene Delivery: Biophysical Characteristics and Transfection Ability. *Pharm. Res.* **15,** 1332–1339 (1998).

46.  Ghilardi, A. *et al.* Synthesis of multifunctional PAMAM-aminoglycoside conjugates with enhanced transfection efficiency. *Bioconjugate Chem.* **24,** 1928–1936 (2013).

47.  Abedi-Gaballu, F. *et al.* PAMAM dendrimers as efficient drug and gene delivery nanosystems for cancer therapy. *Appl. Mater. Today* **12,** 177–190 (2018).

48.  Sun, X., Zhang, N. Cationic Polymer Optimization for Efficient Gene Delivery. *Mini-Reviews Med. Chem.* **10,** 108–125 (2010).

49. Creusat, G. *et al.* Proton Sponge Trick for pH-Sensitive Disassembly of Polyethylenimine-Based siRNA Delivery Systems. *Bioconjugate Chem.* **21,** 994–1002 (2010).

50. Wang, H. Tor, Y. Electrostatic interactions in RNA aminoglycosides binding. *J. Am. Chem. Soc.* **119,** 8734–8735 (1997).

51. Hermann, T. Westhof, E. Docking of cationic antibiotics to negatively charged pockets in RNA folds. *J. Med. Chem.* **42,** 1250–1261 (1999).

52. Arya, D. P. *et al.* Neomycin binding to watson-hoogsteen (W-H) DNA triplex groove: A model. *J. Am. Chem. Soc.* **125,** 3733–3744 (2003).

53. Arya, D. P., Coffee, R. L., Willis, B., Abramovitch, A. I. Aminoglycoside-nucleic acid interactions: remarkable stabilization of DNA and RNA triple helices by neomycin. *J. Am. Chem. Soc.* **123,** 5385–95 (2001).

54. Belmont, P. *et al.* Aminoglycoside-derived cationic lipids as efficient vectors for gene transfection in vitro and in vivo. *J. Gene Med.* **4,** 517–526 (2002).

55. Napoli, S., Carbone, G. M., Catapano, C. V., Shaw, N., Arya, D. P. Neomycin improves cationic lipid-mediated transfection of DNA in human cells. *Bioorganic Med. Chem. Lett.* **15,** 3467–3469 (2005).

56. Sainlos, M. *et al.* Kanamycin A-derived cationic lipids as vectors for gene transfection. *ChemBioChem* **6,** 1023–1033 (2005).

57. Desigaux, L. *et al.* Self-assembled lamellar complexes of siRNA with lipidic aminoglycoside derivatives promote efficient siRNA delivery and interference. *Proc. Natl. Acad. Sci.* U.S.A **104,** 16534–16539 (2007).

58. Zhang, Y. *et al.* Lipid-modified aminoglycoside derivatives for in vivo siRNA delivery. *Adv. Mater.* **25,** 4641–4645 (2013).

59. Le Gall, T. *et al.* Synthesis and transfection properties of a series of lipidic neamine derivatives. *Bioconjugate Chem.* **20,** 2032–2046 (2009).

60. Mével, M. *et al.* Paromomycin and neomycin B derived cationic lipids: Synthesis and transfection studies. *J. Control. Release* **158,** 461–469 (2012).

61. Habrant, D. *et al.* Design of Ionizable Lipids to Overcome the Limiting Step of Endosomal Escape: Application in the Intracellular Delivery of mRNA, DNA, and siRNA. *J. Med. Chem.* **59,** 3046–3062 (2016).

62. Colombani, T. *et al.* Self-assembling complexes between binary mixtures of lipids with different linkers and nucleic acids promote universal mRNA, DNA and siRNA delivery. *J. Control. Release* **249,** 131–142 (2017).

63. Yadav, S. *et al.* Multifunctional self-assembled cationic peptide nanostructures efficiently carry plasmid DNA in vitro and exhibit antimicrobial activity with minimal toxicity. *J. Mater. Chem. B* **2,** 4848–4861 (2014).

64. Iwata, R. *et al.* Synthesis and properties of vitamin e analog-conjugated neomycin for delivery of RNAi drugs to liver cells. *Bioorg. Med. Chem. Lett.* **25,** 815–819 (2015).

65.    Chen, M. *et al.* Hyperbranched glycoconjugated polymer from natural small molecule kanamycin as a safe and efficient gene vector. *Polym. Chem.* **2,** 2674–2682 (2011).

66.    Chen, M. *et al.* Multifunctional hyperbranched glycoconjugated polymers based on natural aminoglycosides. *Bioconjugate. Chem.* **23,** 1189–1199 (2012).

67.    Potta, T. *et al.* Discovery of antibiotics-derived polymers for gene delivery using combinatorial synthesis and cheminformatics modeling. *Biomaterials* **35,** 1977–1988 (2014).

68.    Miryala, B., Zhen, Z., Potta, T., Breneman, C. M., Rege, K., Parallel Synthesis and Quantitative Structure-Activity Relationship (QSAR) Modeling of Aminoglycoside-Derived Lipopolymers for Transgene Expression. *ACS Biomater. Sci. Eng.* **1,** 656–668 (2015).

69.    Miryala, B., Feng, Y., Omer, A., Potta, T. Rege, K. Quaternization enhances the transgene expression efficacy of aminoglycoside-derived polymers. *Int. J. Pharm.* **489,** 18–29 (2015).

70.    Miryala, B. *et al.* Aminoglycoside-derived amphiphilic nanoparticles for molecular delivery. *Colloids Surf. B* **146,** 924–937 (2016).

71.    Huang, Y., Ding, X., Qi, Y., Yu, B., Xu, F.J. Reduction-responsive multifunctional hyperbranched polyaminoglycosides with excellent antibacterial activity, biocompatibility and gene transfection capability. *Biomaterials* **106,** 134–143 (2016).

72.    Oroojalian, F., Rezayan, A. H., Shier, W. T., Abnous, K., Ramezani, M. Megalin-targeted enhanced transfection efficiency in cultured human HK-2 renal tubular proximal cells using aminoglycoside-carboxyalkyl-polyethylenimine -containing nanoplexes. *Int. J. Pharm.* **523,** 102–120 (2017).

# Chapter II: Triazine as core for the synthesis of AGs based cationic lipids for gene delivery.

## 2.1 Background

1,3,5-triazine scaffolds allow for versatile modifications without regiochemical concerns in a multigram-scale. Moreover, 1,3,5 triazine have been used in the synthesis of a wide range of biologically active compounds and have been probed for various medicinal purposes such as antibacterial,[1,2] imaging probes,[3] or anticancer agents.[4,5]

Triazines have also found their application in gene delivery. Merkel and coworkers have extensively investigated triazine-based dendrimers as transfectant agents to elucidate whether size, internal structure and peripherical groups of the dendrimers can influence the transfection efficiency.[6,7] The correlation between the structure and the transfection efficiency is, in fact, a valuable information to further modified the structure of the dendrimers and optimize their delivery properties.

Our group has previously developed a series of triazine-based CL vectors exploring various alkyl chains of different lengths. These CLs exhibited low cytotoxicity and high transfection efficiency, without the need of any formulation with co-lipids.[8]

The triazine scaffold makes easy to synthesize CLs with high tranfection efficiency, therefore, we use this molecule to synthesize a library of CLs with a triazine core in which the polar head is constituted by an AG chosen between neomycin or paromomycin, in combination with different lipophilic moieties. The compounds were characterized through NMR and by mass spectroscopy. Finally, they underwent preliminary biological validation.

## 2.2. Materials and methods

### 2.2.1 Materials and reagents

Starting materials and solvents were purchased from commercial suppliers (Alfa Aesar, Apollo Scientific, Fluka, FluoroChem, Honeywell, Sigma Aldrich, TCI) and used without further purification. HeLa (human cervix carcinoma) cells were purchased from the American Type Culture Collection (ATCC, Manassas, VA, USA).

AlamarBlue Cell Viability Assay was purchased from Life Technologies Italia (Monza,Italy), while BCA Protein Assay Kit was from ThermoFisher (Monza,Italy). pDNA encoding the modified firefly luciferase (pGL3-Control Vector, 5.2 kbp; hereafter referred to as pGL3) and Luciferase Assay System were obtained from Promega (Milan, Italy).

## 2.2.2 Synthesis of the conjugates
See Supporting Information 2.6

## 2.2.3 Biological assays
**Preparation of transfectant solutions**: Compound **15** to **20** were diluted in $dH_2O$ to a final nitrogen concentration ([N]) of 13 mM. 25 kDa bPEI was diluted in 10mM HEPES to a final concentration of 0.86 mg/mL and a [N]=20 mM, considering that there is one nitrogen per repeat PEI unit (-NHCH2CH2-, Mw=43 Da).[9]

**Complexes preparation** pDNA was amplified, isolated, purified and diluted in 0.1×TE buffer (1mM Tris, pH 8; 0.1mM EDTA) as previously described.[10] Lipoplexes were prepared at r.t. by mixing the aqueous solutions of pGL3 to compound **15** to **20** at the desired lipid concentration, yielding different charge ratios (N/P) and a final DNA concentration in transfection solution of 20 ng/µL. N/P is defined as the number of amines (N, cationic) of the AG which is used to complex the phosphate groups (P, anionic) of a given quantity of DNA (i.e. cationic vs. anionic charge ratio). pDNA/**15** to **20** complexes were prepared in $dH_2O$ and incubated for 20 min at r.t. prior to use.

**Cell cultures**: Mycoplasma-free HeLa cells were cultured in Dulbecco's modified Eagle's medium (DMEM) containing 1mM sodium pyruvate, 10mM HEPES buffer, 100 U/mL penicillin, 0.1 mg/mL streptomycin, 2mM glutamine and supplemented with 10% (v/v) fetal bovine serum (FBS) (hereafter referred to as complete culture medium, cDMEM) in a humidified atmosphere under constant supply of 5% $CO_2$ and at 37 °C (hereafter referred to as standard culture conditions).

**In vitro cells transfection:** Cells were passaged 24 h before plating in 96-well plates at a density of $2×10^4$ cells/$cm^2$ and maintained in standard culture conditions. Twenty-four hrs after seeding, 160 ng/well of pGL3 were complexed in $dH_2O$ with compounds **15** to **20** solutions to yield different N/P as described herein above, and cells were incubated with complexes in 100 µL/well of cDMEM under standard culture conditions for further 24 hrs. Cells transfected with 25 kDa bPEI/DNA complexes at varying N/P were used as the internal reference. Twenty-four hr-post transfection, cytotoxicity was evaluated by means of AlamarBlue assay according to manufacturer's instructions. Briefly, medium was removed, and each well was loaded with 100 µL of cDMEM containing 1×resazurin dye. Cells were next incubated in standard culture conditions for 2 hrs, then the fluorescence of the medium was read with a GENios Plus reader

(Tecan, Italy) (λex=540 nm; λem=595 nm). Viability of untransfected cells (CTRL) was assigned to as 100%.

Transfection efficiency was evaluated measuring the luciferase activity by means of the Luciferase Assay System, according to manufacturer's instructions. Briefly, cells were washed with phosphate buffered saline (PBS) and lysed with 110 μL/well of Cell Culture Lysis Reagent (Promega, Italy). Following a freeze-thawing cycle to improve cell disruption, 20 μL of cell lysates were mixed with 50 μL of Luciferase Assay Reagent and luminescence was measured by means of a GENios Plus reader. The luminescence signal (expressed as relative light units, RLU) of each sample was normalized to its protein content, determined by BCA assay and data are expressed as RLU/mg of proteins.

## 2.3 Results and discussion

Synthesis of triazine based non-viral vectors can be obtained by starting from the cheap and easily available cyanuric chloride. This starting material allows for a smooth introduction of structural diversity by subsequent nucleophilic dechloroaminations of the trichloro-triazine by different amines by controlling the reaction conditions, i.e. the temperature. A sequential substitutions of the chlorine with amine nucleophiles can afford selective synthesis with high yielding.[8,11]

Besides, AGs with their inherent high affinity for a variety of anions[12] and NAs[13] are a promising candidate in gene delivery. For these reasons they have been already used in the synthesis of highly efficient non-viral vectors.[14,15] The group of Prof. Lehn gave some insight into the structure-activity relationship of a series of amphiphilic vectors constituted by various AGs such as kanamycin[16], neamine[17] and paromomycin.[18] They elucidated that highest levels of transfection efficiency are reached when the AG is used in combination with cholesterol[19] or $C_{18}$ alkyl chains.[17,18]

Bearing these considerations in mind, we chose to develop a panel of CLs by using three different lipophilic moieties, namely stearyl, oleyl and cholesterol in combination with AGs. Specifically, two set of derivatives were synthesized, in the first case, we developed single-tailed molecules with paromomycin or neomycin as polar head. A second set of CLs, composed of double-tailed derivatives with homo- and hetero-combinations of the three lipophilic structures, was then arranged with neomycin.

## Nomenclature adopted

In this chapter the compounds are named according to their structural features: the cationic head will be indicated as neo (neomycin) and paro (paromomycin), meanwhile the lipidic moiety will be referred to as chol (cholesterol), oleyl (oleylamine) stearyl (octadecylamine).

## 2.3.1 Unsuccessful synthetic strategy

In this paragraph, the first attempt performed to obtain AG-triazine based CLs is described even if it was found to be unsuccessful.

Cyanuric chloride was first reacted with one oleylamine in order to displace the first chlorine (Fig. 18 step *i*). The reagents were allowed to stir few hours in an ice bath in a mixture of 1/1 v/v of acetone/ water in the presence of NaHCO$_3$. The desired product was afforded in high yield (Fig 18a). This compound underwent a further displacement of the chlorine with a second oleylamine obtaining the di-substituted derivative (Fig. 18b step *ii*).
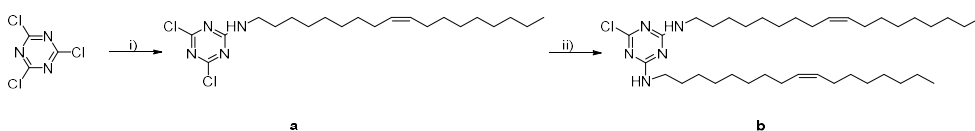


**Fig. 18 Synthetic pathway**: *A first oleylamine was introduced in step i) at 0°C in a H$_2$O/acetone mixture. In step ii) a second oleylamine was used to displace the second chlorine at r.t in a H$_2$O/acetone mixture.*

At this point we tried to substitute the third chlorine and introduce the AG exploiting the Neo-NH$_2$ intermediate (Fig 19a), that was synthesized according to literature.[20] We chose to introduce the AG in the last step for two reasons. On one hand it is an intermediate that required several synthetic steps, thus we want to use the minimum amount needed in the process. On the other hands the purification steps are thus facilitated. The reaction was conducted at 60°C in an acetone-H$_2$O mixture, however only starting materials were recovered.
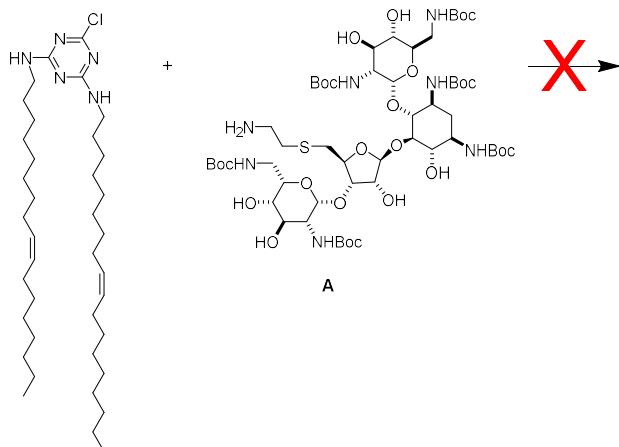
**Fig. 19 Unsuccessful attempt:** *The Neo-NH$_2$ derivative A was not able to displace the third chlorine of the triazine.*

In order to verify whether the reaction was ineffective due to an unsuitable mixture of solvents or due to steric factors, the di-oleyl-triazine was reacted with a generic amine by using the same reaction conditions (Fig. 20). The third substitution was successfully achieved after 24hrs by using dodecylamine. The trisubstituted triazine was obtained in a 48% yield.
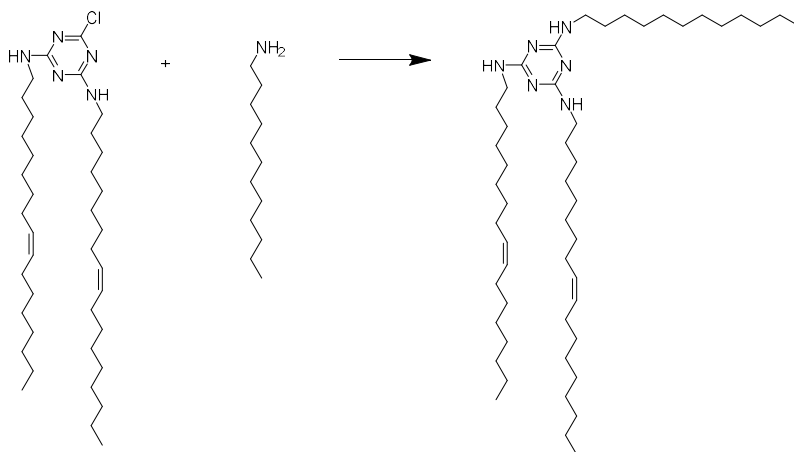


**Fig. 20 Testing the reaction conditions**: *The third chlorine displacement was obtained by using dodecylamine.*

We concluded that the reaction between Neo-NH$_2$ was prevented by steric factors.

In a second attempt we shifted the functionalization of the triazine with the AG in the previous step (Fig. 21, step i). The oleyl-triazine derivative was reacted with Neo-NH$_2$

affording the desired product in a 48% yield. Then we proceeded with the third substitution of the chlorine of the triazine core with the second oleylamine (Fig 21 step *ii*)). The reaction was carried out at 60°C for two days. Unfortunately, we could not detect the final compound and moreover, the starting material was degraded.
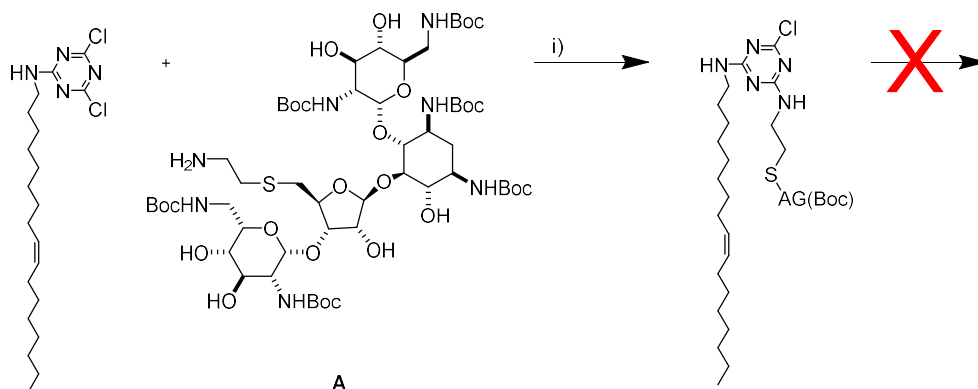


**Fig. 21 Unsuccessful attempt**: *Neo-NH2 successfully displaced the second chlorine (step i), however, when we tried to introduce the oleylamine as third substituent, the conjugates was degraded.*

At this point we decided to use a NH2-PEG-N3 linker to tether the AG to the triazine core. The amine of the linker will be used to conjugate with the triazine scaffold, meanwhile the azido group will be employed in click chemistry with a proper modified AG. This strategy allows for the introduction of the AG in the last step and in mild reaction conditions.

## 2.3.2 Synthesis of the single-tailed conjugates

Cyanuric chloride (Fig. 22) was first reacted with a NH2-PEG-N3 linker at 0°C to afford intermediate **5** in presence of NaHCO3 in 80% yield. This spacer will be further exploited in the last step for coupling the AG by means of click chemistry. The second substitution was performed at room temperature to introduce a second amine residue that will constitute the lipophilic part of the vector. Three different amines were used to introduce the hydrophobic domain: octadecylamine, oleylamine and compound **4**, based on cholesterol. The choice of these amines was based on Prof. Lehn previous considerations. In the last ten years his group thoroughly studied the impact of the lipidic chain on the carrying capacity of AG-based CLs. According to their results, the higher value of transfection efficiency were obtained in the presence of cholesterol and saturated or unsaturated C18 chains.[17,18,21]
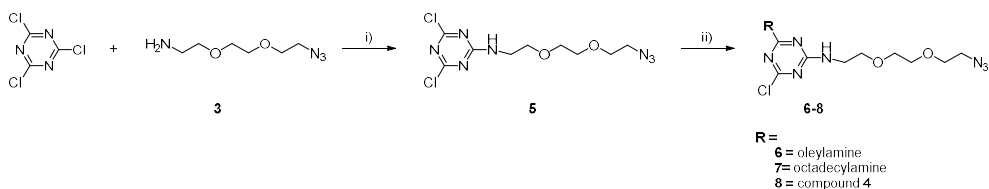
***Fig. 22 Synthetic pathway****: To subsequently substitute two chlorine with amine moieties. i) NaHCO₃, 0°C, H₂O-acetone ii) R-NH₂, NaHCO₃, rt, H₂O-acetone.*

In order to obtain compound **4** we started from cholesterol exploiting as site of modification the hydroxyl group. Cholesterol was allowed to react with CDI and subsequently with 1,4 diaminobutane (Fig. 23). The final compound bore a biodegradable carbamate group that was demonstrated to lower the cytotoxicity of the CLs, if compared with chemically stable ether.[22] Moreover it promotes cellular uptake.[23]
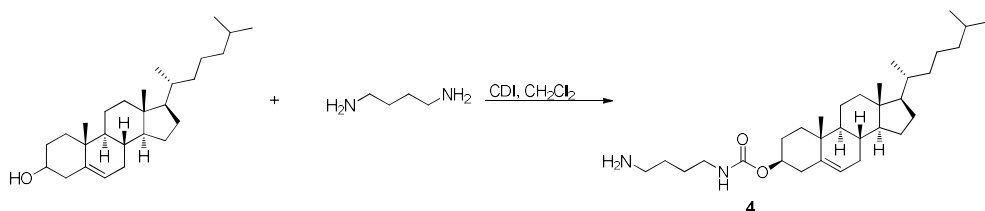


***Fig. 23 Modification of cholesterol****: Cholesterol was first treated with CDI and then with 1,4 diaminobutane in order to obtain a NH₂ terminal derivative suitable to displace a chlorine in the triazine scaffold.*

On the other hand, neomycin and paromomycin underwent proper functionalization to introduce a terminal alkyne group suitable for click chemistry (Fig. 24). We thus exploited the unique less hindered hydroxyl group for neomycin and the unique amino-methylene function of paromomycin in order to obtain compound **1** and **2** as reported in literature (see chapter III for the complete synthetic pathways).[14,24]
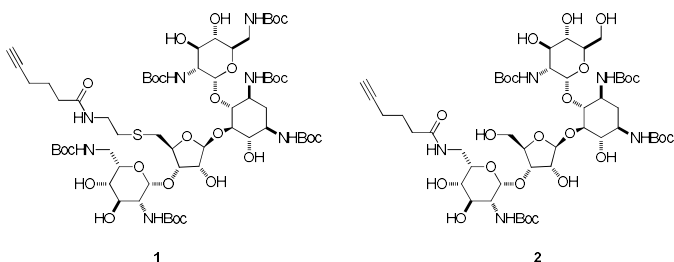


***Fig. 24 Modified AGs:*** *Neomycin 1) and paromomycin 2) were modified by introducing a terminal alkyne suitable for click chemistry.*

The AG-based CLs were obtained by exploiting a click reaction between the azido group of the linker introduced in the first substitution and the terminal alkyne of the AGs (Fig. 25). After treating with TFA, the compounds were characterized through NMR and mass spectroscopy.
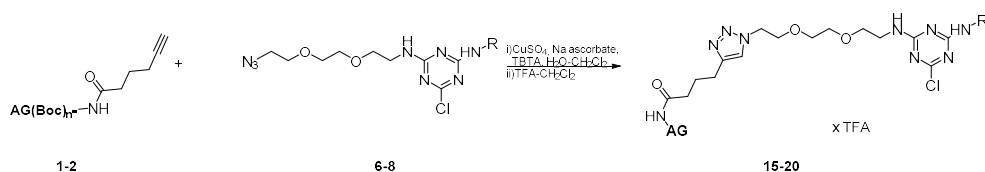


**Fig. 25 Final steps:** *The AG-derivatives were obtained by exploiting a click reaction between the AGs and the azido group of the linker. After treatment with TFA we obtained the AGs-based CLs.*

In total, we obtained six (Fig. 26 and 27) derivatives: three for each AG as polar head and oleyl or stearyl or cholesterol as lipophilic moiety.
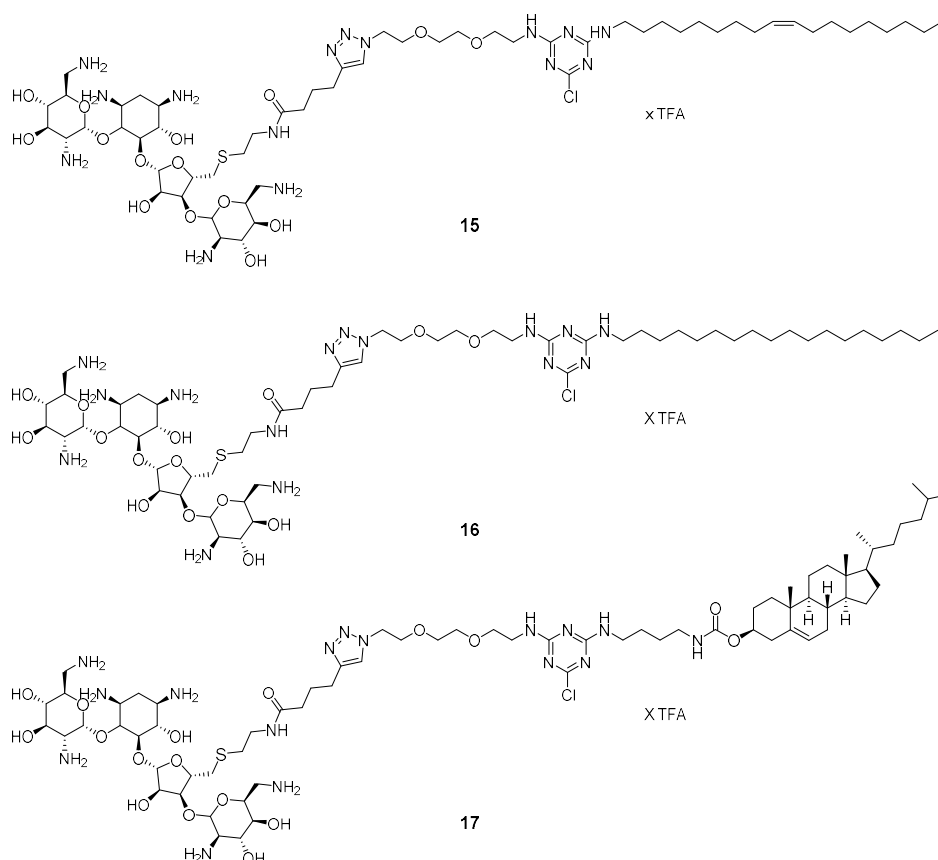


**Fig. 26 Single-tailed conjugates:** *Neomycin (15-17) in combination with three different lipophilic moieties.*
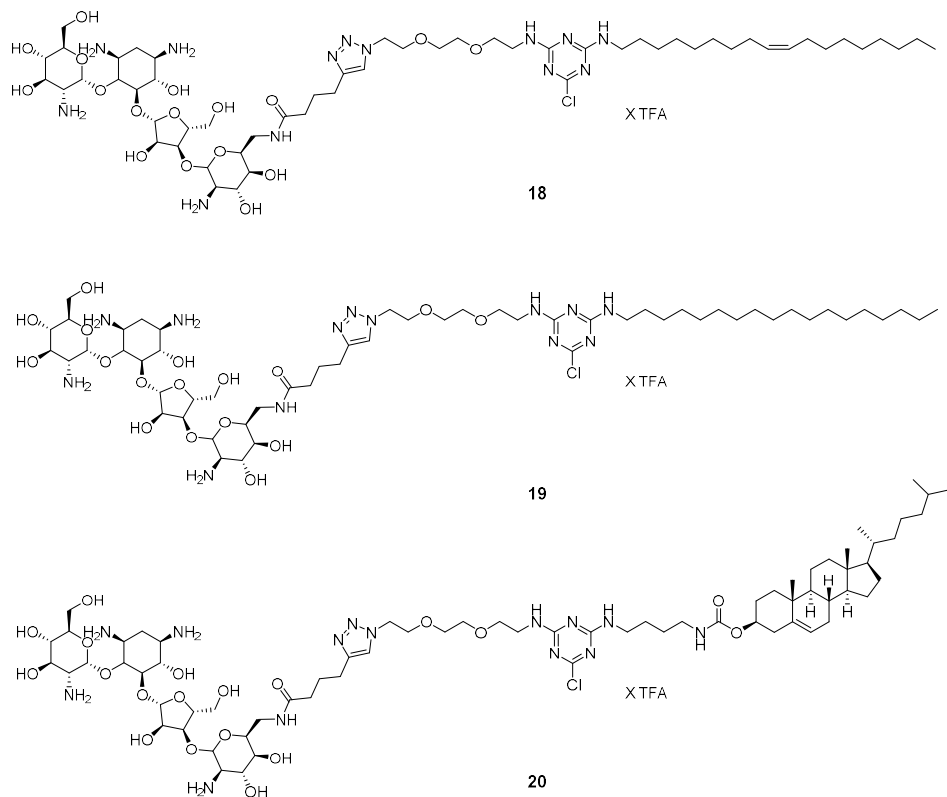
**Fig. 27 Single-tailed conjugates:** *Paromomycin (18-20) in combination with three different lipophilic moieties.*

### 2.3.3 Preliminary biological assays

This first panel of CLs were characterized in biological assays in order to evaluate their effectiveness as transfectants. bPEI was chosen as reference since it is considered the gold standard among transfectants.[25]

Each derivative was tested at N/P 10 and 40 in HeLa cells to obtain a screening of their cytotoxicity and transfection activity (Fig. 28). Some preliminary conclusion can be drawn. As depicted in Fig. 28 the compounds were largely ineffective in this cell line at N/P 10. However, PEI itself did not show significant transfection efficiency at this N/P.

An improvement in the transfection efficiency values can be observed at N/P 40. Despite the derivatives still displayed a lower value of transfection efficiency if compared to bPEI three derivatives displayed enhanced transfection activity. It is worth noting that compounds **17** (Neo-chol) and **20** (Paro-chol) were among the more effective vectors. Above all, the most efficient derivative was proven to be compound **19** (Paro-stearyl).

The viability tests evidenced that all compounds have low cytotoxicity in this cell line. Cells invariably showed a viability higher than 70%, that is considered the toxicity limit.

Overall, this screening highlighted the low cytotoxicity of the CLs. Nevertheless, there are still areas of improvement concerning the transfection activity. Moreover, all these derivatives bear a single chain that can be somehow insufficient to balance their hydrophilic area. It was demonstrated, in fact, that a larger lipophilic area with respect to the head group can promote transfection efficiency. In this case the CLs tend to adopt an inverted hexagonal phase, that has a pivotal role in the transfection of genes and oligonucleotides, because it favours the fusion of the complexes and the release of the NA.[26]
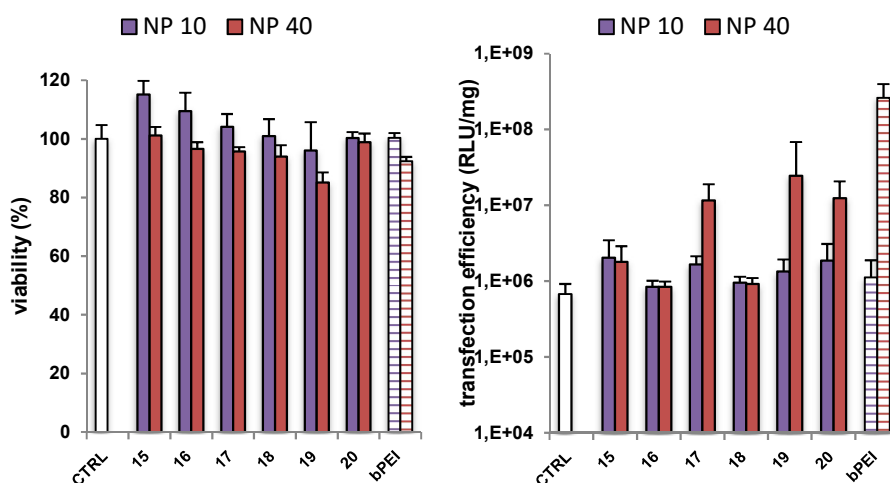


**Fig. 28** *Viability and transfection efficiency of single-tailed derivatives in HeLa cells.*

## 2.3.4 Synthesis of double-tailed derivatives

Transfection efficiency depends on the combination of the polar head and the lipophilic chain. This means that these elements are not determinant of the transfection activity by their own.[27] In general, few examples are reported in which single-tailed CLs are efficient transfection agents.[28,29] It was reported by Cameron and coworkers that CLs with two lipophilic chains not only give higher level of transfection efficiency, but also display a good level of viability.[30]

Bearing this in mind, we hypothesize that the transfection activity of our triazine-based CLs could be enhanced by introducing a second lipophilic moiety. A second set of compounds was then synthesized introducing two lipophilic chains.

The first two steps were analogues to those reported above, but a third amine was introduced by displacing the third chloride heating up to 80°C to introduce a second lipophilic derivative (Fig. 29). The tri-substituted-triazine were obtained with 45-60% yields depending on the amine used.
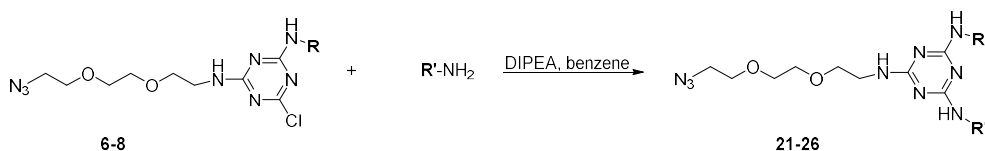


**Fig. 29 Synthesis of the tri-substituted-triazine**: *The last chlorine was displaced by using different amines.*

Then, the final conjugation with the AG was obtained again by using click chemistry with neomycin as polar head (Fig. 30). Unfortunately, it was not possible to obtain the corresponding compounds with paromomycin. In fact, the final click was ineffective probably due to steric factors. Paromomycin **2** was prepared by directly coupling the amine group of the AG with 5-hexynoic acid, meanwhile neomycin has a longer spacer due to intermediate steps in the synthesis.
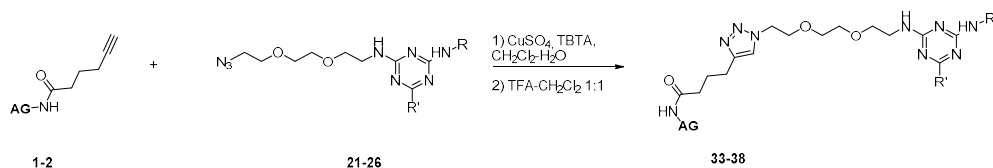


**Fig. 30 Final coupling with the aminoglycoside-alkyne followed by amines deprotection**. *i) CuSO$_4$, TBTA, CH$_2$Cl$_2$-H$_2$O ii) TFA-CH$_2$Cl$_2$.*

All the combinations of the various lipophilic chains were explored. This means that three derivatives with homo- chains (double oleyl, double stearyl and double chol) were synthesized (Fig. 31).
We also obtained three derivatives with asymmetric hydrophobic domain (Fig. 32). It is reported that the activities of the asymmetric CLs are usually superior if compared with symmetric-tailed derivatives.[31] It was shown that the presence of two different chains lead to an up to 10-folds increase in transfection efficiency, probably due to a balance between the rigidity and fluidity of the layer[32] or either to a higher fusogenic capacity gained from an asymmetric structure.[31] Biological tests on these second set of derivatives are still ongoing.
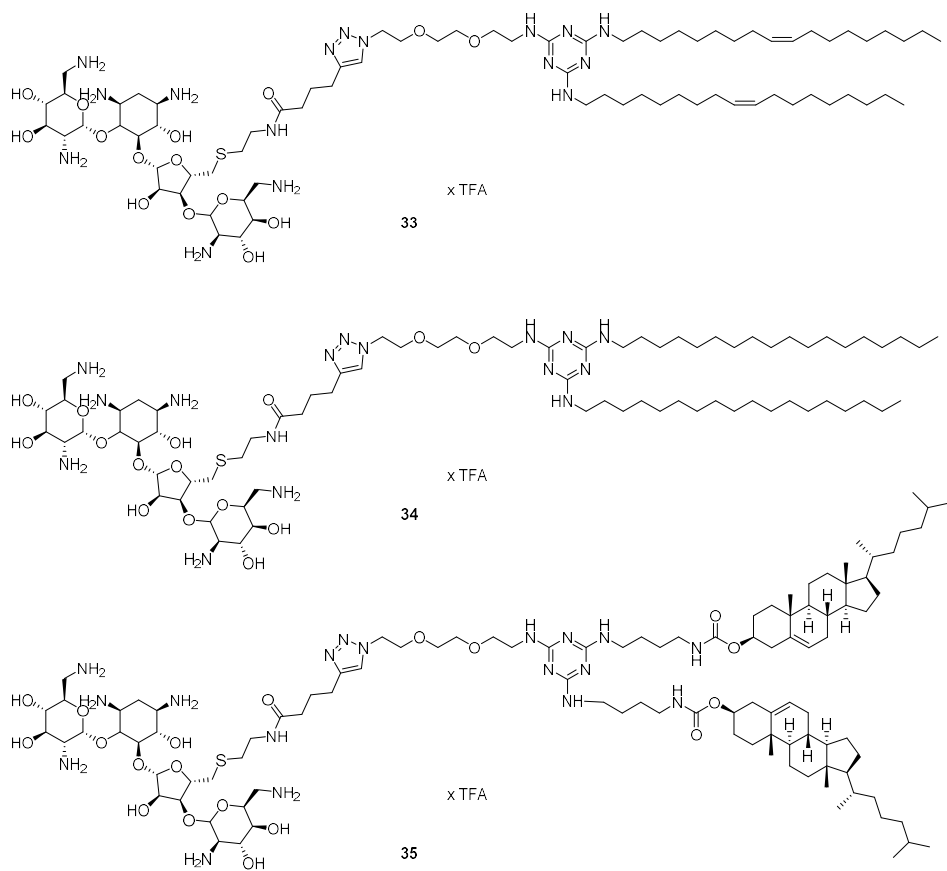
**Fig. 31 Double-tailed derivatives:** *CLs obtained by combining neomycin with a homo-combination of C18, oleyl and cholesterol as lipophilic domain.*
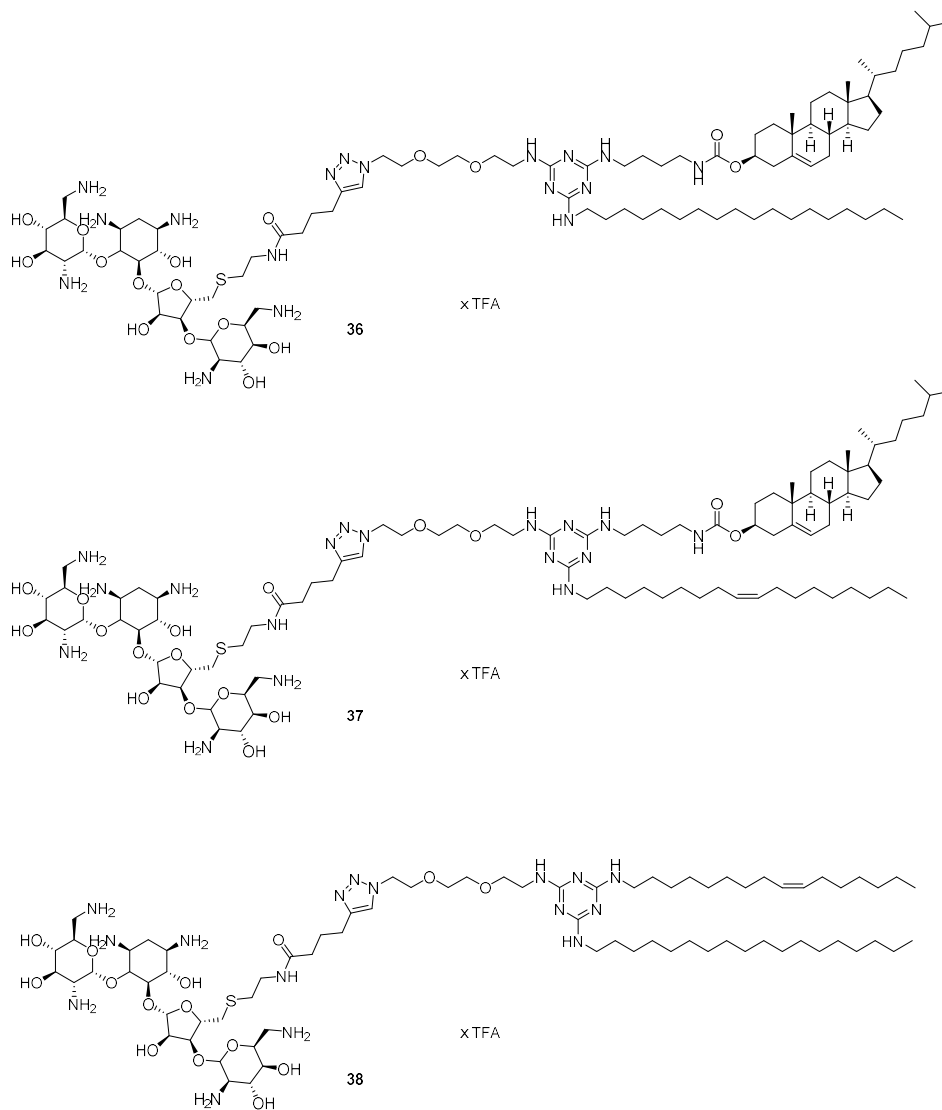
**Fig. 32 Double-tailed derivatives**: *CLs obtained by combining neomycin with a hetero-combination of C18, oleyl and cholesterol as lipophilic domain.*

## 2.4 Conclusion

We have developed amphiphilic molecules with a triazine core for gene delivery purposes. This library of compounds includes two set of conjugates. In the first set, which is composed of six compounds, the polar head is constituted by two different AGs, namely neomycin and paromomycin. The AGs are linked through a spacer to

the triazine core which is connected, in turn, to different lipophilic moieties, namely oleyl, stearyl and cholesterol.

These derivatives underwent preliminary biological tests with the purpose of studying their cytotoxicity and transfection efficiency. All the compounds showed low cytotoxicity in HeLa cell. Although they were found to be inefficient at N/P 10, there was an improvement in their transfection activity at N/P 40. Neo-chol **17**, Paro-chol **20** and Paro-oleyl **18** showed the best transfection activity. We then hypothesized that the transfection efficiency could be enhanced by enlarging the lipophilic moiety. We explored the synthesis of CLs with neomycin and paromomycin combined with a larger lipophilic moiety. However, it was not possible to obtain derivatives based on paromomycin probably because of steric hinderance. We thus synthesized a second set of derivatives bearing a neomycin as polar head. Six derivatives were obtained by exploiting all the combination between oleyl, cholesterol and stearyl as lipid domain. These derivatives are currently undergoing biological testing.

# 2.5 Future perspectives

An essential requirement for an efficient gene vector is its ability to strongly and rapidly bind to NAs.[33] In order to assess whether the synthesized compounds have efficient complexation abilities with NAs, further tests will be performed. Their binding properties will be studied at different N/P to determine the minimum amounts of CLs needed to efficiently complex NAs.

On the other hand, the release of the NAs from lipoplexes is equally important to achieve an efficient gene expression.[34] In this sense, their release capacity is going to be subsequently tested with further experiments. The information on the binding-releasing NAs properties of the compounds will give us more precise indications on which N/P is more convenient for further transfection experiments.

Once determined the ideal N/Ps to be used according to their binding-releasing properties, the compounds will undergo further cytotoxicity and transfection efficiency assays on different cell lines. The physico-chemical properties of lipoplexes will be determined, this means that sizes and charges of the CLs-plasmid complexes will be measured. This characterization will help us to elucidate whether there is a correlation between the physico-chemical properties of the assemblies and the transfection efficiency.[35,36]

Finally, considering that AGs have inherent antibacterial activity against Gram-negative bacteria[37] and the triazine[1] scaffold itself displays bactericidal properties, it will be interesting to probe the antibacterial activity of this panel of compounds.

## 2.6 Supporting information

**Compound 1** was obtained according to literature from commercial neomycin.[24]

**Compound 2** was obtained according to literature from commercial paromomycin.[14]

**Compound 3** was synthesized according to literature.[38]

**Compound 4:** Cholesterol (420 mg, 1 mmol) was dissolved in 50 mL of $CH_2Cl_2$, then CDI (529 mg, 3 mmol) was added. The reaction mixture was stirred 3 hrs at rt. Then it was cooled to 0°C and 1,4-diaminobutane (264 mg, 3 mmol) was added to the mixture. After reaching rt the reaction was stirred 1 hr. The crude was washed with $H_2O$ and brine, dried over $Na_2SO_4$ and concentrated. The product was used without further purifications. Yield 30% in two steps. ^{1}H NMR (400 MHz, $CDCl_3$) δ 5.33 (s, 1H), 4.98 (s, 1H), 3.13 (b, 2H), 2.69 (b, 2H), 2.30 (m, 2H), 2.01-1.80 (m, 10H), 1.47 (m, 11H), 1.09-0.84 (m, 21H), 0.64 (s, 3H). ^{13}C NMR (101 MHz, $CDCl_3$) δ 156.35, 139.97, 122.53, 74.28, 56.80, 56.26, 50.13, 43.41, 42.42, 41.75, 40.82, 39.85, 39.62, 38.71, 37.11, 36.66, 36.29, 35.89, 31.99, 30.66, 28.93, 28.32, 28.09, 27.54, 24.38, 23.94, 22.90, 22.65, 21.15, 19.43, 18.82, 11.95. Calcuated for $C_{32}H_{56}N_2O_2$ 500.43 Found ESI *m/z* 501.7 $[M+H^+]^+$
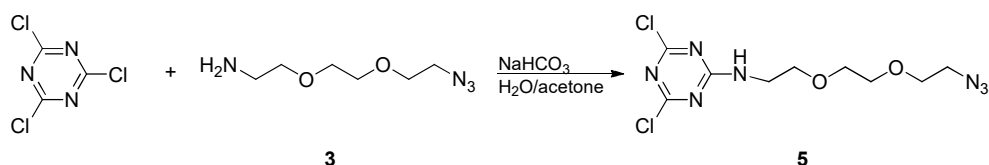


**Compound 5:** Cyanuric chloride (500 mg, 2.7 mmol) was dissolved in 20 mL of a 1:1 (v/v) mixture of $H_2O$/acetone and cooled in an ice bath. Compound **3** (472 mg, 2.7 mmol) was dissolved in the minimum amount of acetone and added dropwise. $NaHCO_3$ (228 mg, 2.7 mmol) was added to the reaction mixture that was stirred at 0°C for 3 hrs. The solvents were evaporated under reduced pressure, then the crude product was dissolved in 20 mL of ethyl acetate and washed with a 1M aqueous solution of HCl (2 x 10 mL), a saturated aqueous solution of $NaHCO_3$ (2 x 10 mL) and brine (2 x 10 mL), dried over $Na_2SO_4$ and concentrated. Flash column chromatography (FCC) of the residue (Hexane-Ethyl acetate 8:2) afforded the desired product as colorless oil in 80% yield. ^{1}H NMR (400 MHz, $CDCl_3$) δ 3.70-3.64 (m, 10H), 3.45 (t, J= 5 Hz, H=2). ^{13}C NMR (101 MHz, $CDCl_3$) δ 170.94, 170.03, 165.90, 70.74, 70.57, 70.24, 69.10, 50.72, 41.39. Calcuated for $C_9H_{13}Cl_2N_7O_2$ 321.05 Found ESI *m/z* 344,0 $[M+Na^+]^+$.
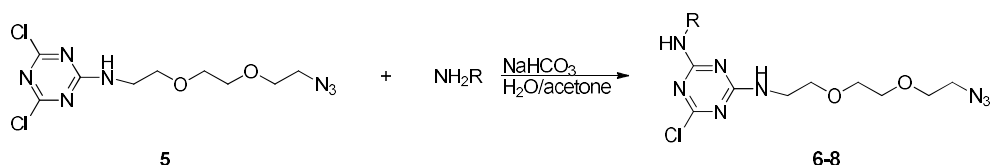
**General procedure for compounds 6-8: 5** (600 mg 1.9 mmol) was dissolved in 15 mL of a 1:1 (v/v) mixture of $H_2O$/acetone. **R-NH$_2$** (2.8 mmol) and NaHCO$_3$ (235 mg, 2.8 mmol) were added to the reaction mixture that was stirred overnight at rt. The volatiles were removed under reduced pressure. The residue was dissolved in $CH_2Cl_2$ and washed with a 1M aqueous solution of HCl (2 x 10 mL) a saturated aqueous solution of NaHCO$_3$. (2 x 10 mL) and brine (2 x 10 mL), dried over $Na_2SO_4$ and concentrated. FCC of the residue (Hexane-Ethyl acetate 7:3) afforded the desired products.
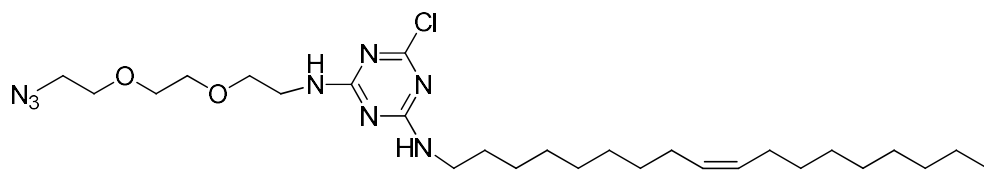


**Compound 6: R-NH$_2$= oleylamine**, white solid in 70% yield. ^{1}H NMR (400 MHz, CDCl$_3$) δ 5.34 (m, 2H), 3.67 (m, 10H), 3.42 (m, 4H), 2.00 (m, 4H), 1.56 (m, 2H), 1.29 (m, 22H), 0.88 (t, J= 7,04 Hz, 3H). ^{13}C NMR (101 MHz, CDCl$_3$) δ 168.30, 165.74, 130.10, 129.86, 70.81, 70.66, 70.28, 69.68, 50.79, 41.07, 40.84, 32.71, 32.01, 29.84, 29.62, 29.42, 27.33, 26.94, 22.78, 14.20. Calcuated for $C_{27}H_{49}ClN_8O_2$ 552.37 Found ESI *m/z* 575,3 [M+Na$^+$]$^+$
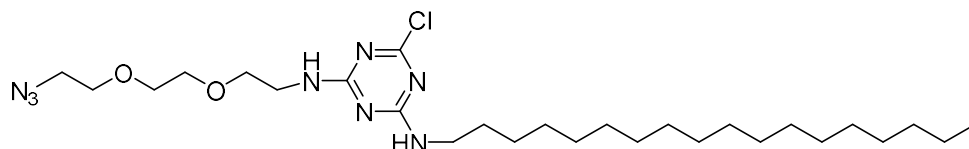


**Compound 7: R-NH$_2$= octadecylamine**, white solid, 70% yield. ^{1}H NMR (400 MHz, CDCl$_3$) δ 3.64 (m, 10H), 3.41 (m, 4H), 1.54 (m, 2H), 1.25 (m, 30H), 0.88 (t, J= 7 Hz, 3H). ^{13}C NMR (101 MHz, CDCl$_3$) δ 168.33, 165.77, 70.84, 70.69, 70.30, 50.81, 41.10, 40.89, 32.07, 29.84, 29.80, 29.69, 29.50, 29.43, 26.96, 22.83, 14.24. Calculated for $C_{27}H_{51}ClN_8O_2$ 554.38 Found ESI *m/z* 577,3 [M+Na$^+$]$^+$
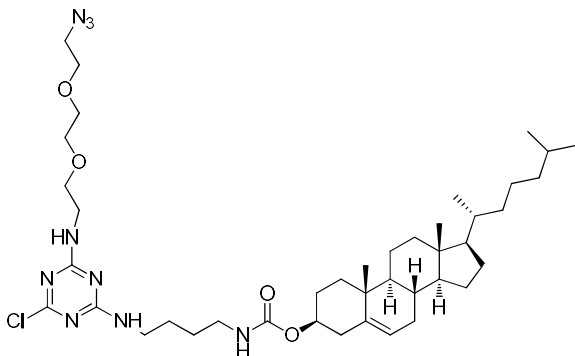
**Compound 8: R-NH₂= compound 4** white solid, 70% yield. $^1$H NMR (400 MHz, CDCl$_3$) δ 5.35 (d, J= 5 Hz, 1H)), 4.47 (br, 1H), 3.64 (m, 10H), 3.39 (m, 4H), 3.17(br, 2H) , 2.32 (m, 2H), 1.97 (m, 2H), 1.84 (m, 3H), 1.66 -0.83 (m, 37H), 0.66 (s, 3H). Calculated for C$_{41}$H$_{68}$ClN$_9$O$_4$ 785.51 Found ESI *m/z* 808,8 [M+Na$^+$]$^+$
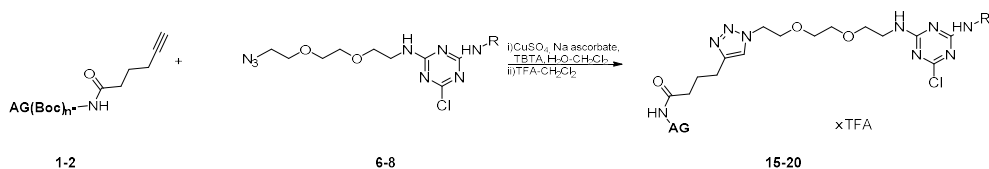


**General procedure 15-20**: Compound **1** or **2** (1eq) were dissolved in CH$_2$Cl$_2$ then compound **6-8** (1.5 eq) were added to the reaction mixture. CuSO$_4$ (0.1eq), Na ascorbate (0.1 eq) and TBTA (0.01 eq) in few drops of water were added to the reaction mixture that was allowed to stir 15 hrs at rt. After evaporating the solvents, the crude was dissolved in EtOAc and washed with a solution of 5% EDTA and brine. FCC (MeOH in CH$_2$Cl$_2$ 0-5%) afforded compounds **9-14.** Then the derivatives were treated with a mixture of TFA:CH$_2$Cl$_2$ 1:1 for 2 hrs. After freeze drying **15-20** were obtained as fluffy solids.
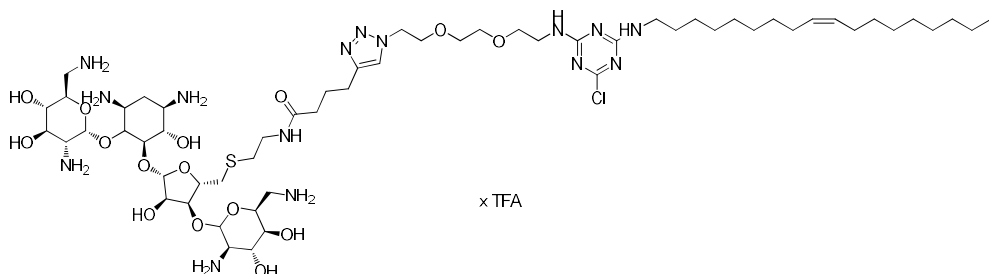
**Compound 9:** ¹H NMR (400 MHz, CD₃OD) δ 7.80 (s, 1H), 5.34 (m, 3H), 5.15 (d, J=2,28 Hz,1H), 4.93 (s, 1H), 4.54 (t, J=5 Hz, 2H), 4.24 (br, 2H), 4.11(m, 1H), 3.90 (m, 4H), 3.77 (m, 2H), 3.65-3.35 (m, 25H), 2.90 (d, J=5,48 Hz, 2H), 2.78-2.71 (m, 4H), 2.28 (t, J=7,36 Hz, 2H), 2.04-1.95 (m, 7H), 1.57 (m, 3H), 1.50-1.40 (m, 54H), 1.32-1.24 (m, 22H), 0.90 (t, J=6,64 Hz, 3H). ESI *m/z* 1944,5 [M+Na⁺]⁺  **Compound 15:** yellowish solid, 35% yield in 2 steps. ¹H NMR (400 MHz, CD₃OD) δ 7.81 (s,1H), 6.05 (d, J=6.2 Hz, 1H), 5.41-5.38 (m, 2H), 5.34 (m, 2H), 4.55 (t, J=4.8Hz, 2H), 4.33 (m, 2H), 4.16 (m, 1H), 3.89 (m, 4H), 3.70 (b, 2H), 3.62-3.35 (m, 25H), 2.72 (m, 6H) 2.28 (t, J=7.2Hz, 2H), 2.03-1.95 (m, 7H), 1.61 (m, 3H), 1.28 (m, 22H), 0.89 (t, J=7.2Hz, 3H). ¹³C NMR (101 MHz, CD₃OD) δ 148.18, 130.88, 130.78, 124.17, 112.07, 96.85, 96.36, 87.62, 79.68, 76.91, 75.30, 74.20, 73.21, 72.14, 71.39, 71.18, 70.39, 70.05, 69.58, 69.21, 55.58, 52.97, 51.34, 50.28, 49.64, 49.43, 49.21, 49.00, 48.79, 48.57, 48.36, 42.10, 41.91, 41.68, 38.42, 36.33, 33.57, 33.02, 32.19, 30.79, 30.73, 30.56, 30.40, 30.29, 30.25, 30.17, 28.09, 27.84, 26.77, 25.71, 23.69, 14.40.
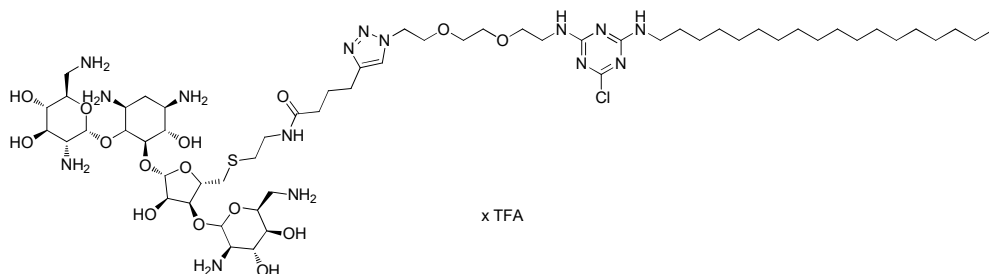


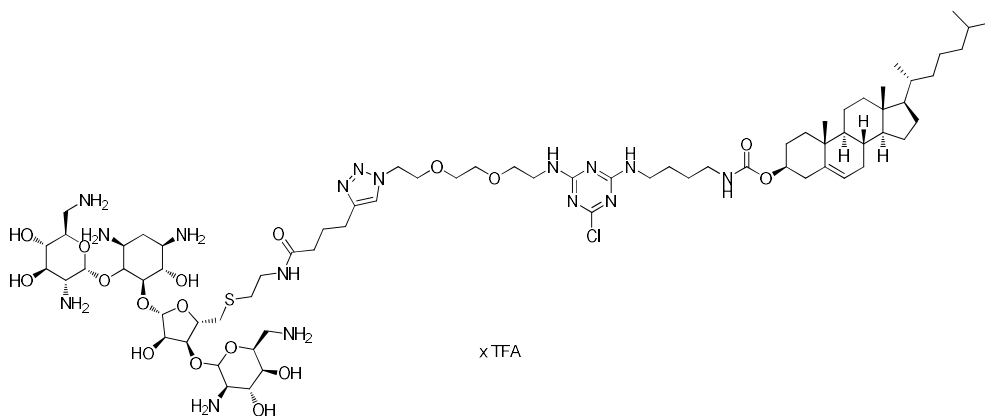**Compound 10:** ¹H NMR (400 MHz, CD₃OD) δ 7.80 (s, 1H), 5.37 (s, 1H), 5.15 (s, 1H), 4.93 (s, 1H), 4.55 (t, J=5Hz, 2H), 4.24 (br, 2H), 4.11 (m, 1H), 3.89 (m, 4H), 3.77 (m, 2H), 3.65-3.35 (m, 25H), 2.90 (d, J=5,5 Hz, 2H) , 2.78-2.71 (m, 4H), 2.29 (7.28 Hz, 2H), 1.97 (m, 3H), 1.64-1.44 (m, 57H), 1.34-1.24 (m, 30H), 0.90 (t, J=6,64, 3H). ESI *m/z* 1946,5 [M+Na⁺]⁺ **Compound 16** white solid, 50% yield in two steps.¹H NMR (400 MHz, CD₃OD) δ 7.83 (s, 1H), 6.06 (d, J=3.72 Hz, 1H), 5.43 (d, J=3,7 Hz, 1H), 5.34 (s, 1H), 4.55 (t, J=4,68 Hz, 2H), 4.44 (t, J= 4,64 Hz, 1H), 4.38-4.31 (m, 3H), 4.20-4.03 (m, 4H), 3.90 (m, 4H), 3.69-3.55 (m, 12H), 3.52-3.35 (m, 12H), 2.73 (, 5H), 2.47 (m, 1H), 2.29 (t, J= 6,92 Hz, 2H), 1.97 (m, 3H), 1.64 (m, 1H), 1.28 (m, 30H), 0.89 (t, 7,36

Hz, 3H). $^{13}$C NMR (101 MHz, CD$_3$OD) δ 175.90, 162.81, 162.48, 158.03, 124.45, 112.03, 96.91, 96.41, 87.51, 82.15, 82.02, 79.69, 76.32, 75.38, 74.14, 73.24, 72.14, 71.37, 70.41, 69.67, 69.38, 69.20, 61.53, 55.53, 52.97, 51.39, 51.19, 50.22, 42.70, 42.49, 41.94, 41.68, 39.56, 36.33, 33.04, 32.13, 30.74, 30.62, 30.43, 30.33, 29.89, 27.79, 23.70, 14.41

.



**Compound 11:**$^1$H NMR (400 MHz, CD$_3$OD) δ 7.80 (s, 1H), 5.38 (m, 2H), 5.15 (s, 1H), 4.93 (s, 1H), 4.55 (s, J=5 Hz, 3H), 3.89 (m, 5H) , 3.77 (m, 3H), 3.61-3.37 (m, 32H), 3.12 (m, 2H), 2.90 (d, J= 4,96 Hz, 1H), 2.75 (m, 4H), 2.30 (m, 3H), 1.97 (m, 5H), 1.86 (m, 2H), 1.60-0.87 (m, 89H), 0.72 (s, 3H). ESI *m/z* 2177,5 [M+Na$^+$]$^+$
**Compound 17:** yellowish solid, 60% yield in two steps. $^1$H NMR (400 MHz, CD$_3$OD) δ 7.85 (d, J=3.2 Hz, 1H), 6.10 (d, J=3.6 Hz, 1H), 5.47 (d, J=4 Hz, 1H), 5.38 (m, 2H), 4.59 (t, J=5.2 Hz, 2H), 4.46 (t, J=4.4 Hz, 1H), 3.93 (m, 2H), 3.69-3.41 (m, 29H), 3.17 (m, 2H), 3.03 (m, 1H), 2.81-2.73 (m, 4H), 2.51 (m, 2H), 2.33 (m, 2H), 2.14 (m, 2H), 1.86 (m, 2H), 1.65-0.86 (m, 46 H), 0.77 (m, 3H). $^{13}$C NMR (101 MHz, CD$_3$OD) δ 175.86, 163.27, 163.20, 162.87, 124.14, 112.02, 96.91, 96.41, 87.53, 82.06, 79.68, 76.33, 75.38, 74.15, 73.23, 72.23, 71.35, 70.42, 69.39, 69.26, 61.49, 58.28, 57.58, 55.54, 52.98, 51.37, 51.18, 50.23, 43.52, 43.42, 42.53, 41.94, 41.69, 40.68, 37.77, 37.36, 37.10, 36.34, 32.97, 32.13, 30.73, 29.52, 29.29, 29.14, 26.78, 25.70, 24.93, 23.18, 22.92, 22.15, 20.84, 19.78, 19.23, 14.45, 12.29.
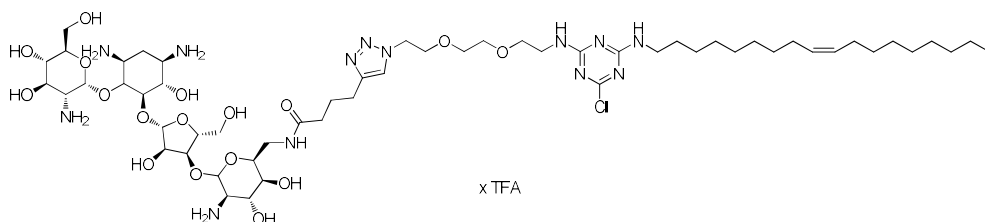
**Compound 12:** $^1$H NMR (400 MHz, CD$_3$OD) δ 7.80 (s, 1H), 5.34 (m, 3H), 5.19 (s, 1H), 4.91 (s, 1H), 4.55 (t, J =5.1Hz, 2H), 4.27 (b, 1H), 4.19 (b, 1H), 4.01-3.43 (m, 33H), 2.73 (t, J=7.48Hz, 2H), 2.29 (t, 2H), 2.08-1.91 (m, 6H), 1.55 (m, 3H), 1.45 (m, 36H), 1.29 (m, 22H), 0.89 (t, =7Hz, 3H). ESI *m/z* 1684,9 [M+Na$^+$]$^+$ **Compound 18:** white solid, 40% yield in 2 steps. $^1$H NMR (400 MHz, CD$_3$OD) δ 7.83 (s, 1H), 5.59 (d, J=3.6Hz, 1H), 5.35 (m, 3H), 5.18 (s, 1H), 4.55 (t, J =4.8Hz, 2H), 4.29 (b, 1H), 4.16 (b, 1H), 4.06-3.34 (m, 33H), 2.75 (b, 2H), 2.47 (m, 1H), 2.32 (m,1H), 2.08-1.76 (m, 6H), 1.64 (m, 3H), 1.29 (m, 22H), 0.89 (t, =6.8 Hz, 3H). $^{13}$C NMR (101 MHz, CD$_3$OD) δ 176.51, 162.70, 158.01, 157.78, 149.07, 130.91, 130.77, 124.24, 111.30, 98.53, 97.32, 85.57, 83.67, 80.81, 77.40, 76.11, 75.60, 74.32, 73.99, 71.79, 71.38, 70.78, 70.42, 69.68, 69.21, 68.29, 62.40, 61.01, 55.77, 53.15, 51.39, 51.24, 50.71, 42.72, 42.50, 40.76, 36.28, 34.70, 33.58, 33.03, 30.81, 30.74, 30.57, 30.50, 30.41, 30.31, 30.26, 30.16, 29.90, 29.78, 28.11, 27.79, 26.67, 26.06, 25.76, 23.70, 14.42.
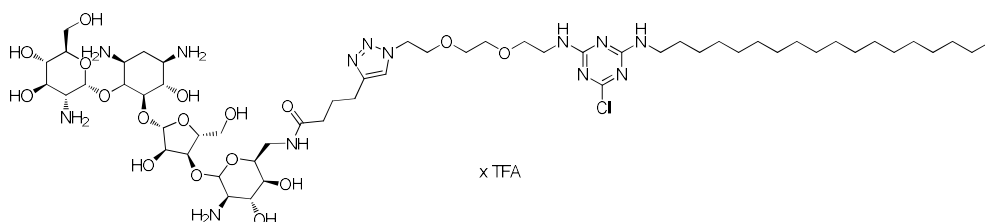


**Compound 13:** $^1$H NMR (400 MHz, CD$_3$OD) δ 7.80 (s, 1H), 5.35 (s, 1H), 5.19 (s, 1H), 4.91 (s, 1H), 4.55 (t, J =5.1Hz, 2H), 4.27 (b, 1H), 4.18 (b, 1H), 4.01-3.43 (m, 31H), 2.73 (t, , J =7.3Hz, 1H), 2.37- 2.21 (m, 4H), 1.97 (m, 2H), 1.81 (m, 1H) 1.57 (b, 3H), 1.45 (m, 36H), 1.29 (m, 30H), 0.90 (t, , J =6.48Hz, 3H ).  ESI *m/z* 1687,2 [M+Na$^+$]$^+$ **Compound 19:** white solid, 35% yield in two steps. $^1$H NMR (400 MHz, CD$_3$OD) δ 7.82 (s,1H), 5.59 (t. J =3.2 Hz, 1H), 5.35 (t, J =2 Hz, 1H), 5.18 (t, 1H), 4.55 (t, J =4.8Hz, 1H), 4.42 (m, 1H), 4.28 (b, 1H), 4.15 (m, 2H), 4.06-3.32 (m, 31H), 2.73 (m, 1H), 2.47 (m, 1H), 2.40-2.21 (m, 4H), 1.98 (m, 1H), 1.84 (m, 2H), 1.62 (m, 1H), 1.28 (m, 30H), 0.90 (t, , J =6.4Hz, 3H). $^{13}$C NMR (101 MHz, CD$_3$OD) δ 176.47, 163.16, 162.82, 111.32, 98.54, 85.59, 80.84, 76.13, 75.67, 74.31, 74.03, 71.79, 71.38, 70.79, 70.39, 69.70, 69.22, 62.40, 55.76, 53.15, 51.38, 51.24, 50.72, 49.64, 49.43, 49.28,

49.21, 49.00, 48.79, 48.57, 48.36, 42.72, 42.49, 36.29, 35.73, 33.05, 30.75, 30.44, 30.34, 29.91, 29.79, 27.80, 25.81, 23.71, 18.66, 14.41.



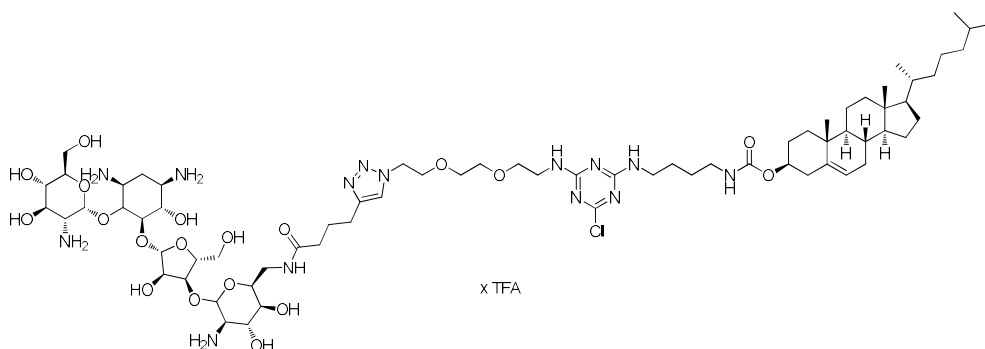**Compound 14:** $^1$H NMR (400 MHz, CD$_3$OD) δ 7.80 (s, 1H), 5.37 (b, 2H), 5.19 (s, 1H), 4.91 (s, 1H), 4.55 (t, 2H), 4.27 (t, 1H), 3.97-3.63 (m, 21H), 3.61-3.44 (m, 16H), 3.11 (b, 2H), 2.73 (t, 2H), 2.35-2.25 (m, 5H), 2.03-1.85 (m, 6H), 1.54-1.38 (m, 48H), 1.15-0.82 (m, 24H), 0.72 (s, 3H). ESI *m/z* 1919,4 [M+Na$^+$]$^+$ **Compound 20:** yellowish solid, 38% yield in two steps. $^1$H NMR (400 MHz, CD$_3$OD) δ 7.84 (s, 1H), 5.59 (s, 1H), 5.36 (b, 2H), 5.18 (s, 1H), 4.56 (b, 1H), 4.42 (b, 1H), 4.16 (b, 2H), 3.99-3.76 (m, 10H), 3.99-3.29 (s, 22H), 3.13 (d, J=5.2 Hz, 2H), 2.74 (b, 2H), 2.50 (m, 2H), 2.31 (s, 2H), 1.99-1.80 (m, 6H), 1.55-0.84 (m, 41H), 0.72(s, 3H). $^{13}$C NMR (101 MHz, CD$_3$OD) δ 176.47, 173.01, 166.86, 162.63, 158.72, 158.01, 141.25, 124.67, 123.42, 117.46, 111.26, 98.48, 97.36, 85.57, 83.67, 80.72, 80.12, 77.47, 76.08, 75.63, 75.49, 74.32, 74.00, 71.77, 71.42, 71.35, 70.77, 70.37, 69.69, 69.17, 68.30, 62.38, 61.53, 60.99, 58.11, 57.56, 55.76, 53.13, 51.61, 51.41, 51.25, 50.71, 43.48, 42.50, 41.68, 41.30, 41.10, 40.76, 40.66, 40.16, 39.69, 38.26, 37.94, 37.72, 37.67, 37.36, 37.09, 36.25, 33.20, 33.00, 30.73, 29.76, 29.29, 29.11, 28.24, 27.11, 26.64, 25.75, 25.29, 24.93, 23.17, 22.93, 22.14, 20.85, 19.77, 19.64, 19.25, 14.44, 12.32.
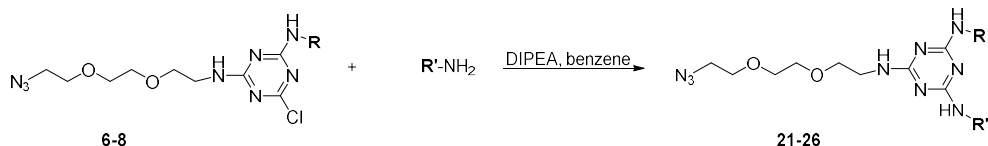
**General procedure for compounds 21-26:** compound **6-8** (1eq) were dissolved in 3 mL of benzene, then DIPEA (1.5 eq) and **R'NH$_2$** (1.5 eq) were added. The reaction was shaken in a sealed vial at 80°C for 2 days. Then the solvent was removed under reduced pressure. The residue was dissolved in CH$_3$Cl and washed with a 1M aqueous solution of HCl, a saturated aqueous solution of NaHCO$_3$ and brine. FCC (hexane:ethyl acetate 1:1) afforded the desired products as powders.
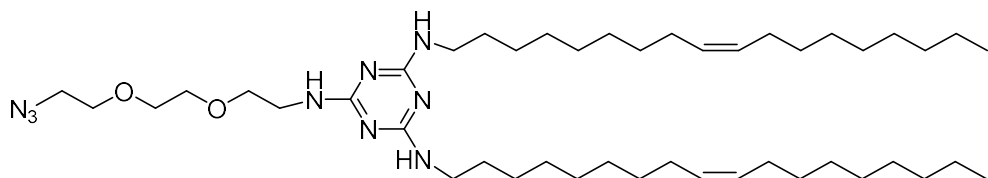


**Compound 21:** white solid. 60% yield. $^1$H NMR (400 MHz, CDCl$_3$) δ 5.34 (m, 4H), 3.68-3.56 (m, 10H), 3.39 (t, J= 4.96 Hz, 2H), 3.33 (d, 4H), 2.02-1.96 (m, 8H), 1.52 (t, 4H), 1.26 (m, 44H), 0.87 (t, J= 6.6 Hz, 6H)**.** Calculated for C$_{45}$H$_{85}$N$_9$O$_2$ 783.68 Found ESI *m/z* 784,9 [M+H$^+$]$^+$
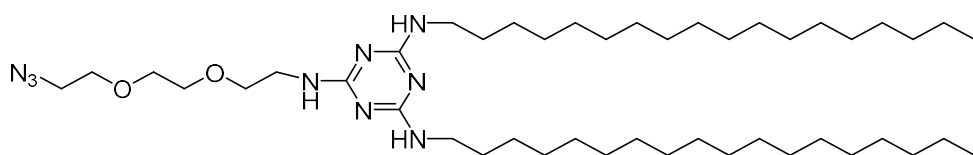


**Compound 22:** yellowish solid, 60% yield.$^1$H NMR (400 MHz, CDCl$_3$) δ 3.71-3.52 (m, 10H), 3.38 (t, J= 5.2 Hz, 2H), 3.31 (m, 4H), 1.52 (m, 4H), 1.24 (m, 60H), 0.87 (t, J= 7 Hz, 6H)**.** Calculated for C$_{45}$H$_{89}$N$_9$O$_2$ 787.71 Found ESI *m/z* 788,6 [M+H$^+$]$^+$
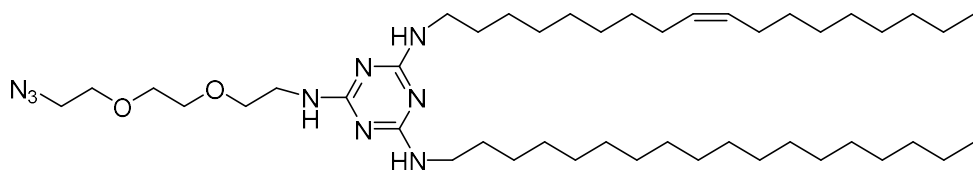


**Compound 23**: white solid, 60% yield. $^1$H NMR (400 MHz, CDCl$_3$) δ 5.33 (m, 2H), 3.69-3.62 (m, 10H), 3.41-3.35 (m. 6H), 2.00 (m, 4H), 1.55 (m, 4H), 1.24 (m, 52H), 0.86 (t, 6H). $^{13}$C NMR (101 MHz, CDCl$_3$) δ 130.08, 129.89, 70.76, 70.56, 70.22, 69.73,

50.81, 41.04, 32.71, 32.03, 29.81, 29.63, 29.57, 29.43, 27.33, 26.97, 22.79.)**.** Calculated for $C_{45}H_{87}N_9O_2$ 785.70 Found ESI *m/z* 787,1 [M+H⁺]⁺.
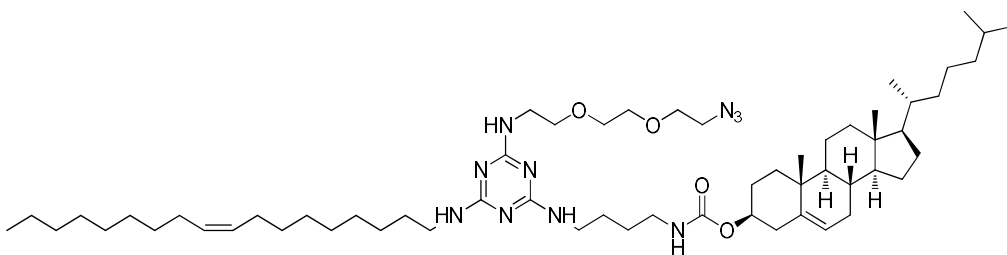


**Compound 24**: white solid, 55% yield. ¹H NMR (400 MHz, CDCl₃) δ 5.34 (m, 3H), 4.48 (b, 1H), 3.69-3.59 (m, 10H), 3.41-3.34 (m, 6H), 3.19 (m, 2H), 2.43-2.11 (m, 2H), 2.03-1.93 (m, 6H), 1.89-1.78 (m, 3H), 1.59-0.79 (m, 64H), 0.67 (s, 3H).¹³C NMR (101 MHz, CDCl₃) δ 156.33, 139.99, 130.09, 129.91, 128.63, 127.67, 127.15, 122.58, 74.40, 70.78, 70.55, 70.22, 69.89, 65.25, 56.83, 56.29, 50.82, 50.17, 42.45, 41.00, 40.75, 39.88, 39.65, 38.74, 37.15, 36.70, 36.32, 35.92, 32.73, 32.02, 29.89, 29.83, 29.78, 29.64, 29.61, 29.44, 29.31, 29.10, 28.35, 28.13, 27.34, 27.04, 24.41, 23.96, 22.93, 22.80, 22.67, 21.18, 19.46, 18.84, 14.22, 11.98. )**.** Calculated for $C_{59}H_{104}N_{10}O_4$ 1016.82 Found ESI *m/z* 1018.1 [M+H⁺]⁺.
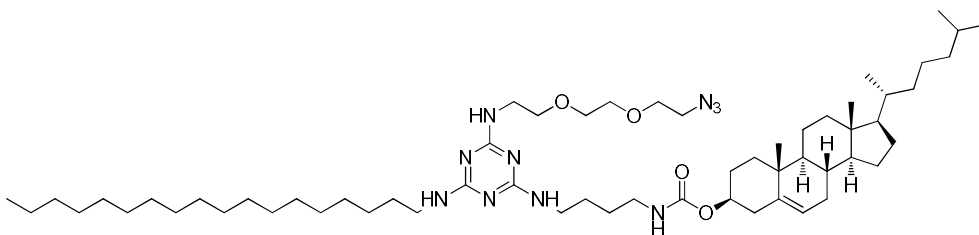


**Compound 25**: white solid, 50% yield. ¹H NMR (500 MHz, CDCl₃) δ 5.37 (s, 1H), 4.49 (bs, 1H), 3.72-3.55 (m, 10H), 3.44-3.29 (m, 6H), 3.21 (m, 2H), 2.40-2.21 (m, 2H), 2.05-1.92 (m, 2H), 1.91-1.78 (m, 3H), 1.65-0.83 (m, 72H), 0.68 (s, 3H). )**.** Calculated for $C_{59}H_{106}N_{10}O_4$ 1018.84 Found ESI *m/z* 1020.0 [M+H⁺]⁺.
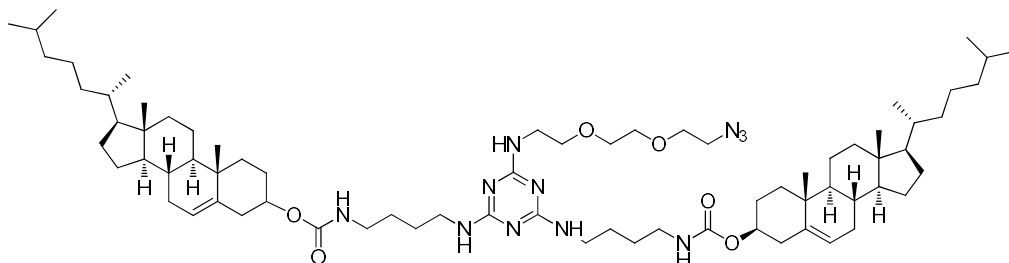
**Compound 26**: white solid, 45% yield. $^1$H NMR (400 MHz, CDCl$_3$) δ 5.36, 4.48, 3.70, 3.51, 3.44, 3.38, 3.20, 3.13, 2.42, 2.19, 2.05, 1.76, 1.59, 0.82, 0.67. $^{13}$C NMR (101 MHz, CDCl$_3$) δ 156.36, 148.60, 139.99, 129.95, 122.60, 74.39, 70.78, 70.56, 70.22, 69.90, 56.84, 56.32, 50.83, 50.16, 42.46, 40.75, 39.89, 39.65, 38.77, 37.15, 36.71, 36.33, 35.93, 32.03, 29.90, 29.65, 29.44, 28.36, 28.13, 27.35, 24.42, 23.99, 22.94, 22.80, 22.69, 21.19, 19.48, 18.85, 14.23, 12.00. ). Calculated for C$_{73}$H$_{123}$N$_{11}$O$_6$ 1249.97 Found ESI *m/z* 1251.0 [M+H$^+$]$^+$.
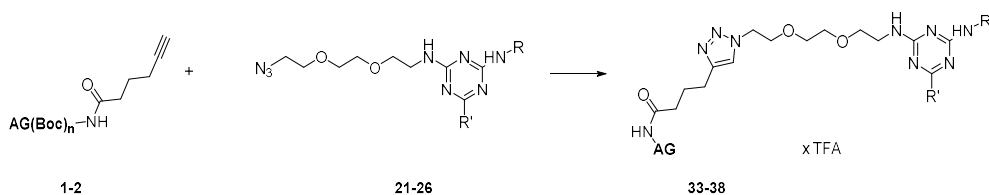


**General procedure 33-38**: Compound **1** (1eq) was dissolved in CH$_2$Cl$_2$ then compound **21-26** (1.5 eq) were added to the reaction mixture. CuSO$_4$ (0.1eq), Na ascorbate (0.1 eq) and TBTA (0.01 eq) in few drops of water were added to the reaction mixture that was allowed to stir 15 hrs at rt. After evaporating the volatiles, the crude was dissolved in EtOAc and washed with a solution of 5% EDTA and brine. FCC (MeOH in CH$_2$Cl$_2$ 0-5%) afforded compounds **27-32.** Then the derivatives were treated with a mixture of TFA:CH$_2$Cl$_2$ 1:1 for 2 hrs. After freeze drying **33-38** were obtained as fluffy solids.
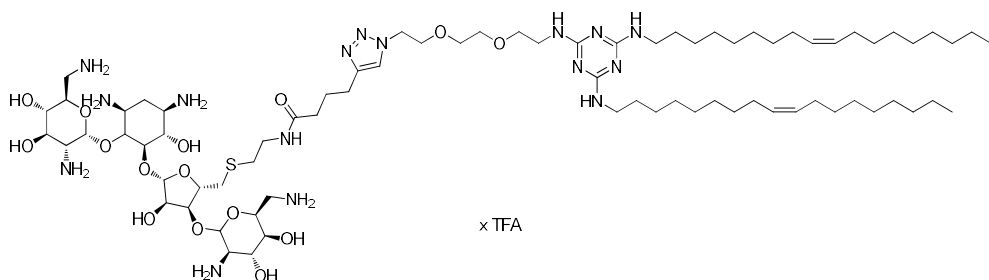
**Compound 27:** $^1$H NMR (400 MHz, CD$_3$OD) δ 7.80 (s, 1H), 5.41-5.32 (m, 5H), 5.15 (s, 1H), 4.93 (s, 1H), 4.54 (t, 2H), 4.24 (b, 2H), 4.11 (m, 1H), 3.91-3.87 (m, 4H), 3.78-3.71 (m, 2H), 3.65-3.36 (m, 27H), 2.88 (d, 2H), 2.77-2.70 (m, 4H), 2.27 (t, 2H), 2.04-1.95 (m, 11H), 1.56 (m, 5H), 1.46 (m, 54H), 1.32(m, 44H) 0.90 (t, 6H). ESI *m/z* 2153,4 [M+H$^+$]$^+$. **Compound 33:** white solid, 20% yield in two steps. $^1$H NMR (400 MHz, CD$_3$OD) δ 7.79 (s, 1H), 6.07 (d, J= 4Hz, 1H), 5.42 (d, J=3.6 Hz, 1H), 5.34 (m, 4H), 5.09 (q, J=6.4Hz, 1H), 4.54 (b, 2H), 4.38 (m, 2H), 4.16 (m, 1H), 3.89-3.87 (m, 4H), 3.67-3.34 (m, 29H), 2.73 (m, 5H), 2.47 (m, 1H), 2.28 (t, J=7.6Hz, 2H), 2.15-1.92 (m, 8H), 1.68 (m, 4H), 1.61 (m, 4H), 1.32 (m, 44H), 0.90 (t, J=6.4Hz, 6H). $^{13}$C NMR (101 MHz, CD$_3$OD) δ 175.80, 163.30, 162.96, 148.31, 130.82, 130.66, 124.09, 112.04, 96.92, 96.36, 87.50, 81.87, 81.31, 79.68, 76.37, 75.35, 74.16, 73.27, 72.17, 71.35, 70.32, 70.07, 69.39, 69.23, 55.49, 52.98, 51.33, 50.22, 41.67, 39.60, 36.32, 35.66, 34.69, 33.06, 32.94, 32.13, 30.75, 30.45, 30.28, 27.96, 26.79, 26.07, 25.72, 23.72, 14.43.
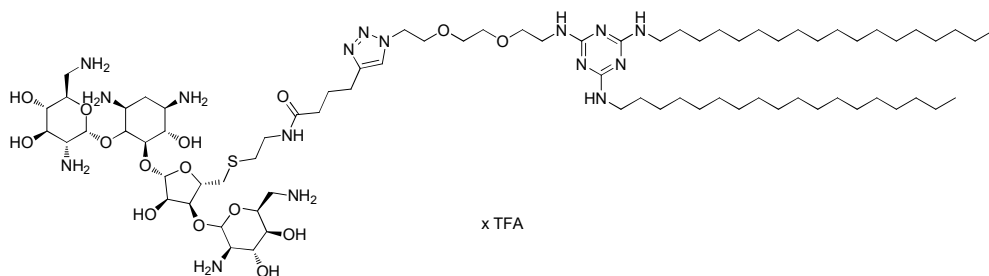


**Compound 28:** $^1$H NMR (500 MHz, CD$_3$OD) δ 7.79 (s, 1H), 5.36 (s, 1H), 5.15 (s, 1H), 4.81 (s, 1H), 4.54 (t, 2H), 4.23 (m, 2H), 4.10 (m, 1H), 3.92-3.87 (m, 4H), 3.78-3.72 (m, 2H), 3.68-3.37 (m, 27H), 2.89 (d, 2H), 2.79-2.69 (m, 4H), 2.27 (t, 2H), 1.97 (m, 3H), 1.56 (b, 5H), 1.45(m, 54H), 1.33-1.29 (m, 60H), 0.90 (t, J=5.7Hz, 6H). ESI *m/z* 2157,4 [M+H$^+$]$^+$ **Compound 34:** white solid, 55% yield in two steps. $^1$H NMR (400 MHz, CD$_3$OD) δ 7.79 (s, 1H), 6.06 (d, J=4 Hz, 1H), 5.43 (d, J= 3.6 Hz, 1H), 5.34 (s, 1H), 4.54 (m, 2H), 4.39-4.28 (m, 2H), 4.16 (t, J=3.2 Hz, 1H), 3.89 (m, 4H), 3.69-3.54 (m, 13H), 3.48-3.33 (m, 16H), 3.31 (m, 2H), 2.73 (m, 4H), 2.29 (t, J= 7.6 Hz, 2H), 1.97 (m, 3H), 1.60 (b, 5H), 1.29 (m, 60H), 0.90 (t, J= 6.8Hz, 6H).
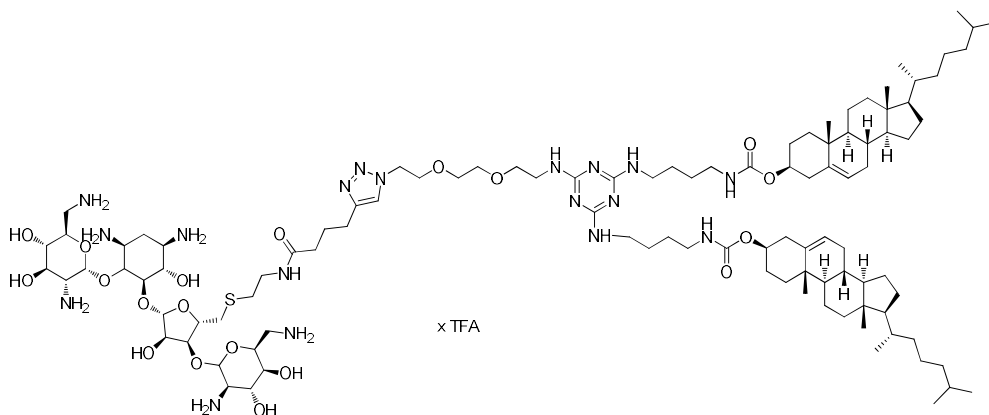
**Compound 29:** ^{1}H NMR (400 MHz, CDCl$_3$) δ 7.63 (s,1H), 6.13 (s, 1H)), 5.86 (s, 1H), 5.62 (s, 1H), 5.36(d, 2H), 4.54 (m, 4H), 3.94 (m, 5H), 3.64-3.18 (m, 41H), 2.96 (b, 1H), 2.72 (b, 4H), 2.39-2.22 (m, 5H), 2.03-1.94 (m, 5H), 1.85-1.80 (m, 4H), 1.56-0.85 (m, 129H), 0.67 (s, 6H)·**Compound 35:** yellowish solid, 55% yield in two steps. ^{1}H NMR (500 MHz, CD$_3$OD) δ 7.80 (s, 1H), 6.09 (s, 1H), 5.42 (s, 1H), 5.37(d, 2H), 5.34(s, 1H), 4.54 (m, 3H), 4.44 (t, 1H), 4.38-4.34 (m, 5H), 3.89 (m, 4H), 3.69 (s, 1H), 3.62-3.35 (m, 36H), 3.13 (m, 5H), 2.72 (m, 5H), 2.30 (m, 5H), 1.87 (m, 4H), 1.61-0.91 (m, 75H), 0.72 (s, 6H).^{13}C NMR (126 MHz, CD$_3$OD) δ 175.93, 161.59, 158.47, 141.31, 132.17, 129.25, 123.46, 112.05, 96.93, 96.41, 87.51, 82.05, 79.71, 76.33, 75.40, 74.16, 73.30, 72.18, 71.44, 71.37, 70.43, 69.41, 69.27, 61.46, 58.17, 55.56, 53.01, 51.41, 51.21, 50.26, 43.55, 41.98, 41.71, 41.17, 40.73, 39.75, 37.78, 36.35, 33.27, 33.05, 32.18, 29.34, 26.78, 25.73, 22.22.
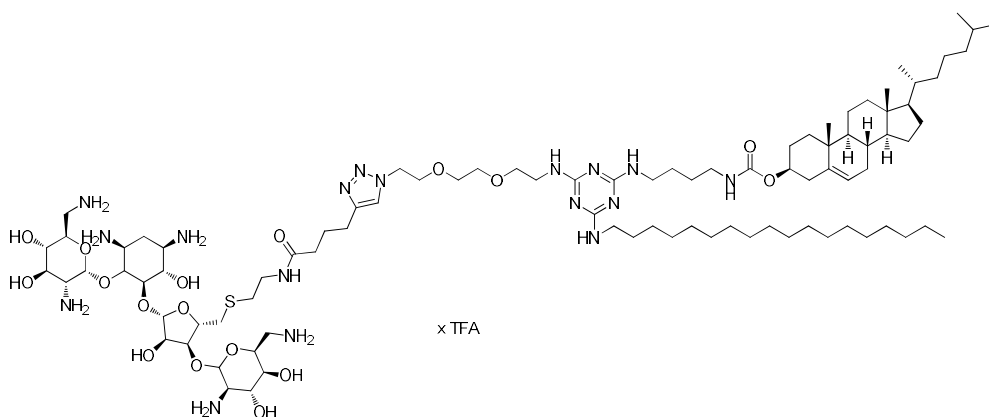


**Compound 30:** ^{1}H NMR (500 MHz, CD$_3$OD) δ 7.80 (s, 1H), 5.37-5.32 (m, 2H), 5.16 (s, 1H), 4.94 (s, 1H), 4.54 (t, 2H), 4.36 (b, 1H), 4.21 (m, 3H), 4.11 (m, 2H), 3.89 (m, 3H), 3.75 (m, 2H), 3.61-3.35 (m, 30H), 3.13 (t, 2H), 2.90 (b, 1H), 2.76 (m, 4H), 2.29 (m, 3H), 2.05-1.95 (m, 5H), 1.86 (m, 2H), 1.60-0.94 (m, 125H), 0.72 (s, 3H). ESI *m/z* 2410.3 [M+H^{+}][+] **Compound 36:** white solid, 44% yield in two steps. ^{1}H NMR (400

MHz, CD₃OD) δ 7.80 (s,1H), 6.06 (d, 1H), 5.43 (s, 1H) , 5.35 (m, 2H), 4.54 (m, 2H), 4.42 (s, 1H), 3.89-3,52 (m, 31H), 3.13 (m, 1H), 2.97-2.81 (m, 4H), 2.65 (m, 2H), 2.45 (m, 2H), 2.29 (m, 2H), 1.61-0.89 (m, 81H), 0.72 (s, 3H). ¹³C NMR (101 MHz, CD₃OD) δ 169.33, 133.60, 132.38, 130.90, 129.86, 123.42, 112.04, 96.90, 96.41, 87.53, 76.34, 75.38, 74.15, 73.26, 72.15, 71.34, 70.41, 70.08, 69.24, 69.13, 58.13, 57.58, 55.53, 52.96, 51.65, 51.35, 51.18, 50.22, 43.50, 41.94, 41.67, 41.13, 40.68, 40.19, 38.30, 37.75, 37.37, 37.10, 36.32, 33.22, 33.03, 32.12, 31.63, 30.83, 30.34, 30.13, 29.30, 29.13, 28.14, 26.78, 25.72, 25.31, 24.96, 24.01, 23.73, 23.17, 22.93, 22.17, 19.80, 19.26, 14.45, 14.37, 12.33, 11.40.
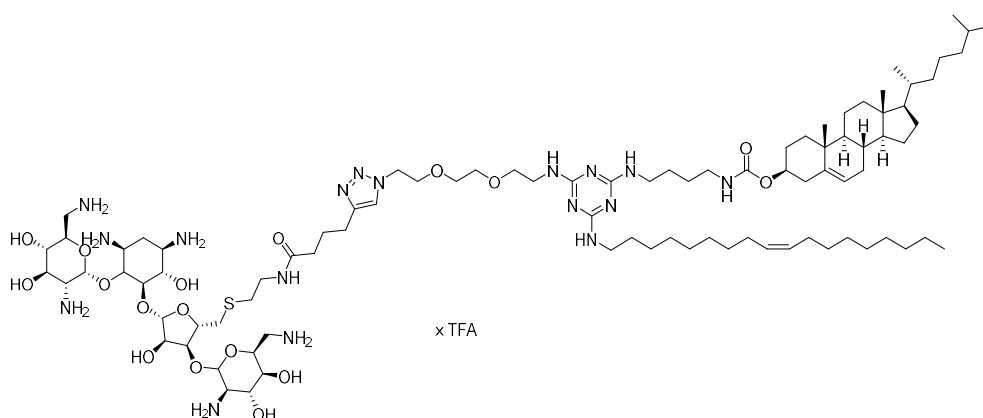


**Compound 31:** ESI *m/z* 2408.3 [M+Na⁺]⁺ **Compound 37:** white solid, 35% yield in two steps. ¹H NMR (400 MHz, CD₃OD) δ 7.80 (s, 1H), 6.06 (s, 1H), 5.42 (d, 1H), 5.34 (s, 4H), 4.54 (bs, 1H), 4.37 (m, 2H), 3.89 (s, 2H), 3.73-3.25 (m, 35H), 3.13 (m, 3H), 2.73 (t, 3H), 2.30 (m, 4H), 2.10-1.87 (m, 6H) 1.69-0.87 (s, 70H), 0.72 (s, 3H).¹³C NMR (101 MHz, CD₃OD) δ 168.99, 162.56, 162.15, 124.16, 119.11, 71.42, 71.29, 69.38, 58.14, 57.59, 51.65, 46.12, 43.51, 41.13, 40.69, 38.29, 37.75, 37.38, 37.11, 36.37, 33.23, 33.07, 30.79, 30.47, 29.31, 29.14, 28.79, 24.95, 23.73, 23.18, 22.94, 22.17, 19.27, 14.44, 12.31.
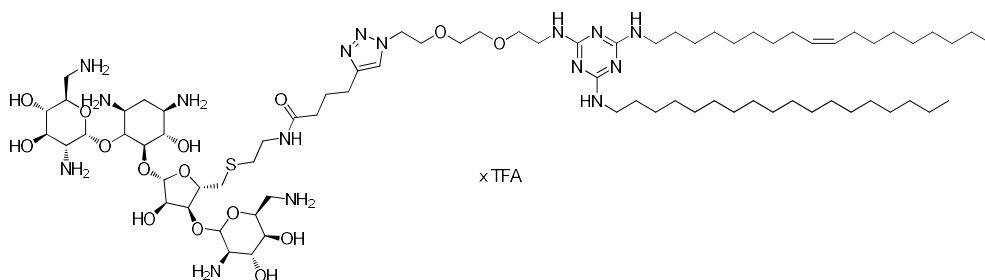
**Compound 32:** $^1$H NMR (400 MHz, CD$_3$OD) δ 7.80 (s, 1H), 5.38 (d, 1H), 5.34 (t, 2H), 5.15 (d, J=2.4 Hz. 1H), 4.93 (s, 1H), 4.54 (t, J=4.8Hz. 2H), 4.25 (b, 2H), 4.12 (m, 1H), 3.88 (m, 4H), 3.80-3.70 (m, 2H), 3.67-3.35 (m, 27H), 2.89 (m, 2H), 2.72 (m, 4H), 2.27 (t, J=7.6Hz, 2H), 2.08-1.93 (m, 7H), 1.56 (b, 1H), 1.53-1.41 (m, 54H), 1.33 (m, 56H), 0.90 (t, J=6.4Hz, 6H). ESI *m/z* 2155,8 [M+H$^+$]$^+$ **Compound 38:** white solid, 40% yield in two steps. $^1$H NMR (500 MHz, CD$_3$OD) δ 7.81 (s, 1H), 6.07 (d, J=2.8Hz, 1H), 5.42 (d, J=3.2Hz, 1H), 5.34 (m, 3H), 4.53 (b, 2H), 4.32  (m, 2H), 4.17 (m, 1H), 3.89 (m, 4H), 3.68-3.35 (m, 29H), 3.15 (m, 2H), 2.81-2.67 (m, 4H) , 2.29 (t, J=4Hz, 2H), 2.13-1.94 (m, 5H), 1.60 (b, 3H), 1.35-1.29 (m, 56H), 0.90 (t, J=4.4Hz, 6H). $^{13}$C NMR (126 MHz, CD$_3$OD) δ 162.09, 130.93, 130.79, 112.03, 96.94, 96.43, 87.62, 82.06, 79.72, 75.41, 74.17, 73.28, 72.18, 71.42, 71.37, 70.42, 69.27, 55.54, 53.00, 51.38, 51.20, 50.25, 41.96, 41.69, 33.05, 30.74, 30.44, 28.13, 26.76, 25.78, 23.71, 14.41

## 2.7 References

1.    Silen, J. L. *et al.* Screening for novel antimicrobials from encoded combinatorial libraries by using a two-dimensional agar format. *Antimicrob. Agents Chemother.* **42,** 1447–53 (1998).

2.    Zhou, C. *et al.* Synthesis and biological evaluation of novel 1,3,5-triazine derivatives as antimicrobial agents. *Bioorg. Med. Chem. Lett.* **18,** 1308–1311 (2008).

3.    Li, H. *et al.* Triazine-based tool box for developing peptidic PET imaging probes: syntheses, microfluidic radiolabeling, and structure-activity evaluation. *Bioconjugate Chem.* **25,** 761–72 (2014).

4.    Liang, T.W., Chen, Y.J., Yen, Y.H., Wang, S.-L. The antitumor activity of the hydrolysates of chitinous materials hydrolyzed by crude enzyme from Bacillus amyloliquefaciens V656. *Process Biochem.* **42,** 527–534 (2007).

5.    Lim, J. *et al.* Design, Synthesis, Characterization, and Biological Evaluation of Triazine Dendrimers Bearing Paclitaxel Using Ester and Ester/Disulfide Linkages. *Bioconjugate Chem.* **20,** 2154–2161 (2009).

6.    Merkel, O. M. *et al.* Triazine Dendrimers as Nonviral Gene Delivery Systems: Effects of Molecular Structure on Biological Activity. *Bioconjugate Chem.* **20,** 1799–1806 (2009).

7.    Merkel, O. M. *et al.* Triazine Dendrimers as Nonviral Vectors for in Vitro and in Vivo RNAi: The Effects of Peripheral Groups and Core Structure on Biological Activity. *Mol. Pharm.* **7,** 969–983 (2010).

8.    Candiani, G. *et al.* Dimerizable Redox-Sensitive Triazine-Based Cationic Lipids for in vitro Gene Delivery. *ChemMedChem* **2,** 292–296 (2007).

9.    Zhang, C. Polyethylenimine strategies for plasmid delivery to brain-derived cells. *Methods* **33,** 144–150 (2004).

10.   Malloggi, C. *et al.* Comparative evaluation and optimization of off-the-shelf cationic polymers for gene delivery purposes. *Polym. Chem.* **6,** 6325–6339 (2015).

11.   Mintzer, M. A., Merkel, O. M., Kissel, T., Simanek, E. E. Polycationic triazine-based dendrimers: effect of peripheral groups on transfection efficiency. *New J. Chem.* **33,** 1918–1925 (2009).

12.   Ohyama, T., Cowan, J. A. Anion coordination by aminoglycosides: structural and charge effects. *Chem. Commun.* **4,** 467–468 (1998).

13.   Wang, H., Tor, Y. Electrostatic interactions in RNA aminoglycosides binding. *J. Am. Chem. Soc.* **119,** 8734–8735 (1997).

14.   Bono, N. *et al.* Design and synthesis of biologically active cationic amphiphiles built on the calix[4]arene scaffold. *Int. J. Pharm.* **549,** 436–445 (2018).

15. Iwata, R. *et al.* Synthesis and properties of vitamin e analog-conjugated neomycin for delivery of RNAi drugs to liver cells. *Bioorganic Med. Chem. Lett.* **25,** 815–819 (2015).

16. Doi, Y., Arakawa, Y. 16S Ribosomal RNA Methylation: Emerging Resistance Mechanism against Aminoglycosides. *Clin. Infect. Dis.* **45,** 88–94 (2007).

17. Le Gall, T. *et al.* Synthesis and transfection properties of a series of lipidic neamine derivatives. *Bioconjugate Chem.* **20,** 2032–2046 (2009).

18. Mével, M. *et al.* Paromomycin and neomycin B derived cationic lipids: Synthesis and transfection studies. *J. Control. Release* **158,** 461–469 (2012).

19. Sainlos, M. *et al.* Kanamycin A-derived cationic lipids as vectors for gene transfection. *ChemBioChem* **6,** 1023–1033 (2005).

20. Ghilardi, A. *et al.* Synthesis of multifunctional PAMAM-aminoglycoside conjugates with enhanced transfection efficiency. *Bioconjugate Chem.* **24,** 1928–1936 (2013).

21. Desigaux, L. *et al.* Self-assembled lamellar complexes of siRNA with lipidic aminoglycoside derivatives promote efficient siRNA delivery and interference. *Proc. Natl. Acad. Sci.* U.S.A **104,** 16534–16539 (2007).

22. Choi, J.S., Lee, E.J., Jang, H.S., Park, J. S. New Cationic Liposomes for Gene Transfer into Mammalian Cells with High Efficiency and Low Toxicity. *Bioconjugate Chem.* **12,** 108–113 (2001).

23. Medvedeva, D. A. *et al.* Novel Cholesterol-Based Cationic Lipids for Gene Delivery. *J. Med. Chem.* **52,** 6558–6568 (2009).

24. Dix, A. V. *et al.* Cooperative, Heparan Sulfate-Dependent Cellular Uptake of Dimeric Guanidinoglycosides. *ChemBioChem* **11,** 2302–2310 (2010).

25. Godbey, W. T., Wu, K. K., Mikos, A. G. Poly(ethylenimine) and its role in gene delivery. *J. Control. Release* **60,** 149–160 (1999).

26. Wasungu, L., Hoekstra, D. Cationic lipids, lipoplexes and intracellular delivery of genes. *J. Control. Release* **116,** 255–264 (2006).

27. Zhi, D. *et al.* Transfection Efficiency of Cationic Lipids with Different Hydrophobic Domains in Gene Delivery. *Bioconjugate Chem.* **21,** 563–577 (2010).

28. Tang, F., Hughes, J. A. Synthesis of a single-tailed cationic lipid and investigation of its transfection. *J. Control. Release* **62,** 345–58 (1999).

29. Wetzer, B. *et al. Reducible cationic lipids for gene transfer*. *Biochem. J* **356,** 747-756 (2001).

30. Cameron, F. H. *et al.* A transfection compound series based on a versatile Tris linkage. *Biochim. Biophys. Acta Biomembr.* **1417,** 37–50 (1999).

31. Balasubramaniam, R. P. *et al.* Structural and functional analysis of cationic transfection lipids: the hydrophobic domain. *Gene Ther.* **3,** 163–72 (1996).

32.    Heyes, J. A., Niculescu-Duvaz, D., Cooper, R. G., Springer, C. J. Synthesis of novel cationic lipids: Effect of structural modification on the efficiency of gene transfer. *J. Med. Chem.* **45,** 99–114 (2002).

33.    Pezzoli, D., Candiani, G. Non-viral gene delivery strategies for gene therapy: A 'ménage à trois' among nucleic acids, materials, and the biological environment: Stimuli-responsive gene delivery vectors. *J. Nanoparticle Res.* **15,** (2013).

34.    Elouahabi, A., Ruysschaert, J. M. Formation and intracellular trafficking of lipoplexes and polyplexes. *Mol. Ther.* **11,** 336–347 (2005).

35.    Pezzoli, D., Giupponi, E., Mantovani, D. Candiani, G. Size matters for in vitro gene delivery: investigating the relationships among complexation protocol, transfection medium, size and sedimentation. *Sci. Rep.* **7,** 44134 (2017).

36.    Mintzer, M. A. Simanek, E. E. Nonviral Vectors for Gene Delivery. *Chem. Rev.* **109,** 259 (2009).

37.    Hancock, R. E. W. Aminoglycoside uptake and mode of action-with special reference to streptomycin and gentamicin II. Effects of aminoglycosides on cells. *J. Antimicrob. Chemother.* **8,** 429-445 (1981).

38.    Schwabacher, A. W., Lane, J. W., Schiesher, M. W., Leigh, K. M., Johnson, C. W. Desymmetrization reactions: Efficient preparation of unsymmetrically substituted linker molecules. *J. Org. Chem.* **63,** 1727–1729 (1998).

# Chapter III: AGs-calix[4]arene conjugates for in vitro gene delivery

## 3.1 Background

Calix[n]arenes are very promising delivery agents due to their well-defined three-dimensional (3D) architecture and their capacity to bear multiple moieties to interact with NAs.[1–4] One of the most striking examples of this point is the work done by Ungaro's group, who has for long time been working on calix[4]arenes. By way of illustration, the conjugation of such macrocyclic molecules at their lower and upper rim with hydrophobic moieties, arginine clusters, and guanidino groups allowed a significant improvement of NAs condensation and delivery abilities of the resulting complexes.[5–7]

In this chapter the synthesis and characterization of a novel class of multicationic-head amphiphiles built on tetramino-tetrahexyloxycalix[4]arene (hereafter referred to as 4A4Hex-calix[4]) is reported. Four units of three different AGs, namely neomycin, neamine, and paromomycin, were grafted by means of isothiocyanate linkers at the upper rim of the calix[4]arene. The efficiency of AGs grafting on 4A4Hex-calix[4] scaffolds was determined by $^1$H and $^{13}$C NMR. Besides, the DNA binding capacity together with the cytotoxicity and the transfection efficiency of such amphiphilic 4A4Hex-calix[4]-AG derivatives were evaluated on two different cell lines and their antibacterial activity was evaluated as well.

## 3.2 Materials and methods

### 3.2.1 Materials and reagents

Refers to 2.2.1. U87-MG (human glioblastoma-astrocytoma epithelial-like) cells were purchased from the American Type Culture Collection (ATCC, Manassas, VA, USA. *Escherichia coli* DSM 3423 (*E. coli* JM109) were purchased from Leibniz Institute DSMZ-German Collection of Microorganisms and Cell Cultures (Braunschweig, Germany), while *Sarcina lutea* (*S. lutea*) ATCC 9341 were from ATCC.

### 3.2.2 Synthesis of the conjugates
Refer to 3.3

### 3.2.3 Biological assays

**Preparation of transfectant solutions:** Refer to 2.2.3

**Complexes preparation and evaluation of DNA complexation ability:**The DNA complexation ability of every 4A4Hex-calix[4]-AG conjugate was monitored by a fluorophore-exclusion titration assay. For each condition, 0.12 µg of pDNA in 2.4 µL of 20×SYBR Green I ($\lambda_{ex}$=497 nm, $\lambda_{em}$=520 nm) were added to 3.6 µL of CL solutions at different concentrations. Afterwards, lipoplexes were incubated for 20 min at r.t., then diluted 1:5 (v/v) in dH$_2$O. Fluorescence measurements (n=3 per condition) were performed with a GENios Plus Reader (Tecan, Segrate, Italy) in 384-well black plates. Data are expressed as relative fluorescence normalized to the fluorescence of uncomplexed pDNA.

**Measurement of size and zeta-potential of complexes:** The hydrodynamic diameter (D$_H$) and the zeta potential ($\zeta_P$) of the lipoplexes were measured at 25 °C by Dynamic Light Scattering (DLS) and Laser Doppler micro-electrophoresis using a Malvern Zetasizer Nano ZS instruments (Malvern, Italy), fitted with a 5 mV HeNe laser ($\lambda$=633 nm) and a scattering angle of 173°. Fifty µL of complexes containing 1 µg of pDNA were prepared as described above, incubated for 20 min at r.t. then diluted 1:9 in dH$_2$O. Samples were equilibrated for 5 min at 25 °C prior the measurement.

**In vitro cells transfection experiments:** Cell cultures and *in vitro* cell transfection: Refers to 2.2.3

<div align="center">

Cytotoxicity was determined as follows:

Cytotoxicity[%] = 100%−Viability[%]

</div>

**Antimicrobial activity of calix[4]-AGs:** *E. coli* JM109 and *S. lutea* bacterial strains were pre-cultured in 5 mL of Luria-Bertani broth at 37 °C under shaking at 130 rpm for 20 hrs, until reach an optical density at $\lambda$=600 nm (OD$_{600}$nm)≈1, corresponding to ≈10$^9$ bacteria/mL. Bacterial suspensions were then diluted to obtain a final concentration of ≈10$^6$ bacteria/mL, hereafter used as the test inoculum. Afterwards, bacterial suspension (50 µL/well) were inoculated in 96-well plates at a density of 1.5×10$^5$ bacteria/cm$^2$ in 50 µL/well of LB containing pDNA/4A4Hex-calix[4]-AGs complexes prepared as described herein above or uncomplexed (i.e. DNA-free) 4A4Hex-calix[4]-AGs solutions (prepared at the same lipid concentration used to complex pDNA), and incubated at 37 °C for 24 hrs. Bacteria inoculated in 50 µL/well of LB were used as positive controls (CTRL⁺) for bacterial growth[8], while bacteria inoculated in 50 µL/well of free AGs solution (i.e. neomycin, neamine, paramomycin

at different AG concentrations) and 4A4Hex-calix[4] were used as internal references. The antibacterial efficacy of every compound was evaluated by means of both indirect (i.e. turbidity–$OD_{600}$nm measurements)[9–11] and direct (i.e. plate count) methods, according to the ISO10932:2010 (E) norm and Taylor[12] *et al*. (1983). The $MIC_{90}$ was as the lowest concentration (or N/P) of every compound that reduced the OD of the inoculum by 90% within a 24 hr-incubation with respect to the $CTRL^+$.[13] Briefly, 24 hrs after inoculation, the $OD_{600\ nm}$ of each well (n≥3 per compound) was read by means of a Sunrise microplate reader (Tecan, Italy). The number of viable bacteria was next counted on LB-agar Petri dishes after serial 10-fold dilutions of the bacterial suspensions and plating. Briefly, for every compound, wells displaying an $OD_{600\ nm}$ across the minimum were plated. The bacterial reduction was calculated according to the following equation:

$$\text{antibacterial reduction [\%]} = [1 - (N_{compound}/N_{CTRL+})] \times 100$$

where N is the number of Colony Forming Units (CFU) specific to every compound.
**Statistical analysis:** Statistical analysis was carried out by GraphPad version 6 (GraphPad software, La Jolla, CA, USA). All data were initially analyzed using D'Agostino & Pearson omnibus normality test. Comparisons among groups were performed by multiple t-test. Significance was retained when $p < 0.05$. Data are expressed as mean ± standard deviation (SD). Experiments were performed at least in triplicate.

## 3.3 Results and discussion

It was reported by Bagnacani and coworkers[5] that calix[4]arenes tethered with a six-carbon lipophilic chain to the lower rim were extremely effective in transfecting a variety of cell lines. Taking a clue from this study, we propose the synthesis of a novel class of lipid vectors displaying a hydrophobic domain consisting of 4A4Hex-calix[4] scaffold (Fig. 33).
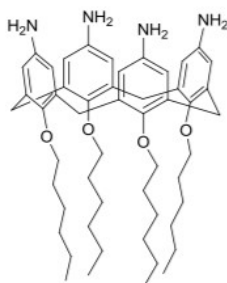


***Fig. 33 Structure of 4A4Hex-calix[4]:*** *Calix[4]arenes tethered with a six-carbon lipophilic chain to the lower rim are effective in transfecting a variety of cell lines.*

Besides, multivalent CLs do generally display enhanced NAs binding and delivery abilities as compared to the mono cationic counterparts.[14] As we have proficiently used AGs as polar heads of polycationic vectors[15], we did tether the calix[4] macrocyclic scaffold with AG headgroups, namely neomycin, neamine and paromomycin.

### 3.3.1 Synthesis and characterization of 4A4Hex-calix[4]-AG derivatives

The synthetic strategy used to graft 4A4Hex-calix[4] is well established in our laboratory[15], and relies on the reaction between the AG-modified with the isothiocyanate-terminated linker and the amine at the upper rim of 4A4Hex-calix[4].

In order to selectively functionalize Neo, we exploited the presence of only one, less hindered primary hydroxyl group in the molecular skeleton. Accordingly, neomycin was treated with Boc$_2$O and the resulting Boc-protected neomycin reacted with TPSCl producing the selective formation of intermediate **5** in good yields (Fig. 34). Substitution with mercaptoethylamine followed by coupling with 5-hexynoic acid lead to the formation of terminal-alkyne derivative **6** (Fig. 34).
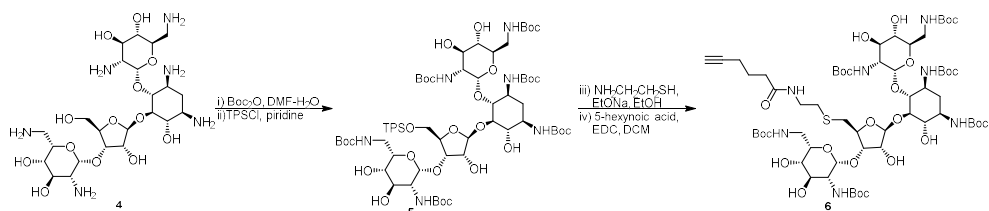


**Fig. 34 Modification of Neomycin:** *Neomycin was treated with Boc$_2$O and then with TPSCl obtaining intermediate **5**. After substitution with mercaptoethylamine followed by coupling with 5-hexynoic acid **6** was obtained.*

On the other hands the isothiocyanate linker **7** was prepared according to literature.[33] Finally, click reaction between **6** and azido-linker **7** bearing the needed isothiocyanate functional group produced in good yields compound **8** (Fig. 35).
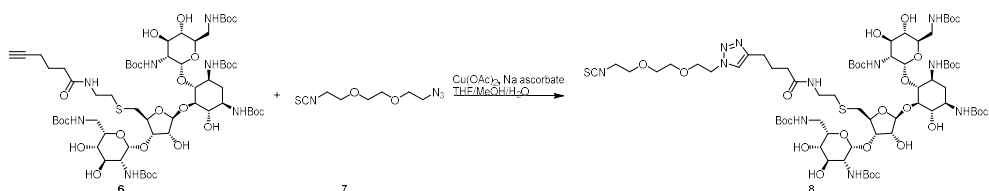


**Fig. 35 Modification of Neomycin**: *Click reaction between the isothiocyanate linker and Neo-Alkyne derivative **6**.*

Instead, for the functionalization of neamine **9** and paromomycin **10** we exploited the presence of only one, less hindered aminomethylene moiety which reacts smoothly with activated p-nitrophenyl ester **11** (for the synthesis, see 3.5). The remaining amines were protected with Boc$_2$O (Fig. 36 for neamine and Fig. 37 for paromomycin) resulting in intermediate **12** (for neamine) and **13** (for paromomycin). Following the same synthetic strategy, alkyne-terminal functionalized AGs **12**, **13** were submitted to click reaction with azido-linker **7** producing the corresponding isothiocyanate-functionalized AG **14**, **15** (Fig. 36 and 37).
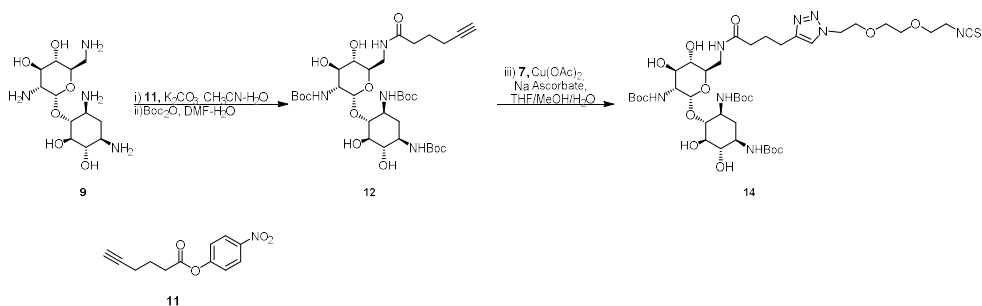


**Fig. 36 Modification of Neamine:** *The less hindered amino-methylene moiety reacts with p-nitrophenyl ester 11. After protection of the remaining amines, derivative 14 is obtained by using click chemistry.*
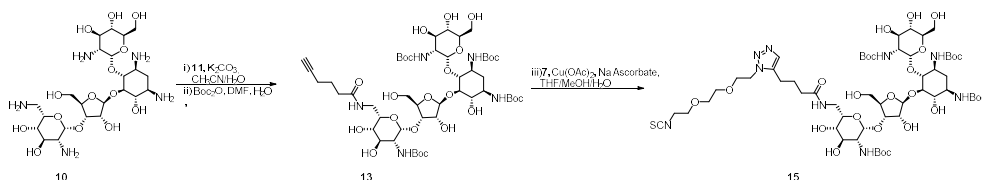


**Fig. 37 Modification of Paromomycin:** *Paromomycin contains a unique, less hindered amino-methylene suitable as site for modification.*

Compound **8**, **14** and **15** were used in the syntesis of 4A4Hex-calix[4]-AG **1-3**. Neat 4A4Hex-calix[4] was dissolved in DMSO and a solution of AG-isothiocyanate linker (1.2 equivalent per NH$_2$) in a minimal volume of DMSO was added (Fig. 38). The solution was stirred at 60°C for 24 hrs in order to maximize the degree of grafting. The compounds were then dialyzed for 8 hrs against MeOH (the solvent reservoir was renewed 3 times, MWCO 1 KDa). The solution was evaporated under reduced pressure to give N-Boc-protected 4A4Hex-calix[4]-AG. After ^{1}H NMR characterization, the resulting conjugates were dissolved in a 1:1 mixture of TFA/DCM and stirred for 30 min at r.t. The excess of TFA was stripped off under reduced pressure, the crude dissolved in dH$_2$O and the solution dialyzed against

dH$_2$O. Lyophilization led to fluffy, white solid products, i.e. the 4AHex-calix[4]-AGs **1**–**3**.
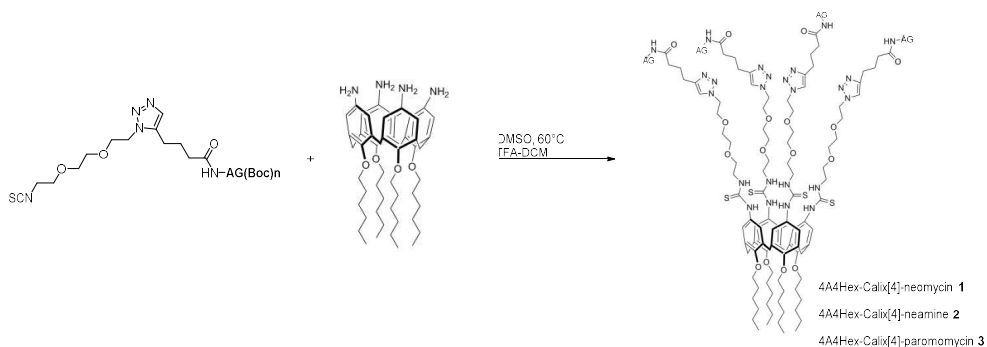


***Fig. 38 Synthesis of 4AHex-calix[4]-AGs 1–3:*** *Compound **8**, **14** and **15** were grafted with 4A4Hex-calix[4] to obtain 4A4Hex-calix[4]-AG **1-3**.*

The conjugates were next characterized through ^{1}H NMR and ^{13}C NMR. Specifically, the efficiency of AG grafting on the 4A4Hex-calix[4] scaffold was determined by ^{1}H NMR. In the spectra of 4A4Hex-calix[4]-AG **3**, reported as typical example in Fig. 39, it is evident the characteristic proton of the triazole at 8.1 ppm, the signals of the three anomeric protons of the AG between 5.3 and 5.9 ppm and the broad singlet of the methyl groups of the terminal hexyl moiety of calix around 1.0 ppm. Their integrations are respectively 4H for each anomeric proton and 12H. This confirms that each amino group of the 4A4Hex-calix[4] was covalently functionalized with an AG. Besides, the aromatic protons of the calix[4]arene result in broad resonances, most likely due to the formation of high molecular weight aggregates and/or for the resonance between the aromatic rings and the thiourea groups. The fact that the ratio between the integrations of the signals belonging to the protons of the AGs and the calix is 4:1, together with the fact that the signals of the anomeric protons do not present any side peaks belonging to the free AG indicates that the conjugates **1**–**3** are pure and that the excess of the free AG used in the "click" isothiocyanate/amine reaction was completely removed by dialysis.
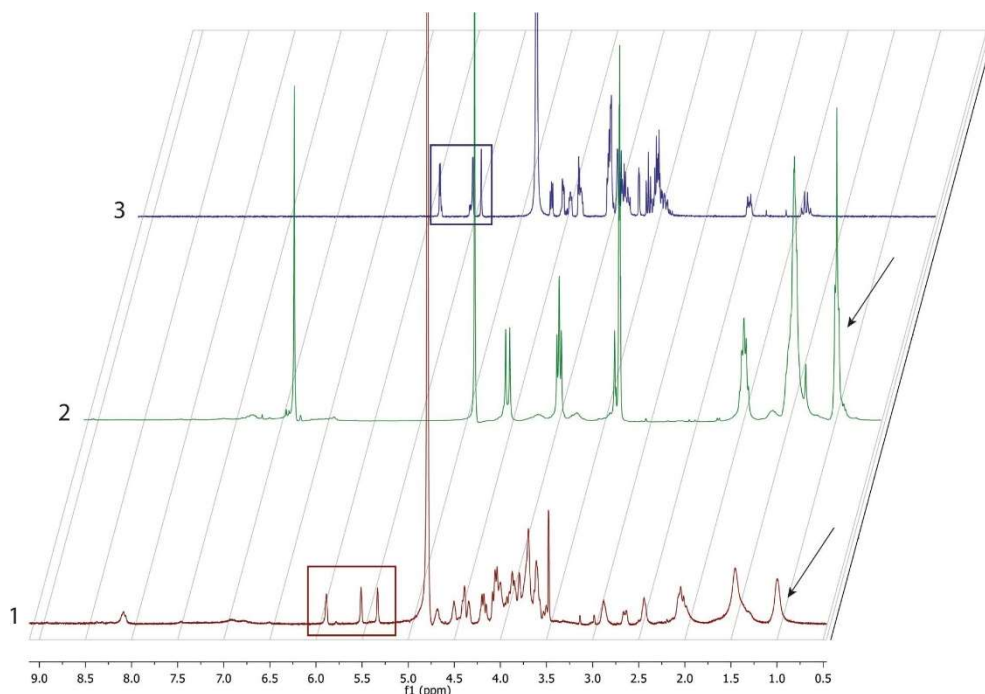
***Fig. 39 Representative ¹H NMR spectra***. *¹H NMR spectra of: 1) 4A4Hex-calix[4]areneparamomycin conjugate **3** (recorded in D₂O), 2) 4A4Hex-calix[4]arene (recorded in CD₃OD) and 3) free paromomycin (recorded in D₂O). The spectrum of the 4A4Hex-calix[4]arene-paromomycin **3** displays the three anomeric protons (spectrum 1, red rectangle) belonging to paromomycin (spectrum 3, blue rectangle) and the terminal methyl groups of the 4A4Hex-calix[4] (spectra 1 and 2, arrows) confirmed that the functionalization has occurred.*

### 3.3.2 Biophysical properties of pDNA/4A4Hex-calix[4]-AGs

The formation of the lipoplexes has known to be driven by electrostatic interactions between the cationic moieties of the transfectant and the anionic phosphates of NAs, leading to the charge neutralization and the compaction of polynucleotides. Accordingly, one of the key requirements of an efficient gene delivery vector lies on its ability to effectively bind and condense NAs. We thus evaluated the ability of every 4A4Hex-calix[4]-AG derivative to complex pDNA as a function of N-to-P (+/−) ratio (N/P). In fluorophore exclusion titration assay (Fig. 40), 4A4Hex-calix[4]-AGs invariably exhibited a maximal complexation ability at N/P≥1.5. This means that they have higher affinity for NAs if compared with the gold standard 25 kDa bPEI, which exhibited a maximal complexation at N/P≥3. A reason for such strong interactions with NA scan be ascribed to multivalent binding, due to the presence of four AGs[16], and to the clustering of the binders on the rigid scaffold calix[4]arene.
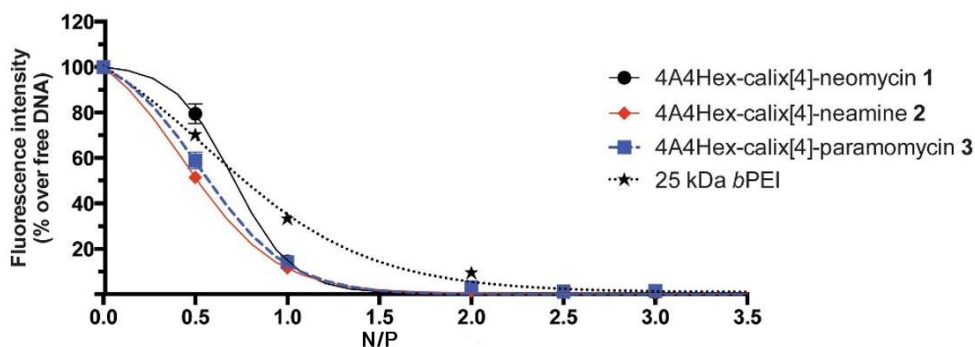
***Fig. 40 DNA complexation ability of 4A4Hexcalix[4]arene-AG conjugates 1–3 vs. 25 kDa bPEI***: *Comparative DNA complexation ability of 4A4Hex-calix[4]arene-neomycin **1** (black circle and solid line), 4A4Hex-calix[4]arene-neamine **2** (red circle and solid line), 4A4Hex-calix[4]arene-paromomycin **3** (blue square and dotted line), evaluated by monitoring the fluorochrome exclusion from complexes as a function of N/P.*

We have recently pointed out a strict relationship between the dimensions of gene delivery complexes and their transfection efficiency.[17] Besides, the surface charge of complexes is considered as an essential factor affecting their biological fate as well.[18] In this context, we evaluated the physicochemical properties of 4A4Hex-calix[4]-AG lipoplexes, i.e. their average $D_H$ and $\zeta_P$, at varying N/P. Since physico-chemical properties of complexes are highly dependent on the N/P, in this study a wide range of N/P was considered, in order to find out the lowest ratio at which DNA was condensed into small and weakly cationic particles. As reported in Fig. 41B–E, every $\zeta_P$ curve displayed a sigmoidal shape as a function of N/P. Very interestingly, the charge-inversion point (0 mV) did correspond to the N/P at which maximal complexation occurred for all the 4A4Hex-calix[4] derivatives. Conversely, the $D_H$ profile of every 4A4Hex-calix[4]-AG derivative was fairly constant at N/P$\geq$5. It is worthy of note that all pDNA/4A4Hex-calix[4] lipoplexes displayed similar $D_H$ ($\approx$150 nm) and $\zeta_P$($\approx$25$\div$40 mV) at 5$\leq$N/P$\leq$80 (p > 0.05 for every derivative series). Nevertheless, derivatives **2-** and **3-**based assemblies displayed high $D_H$ at N/P 80, although not significantly greater than those at other N/Ps (N/P80 vs. N/P 10-20-40; p > 0.05 for all). The $D_H$ and $\zeta_P$ profiles of bPEI/DNA complexes were similar to those of 4A4Hex-calix[4]-AGs **1**–**3**. The ability of 4A4Hex-calix[4]-AG derivatives to effectively bind the DNA, together with their biophysical behavior similar to those of the gold standard bPEI, prompted us to challenge cells in vitro with such vectors.
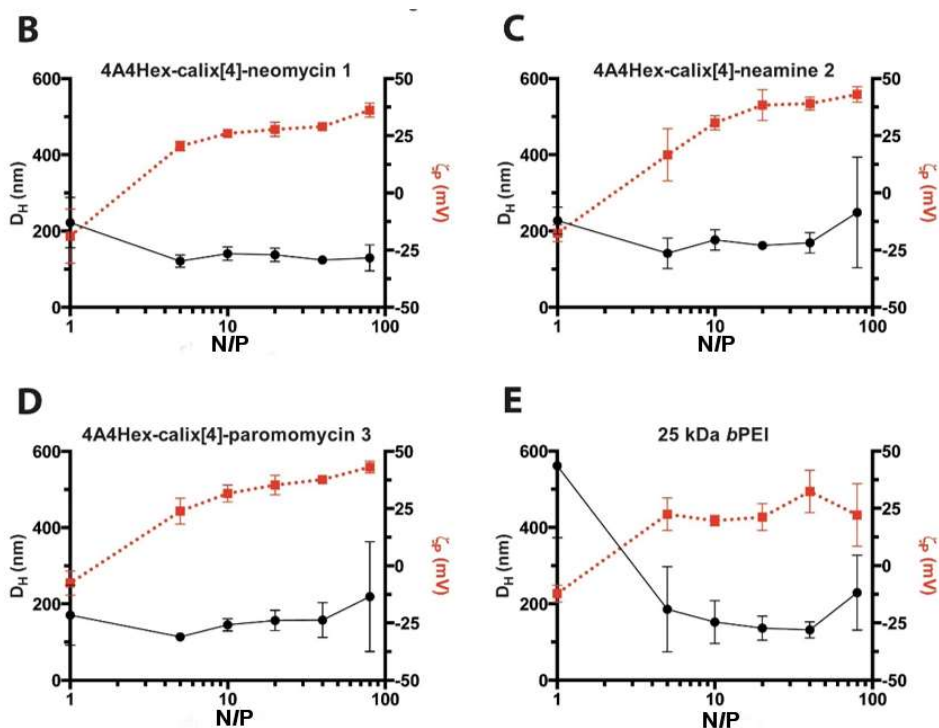
**Fig. 41 Physico-chemical characterization of 4A4Hexcalix[4]arene-AG conjugates 1–3 vs. 25 kDa bPEI**: *Mean hydrodynamic diameter ($D_H$; black circle and solid line) and overall charge ($\zeta_P$; red square and dotted line) of B) 4A4Hex-calix[4]arene-neomycin **1**, C) 4A4Hex-calix[4]arene-neamine **2**, D) 4A4Hex-calix[4]arene-paromomycin **3** and E) 25 kDa bPEI, measured by Dynamic Light Scattering (DLS) and Laser Doppler microelectrophoresis. Results are expressed as mean ± SD (n=3).*

### 3.3.3 In vitro transfection of pDNA/4A4Hex-calix[4]-AGs

To investigate the influence of biophysical properties of pDNA/4A4Hex-calix[4]-AG lipoplexes on the gene delivery behavior, we evaluated their transfection effectiveness at varying N/Ps. Besides physico-chemical properties, biological activity of complexes is highly dependent on the N/P as well. Accordingly, we tested lipoplexes prepared over a wide range of N/P to find out the minimal ratio to attain high gene expression and low cytotoxicity. Since bPEI is a gold standard transfectant[15,18–20], for the sake of comparison, bPEI/DNA complexes were herein used as the reference. pGL3 encoding the firefly luciferase was used to check the transfection efficiency in two extensively used cell lines, namely HeLa and U87-MG cells.[20] As expected, the transfection profiles of 4A4Hex-calix[4]-AG derivatives **1–3** were strongly dependent on the N/P (Fig.42 A and B). More into detail, amphiphilic

derivative **1** exhibited the highest transfection efficiency in both cell lines at N/P 20, while 4A4Hex-calix[4]-neamine conjugate **2** and -paromomycin conjugate **3** did display a different N/P-dependent and cell-dependent transfection behavior. Indeed, derivative **2** was more effective at N/P 20 and 40 when used to transfect HeLa and U87-MG cells, respectively. Derivative **3**, instead, did show higher transfection levels at N/P 80 and 20, in HeLa and U87-MG cells, respectively. Most important, it is worth noting that every derivative, when tested at each respective optimal N/P, invariably exhibited similar or even greater transfection efficiency than the gold standard 25 kDa bPEI used in the most effective conditions, that were N/P 10 and N/P 40 for HeLa and U87-MG cells, respectively (Fig. 42). Yet, without exception, pDNA/4A4Hex-calix[4]-AG lipoplexes exhibited very low toxicity on HeLa cells, close to that of bPEI-based complexes ($p > 0.05$) (Fig. 42C). Similar results were found with U87-MG cells as well, even though slightly greater cytotoxicity levels were found as compared to HeLa cells (Fig. 42D). From a general point of view, we found no strict relationship between the physico-chemical features (i.e. $D_H$ and $\zeta_P$) and the transfection efficiency of pDNA/4A4Hex-calix[4]-AG derivatives. In fact, even though different lipoplex types displayed similar size and surface charge, the different surface chemistry of each specific assembly might account for some differences in transfection. Overall, gene delivery studies highlight the pretty good transfection properties and low cytotoxicity of amphiphilic 4A4Hex-calix[4]-AG derivatives. Interestingly, such remarkable results were obtained with pure 4A4Hex-calix[4]-AG, therefore without the inclusion of any helper lipids in lipoplex formulations. Indeed, a lipid adjuvant, such as the neutral phospholipid DOPE, is sometimes used to substantially improve the transfection efficiency of CLs.[5,21,22] This underlines the inherent gene delivery efficacy of this novel class of cationic amphiphile.
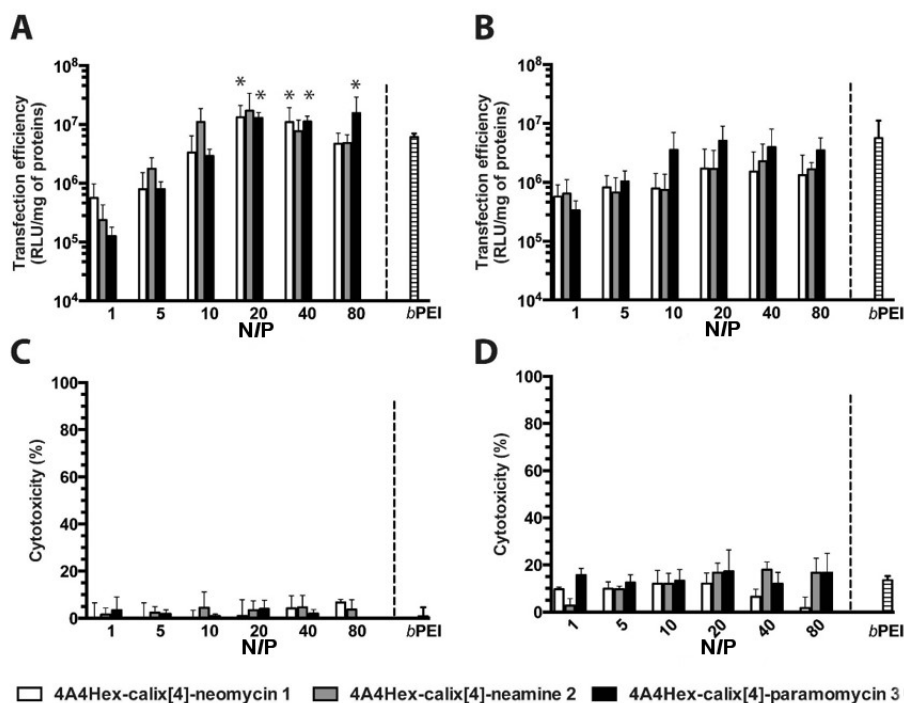
**Fig. 42 Transfection efficiency and cytotoxicity and of 4A4Hex-calix[4]arene derivatives in HeLa and U87-MG cells:** *Comparative transfection efficiency of complexes prepared by mixing pGL3 with 4A4Hex-calix[4]arene-AG derivatives 1–3 at different N/P and 25 kDa bPEI, expressed as luminescence signal (RLU) normalized to the total protein content in each cell lysate: A) HeLa cells; B) U87-MG cells. Cytotoxicity of the aforementioned complexes on C) HeLa and D) U87-MG cells. Results are expressed as mean ± SD (n ≥ 3) (*p < 0.05 vs. 25 kDa bPEI).*

### 3.3.4 Antibacterial properties of 4A4Hex-calix[4]-AG derivatives and pDNA/4A4Hex-calix[4]-AGs

An important feature sometimes undervalued or ignored by fundamental scientists but receiving considerable attention from clinical investigators is the desired side antibacterial effect of medicinal drugs, especially when diseases associated with immune suppression, such as certain types of cancer, are treated. We hypothesized that 4A4Hex-calix[4]-AGs, found to be effective as gene delivery agents, would also be suited to this purpose. It is worthy of note that, AGs are a group of clinically relevant antibiotics, which function through the binding to the 30S subunit of ribosomes. In turn, this perturbs the elongation of the nascent protein chain by impairing the proof-reading process controlling translational accuracy. The use of AGs as potential antiviral (HIV) agents has also been reported.[23] On the other hand, calix[n]arenes

have been extensively used in the last few years as molecular platforms to attach binding moieties for the selective recognition of molecular species.[24] Due to their three-dimensional architecture and the possibility to be specially tethered with different groups at their lower and upper rim, calix[n]arenes are well suited to engage in multivalent interactions, allowing these compounds to possibly interfere with the function of critical bacterial virulence determinants. In these context, several pharmacological properties, including antibacterial[25], antifungal, and antiviral activities of calix[n]arene derivatives have been already reported in literature[26]. We therefore tested and compared the potential antimicrobial activity of 4A4Hex-calix[4]-AG conjugates **1**–**3,** used as aqueous (lipid)solutions and in the form of suspensions of pDNA/4A4Hex-calix[4]-AG complexes, and compared their performances to those of free AGs and the 4A4Hex-calix[4] lipophilic scaffold. The antibacterial activity of such free molecules and particles were tested against Gram-negative *E. coli* and Gram-positive *S. Lutea* bacteria, which are part of the human flora (*E. coli* are found in gut microbiota, while *S. lutea* may be found in the skin and large intestine). In solution, 4A4Hex-calix[4]-neomycin derivative **1** displayed the strongest antibacterial activity as it was largely more effective in inhibiting Gram-negative *E. coli* growth with respect to the 4A4Hex-calix[4]-neamine **2** and the 4A4Hex-calix[4]-paromomycin **3** (Fig. 43). It is worth noting that the antibacterial activity of 4A4Hex-calix[4]-AGs was not affected by their association with pDNA, as previously pointed out by Kichler and colleagues for other transfectants.[27] In our hands, the antibacterial efficiencies of 4A4Hex-calix[4]-AGs complexed with pDNA were even greater than the same derivatives in solution (DNA-free lipids), but were slightly less active against *E. coli* than the corresponding free AGs (Fig. 43).

**Fig. 43 Antibacterial activity of 4A4Hex-calix[4]arene derivatives in solution and pDNA/4A4Hex-calix[4]-AG assemblies against Gram-negative E. coli.** *Complexes were prepared by mixing pDNA with 4A4Hex-calix[4]arene-neomycin 1 (A), -neamine 2 (B), and -paromomycin 3 (C) at different N/P, and 25 kDa bPEI (D). Data are expressed as mean absorbance (OD$_{600 \ nm}$) ± SD (n ≥ 3). Free AGs, namely neomycin (A), neamine (B), paromomycin (C), and 4A4Hex-calix[4]arene lipophilic scaffold (D) were used as internal references.*

For derivative **1**-based lipoplexes, the MIC$_{90}$ was found at N/P 40 (corresponding to 9.4 µg of Neo per mL) (Fig. 43A), with a bacterial reduction of ≈100% (plate count method, Table 1), while its free lipid counterpart displayed a bacterial reduction of 76% at the same lipid concentration. For derivative **3**, lipoplexes and free lipid showed a 100% bacterial reduction at its MIC$_{90}$, that is at N/P 80 (corresponding to an AG concentration of 28.2 µg/mL). On the other hand, neomycin and paromomycin, tested

as free AGs, displayed the $MIC_{90}$ at $\approx$4 µg/mL, a slightly lower concentration with respect to their conjugated counterparts (Figs. 43A and C and Fig. 44A and C), while 4A4Hex-calix[4] lipophilic scaffold alone was roughly ineffective (Fig. 43D). Of note, it is evident that 4A4Hexcalix[ 4]-AG conjugates hide in a sort of way the antimicrobial potential of free AGs. Specifically, derivatives **1** and **3** exerted strong antibacterial effects at N/P≥20 (Table 1) while, irrespective of the complexation with DNA, derivative **2** (and PEI as well) was found to be ineffective against *E. coli* (Fig. 43 B and D). Of note, the $MIC_{90}$ of neamine was found at 32 µg/mL (Fig. 44B), therefore the lack of antibacterial properties cannot be ascribed to the ineffectiveness of the AG per se, but may rely on the conjugation of the antibiotic and the 4A4Hex-calix[4] scaffold. These data about the MIC of free AGs are in good agreement with the literature[11,13].

**Table 1**. *Antibacterial efficiency of 4A4Hex-calix[4]-neomycin 1, 4A4Hex-calix[4]-neamine 2, 4A4Hex-calix[4]-paromomycin 3 lipids and lipoplexes, their parent AGs, as determined by means of the (direct) plate count method.*

| Compound | Antibacterial Activity (%) | | |
|---|---|---|---|
| | **N/P20** | **N/P40** | **N/P80** |
| 4A4Hex-calix[4]-neomycin **1** | 73 | 76% | 100% |
| 4A4Hex-calix[4]-neomycin **1**/pDNA | 73 | 95% | 100% |
| 4A4Hex-calix[4]-neamine **2** | n.a. | n.a. | n.a. |
| 4A4Hex-calix[4]-neamine **2**/pDNA | n.a. | n.a. | n.a. |
| 4A4Hex-calix[4]-paromomycin **3** | 65% | 90% | 100% |
| 4A4Hex-calix[4]-paromomycin **3**/pDNA | 75% | 90% | 100% |
| bPEI | n.a. | n.a. | n.a. |
| bPEI/pDNA | n.a. | n.a. | n.a. |
| Neomycin | 100% | 100% | 100% |
| Neamine | n.a. | n.a. | n.a. |
| Paromomycin | 98% | 100% | 100% |
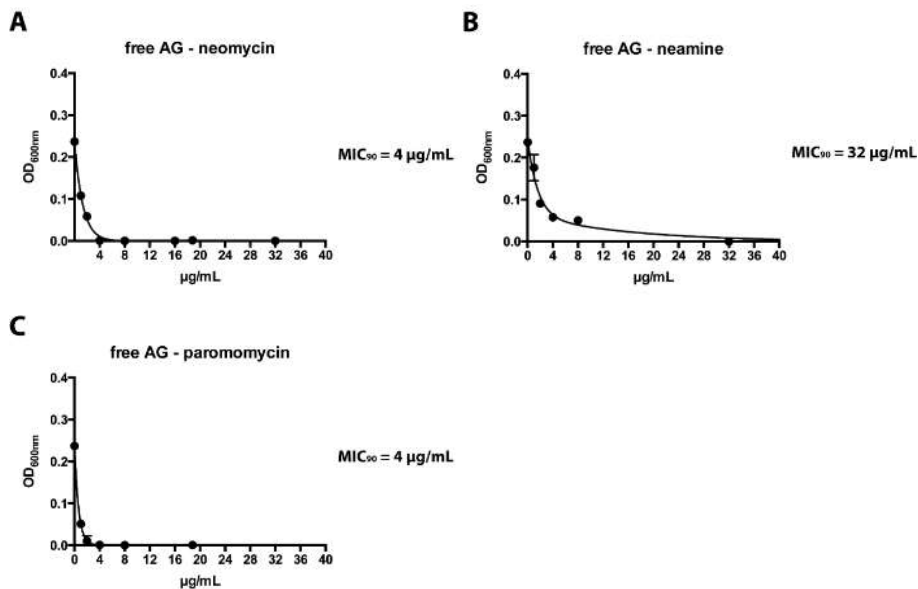
**Fig. 44**. *Minimum Inhibitory Concentration (MIC) of free AGs. Minimum Inhibitory Concentration ($MIC_{90}$) of free AGs evaluated against Gram-negative E. coli: A) free neomycin; B) free neamine; C) free paromomycin. Results of $OD_{600\,nm}$ are expressed as mean ± SD (n≥3).*

We evaluated the antibacterial activity of 4A4Hex-calix[4]-AG derivatives also against Gram-positive bacteria. We found a mild effect of such compounds against *S. lutea* (Fig. 45), and it was not particularly surprising because parent AGs are known to be mostly effective against Gram-negative bacteria.[28–30]
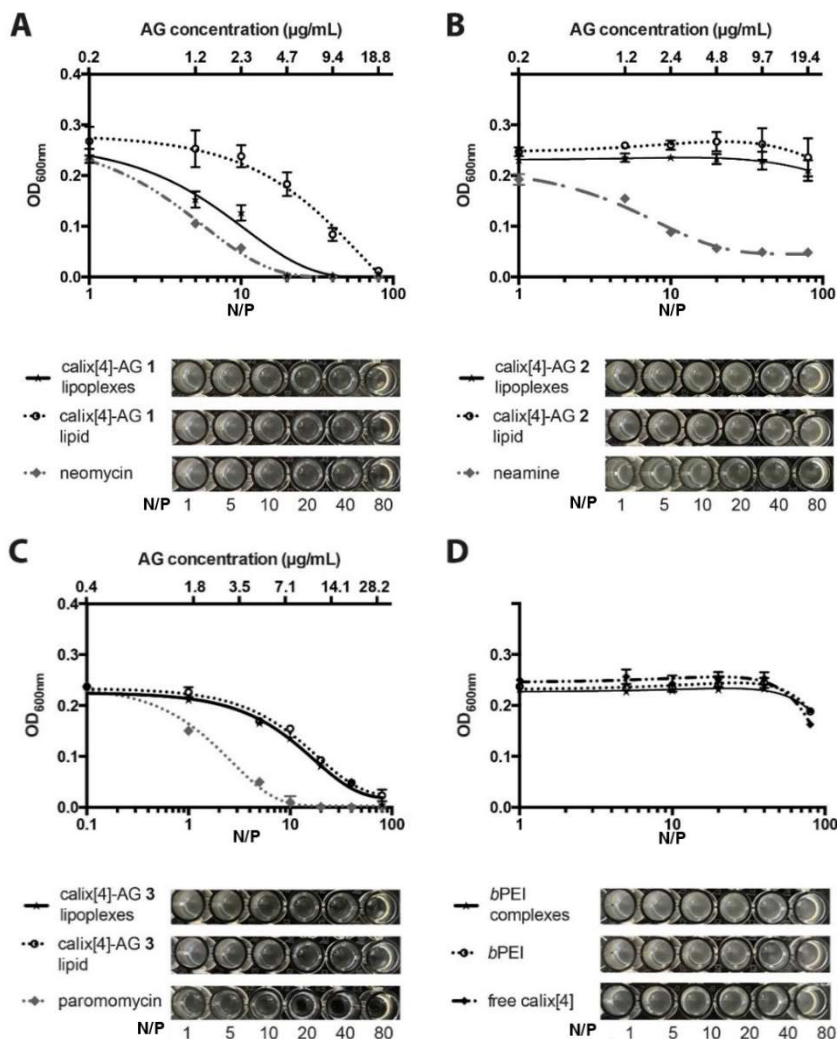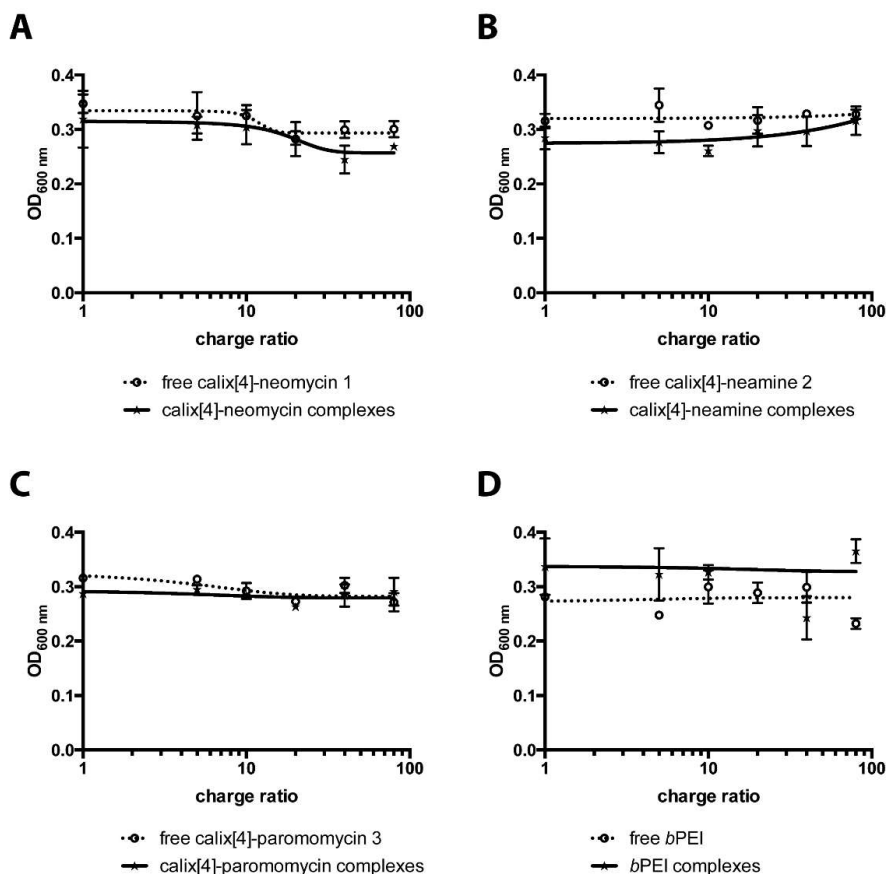
**Fig. 45 Antibacterial activity of 4A4Hex-calix[4]arene derivatives in solution and pDNA/4A4Hex-calix[4]-AG assemblies against Gram-positive S. lutea.** *Lipoplexes were prepared by complexing pDNA with 4A4Hex-calix[4]arene-neomycin **1** (A), -neamine **2** (B), -paromomycin **3** (C), and 25 kDa bPEI (D) at different N/P. Data are expressed as mean absorbance (OD$_{600\,nm}$) ± SD (n ≥ 3).*

Altogether these results disclosed 4A4Hex-calix[4]-AG derivatives **1** and **3** as potential antimicrobials against Gram-negative bacteria, especially when complexed with DNA. Besides, since in every conjugate the AGs were found to be covalently bound to the 4A4Hex-calix[4] as shown by NMR analysis (which means that no free AG is detectable), the antibacterial activity displayed by 4A4Hex-calix[4]-AG as free lipids and their relative lipoplexes can be ascribed to the compounds themselves rather than to the presence of some free AGs. Indeed, due to their cationic nature, 4A4Hex-calix[4]-AG derivatives **1** and **3** did display antimicrobial properties, probably because of the interactions happening with the bacterial wall, as reported for other bioactive chemicals.[31] Taken together, these data disclose 4A4Hex-calix[4]-AGs as effective gene delivery tools with inherent antibacterial properties.

## 3.4 Conclusion

We have herein reported the synthesis and characterization of a novel class of multivalent CLs through the tethering of the upper rim of the 4A4Hex-calix[4] scaffold with three different AGs, namely neamine, neomycin, and paromomycin. 4A4Hex-calix[4]-AG derivatives **1**–**3** did induce very effective DNA complexation, as demonstrated by the fluorophore exclusion assay, thus giving rise to nano-assemblies ($D_H \approx 150$ nm) with superior transfection efficiencies in vitro and weak cytotoxicity on HeLa and U87-MG cells. Besides, these nano-assemblies displayed inherent antimicrobial activity against Gram-negative (*E.coli*) bacteria. In order to provide more insight into the structure–activity relationship, further studies will aim to elucidate the mechanisms involved in cellular uptake and intracellular trafficking of this class of multivalent and multifunctional gene delivery vectors and to shed light on their mode of actions against Gram-negative bacteria. Altogether, these findings highlight the potential of 4A4Hex-calix[4]-AGs assemblies as efficient multifunctional carries capable of delivering NAs and blunting Gram-negative bacterial infections at once.

## 3.5 Supporting Information



**7**
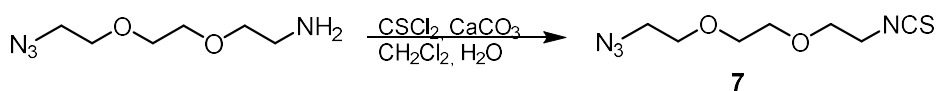
*Compound 7:* To a solution of 13 (780 mg, 4.50 mmol) in 1:1 mixture of DCM/$H_2O$ (30 mL), solid $CaCO_3$ (1.350 g, 13,5mmol) was added. Thiophosgene (1.0 g, 9.0 mmol) was added drop wise over 5 minute and the resultant biphasic mixture vigorously stirred at RT overnight. The reaction mixture was diluted with water (40 mL) and the organic phase was separated. The aqueous layer was extracted with DCM (2 x 40 ml) and the combined organic layers were washed with water (50ml), dried over $Na_2SO_4$ and concentered in vacuo to give a yellow oil (660 mg, 3,06 mmol) in 68% yield. Rf = 0,4 (hexane:AcOEt 50:50); ^{1}H-NMR (400 MHz, $CD_3Cl$): δ = 3.72-3.68 (m, 10H), 3.41 (t, J = 5.2 Hz, 2H); ^{13}C-NMR (101 MHz, $CD_3Cl$): δ = 70.85, 70.78, 70.1, 69.4, 50.8, 45.3; ESI (m/z) 239.0 [M+Na]+.



**11**
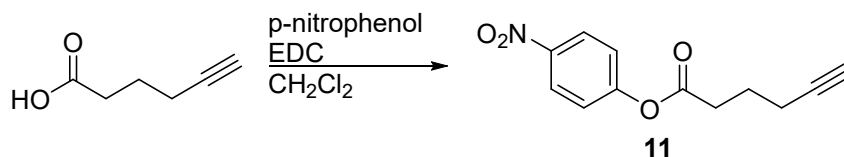
**Compound 11:** 500 mg of 5-hexynoic acid (4.46 mmol) were dissolved in $CH_2Cl_2$, then 744 mg of 4-nitrophenol (5.36 mmol) and 1 g of EDC (5.36 mmol) were added and then the reaction mixture was stirred for 24 hrs at r.t. The resulting mixture was then washed with 20 mL of 10% $Na_2CO_3$ solution in $dH_2O$ (3 times). Following the separation, the organic phase was let dry over $Na_2SO_4$ and concentrated under reduced pressure. The crude was then purified by flash chromatography (20% ethyl acetate in hexane) leading to the compound **6** as an oil in 60% yield. ^{1}H NMR (400 MHz, $CDCl_3$) δ 8.16 (d, J = 9.2Hz, 2H), 7.19 (d, 2H), 2.68 (t, J = 7.2, 2H) 2.27 (td, J = 2.8, 2H), 1.95 (t, 1H), 1.89 (p, 2H). ^{13}C NMR (101 MHz, $CDCl_3$) δ 170.65, 160.53, 149.61, 127.68, 125.43, 81.77, 71.33, 36.61, 25.06, 19.38.

**Syntesis of 4A4Hex-calix[4]-neomycin conjugate 1**

*Compound 8:* 150 mg of **6** (0.11 mmol) were dissolved in 6 mL of THF/$CH_3OH$/$H_2O$ mixture (5:4:1 (v/v/v)). Next, 28 mg of sodium ascorbate (0.14 mmol) and 26 mg of $Cu(OAc)_2$ (0.143 mmol) were added to the reaction mixture, then 32 mg of **7** (0.23 mmol), dissolved in a minimum amount of THF, were added. The mixture was sonicated until the disappearance of the starting material that was detected by TLC monitoring (30 min × 3 times). The mixture was concentrated under reduced pressure

then diluted in $CH_2Cl_2$. The organic layer was washed with saturated $NH_4Cl$, dried over $Na_2SO_4$ and filtered. The solvent was then removed under reduced pressure. The crude was purified by flash chromatography leading to the compound **8** in 85% yield *Rf* = 0.33 ($CH_2Cl_2$:$CH_3OH$ 95:5); ^{1}H NMR (400 MHz, $CDCl_3$): δ = 7.94 (s, 1H), 5.35 (s, 1H), 5.17 (s, 1H), 4.95 (s, 1H), 4.57 (s, 2H), 4.25 (s, 2H), 4.11 (s, 1H), 3.92 (s, 4H), 3.80 (d, J=6.0 Hz, 2H), 3.6-3.17 (m, 22H), 2.92 (s, 2H), 2.78(s, 4H), 2.31 (s, 2H), 2.02 (s, 3H), 1.45 (broad s, 56H). ^{13}C NMR (101 MHz, $CD_3OD$): δ = 174.12, 157.5, 157.1, 156.9, 156.8, 156.4, 156.2,132.27 122.99, 110.1, 99.3, 97.8, 86.2, 79.7, 79.3, 79.0, 74.5, 74.3, 73.2, 72.0, 71.56, 70.25, 70.16, 70.12 69.9, 69.6, 69.06, 55.57, 53.37, 52.3, 51.2, 50.2, 49.8, 47.64, 47.22, 47.01, 45.01, 44.8, 41.6, 40.7, 38.74, 35.06, 34.47, 34.34, 27.6, 27.5, 27.4, 27.3; 25.38, 24.53. ESI (*m/z*) 1606.76 [M+Na]+.

**Compound 1**: ^{1}H NMR (400 MHz, $D_2O$) δ 8.44 (bs, 4H, triazole), 7.76-6.97 (bs, 8H), 6.52 (d, 4H, anomeric), 5.88 (d, 4H, anomeric), 5.79 (s, 4H, anomeric), 5.04 (bs, 4H), 4.63-4.33 (m, 32H), 4.23-3.80 (m, 80H), 3.53 (dd, 4H), 3.38- 3.16 (m, 20H), 3.01 (m, 4H), 2.75 (m, 8H), 2.40 (m, 20H) , 1.77 (m, 32H), 1.31 (bs, 12H, terminal methyl of calix). ^{13}C NMR (101 MHz, $D_2O$) δ 175.55, 145.31, 144.34, 126.60, 125.52, 112.07, 110.48, 95.76, 95.01, 85.56, 80.32, 78.89, 75.16, 73.81, 72.61, 70.90, 70.32, 69.92, 69.76, 69.62, 68.22, 67.74, 67.63, 67.60, 53.84, 53.79, 51.12, 49.81, 49.10, 48.72, 40.69, 40.42, 38.74, 38.66, 34.95, 34.89, 34.35, 31.97, 30.71, 28.10, 24.44, 23.15, 22.71, 13.76. ESI (*m/z*) 1586.81 [M + 3H+]3+

**Syntesis of 4A4Hex-calix[4]-neamine conjugate 2**
Neamine was synthesized according to literature.[34]
**Compound 14:** 125 mg of **12** (0.13 mmol) were dissolved in 10 mL of THF/$CH_3OH$/$H_2O$ mixture (5:4:1 (v/v/v)). Next, 20 mg of sodium ascorbate (0.1 mmol) and 18 mg of $Cu(OAc)_2$ (0.09 mmol) were added to the reaction mixture. Then, 36 mg of **7** (0.26 mmol), dissolved in a minimum amount of THF, were added. The mixture was next sonicated until the disappearance of the starting material that was detected by TLC monitoring (30 min × 3 times). The mixture was concentrated under reduced pressure then diluted in $CH_2Cl_2$. The organic layer was washed with saturated $NH_4Cl$, dried over $Na_2SO_4$ and the solvent was removed under reduced pressure. The crude was purified by flash chromatography leading to the compound **14** in 82% yield. *Rf* = 0.30 ($CH_2Cl_2$:$CH_3OH$ 95:5. ^{1}H NMR (400 MHz, $CD_3OD$): δ =7.91 (s, 1H), 5.40 (s, 1H), 4.61 (s, 2H), 4.53 (m, 1H), 4.28 (m, 2H), 4.01-3.64 (m, 88H), 3.40 (m, 8H), 3.25 (m, 3H), 2.85 (t, J = 4Hz, 2H), 2.47 (t, J = 5Hz, 2H), 2.21 (m, 2H), 1.53 (bs, 29H). ^{13}C NMR (101 MHz, $CD_3OD$): δ =174.77, 157.55, 155.63, 147.61, 137.63, 126.76, 99.35, 80.62, 80.11, 79.69, 75.33 73.93, 72.09, 71.78, 71.57, 69.93,

69.60, 68.94, 56.74, 52.14, 51.76, 48.95, 43.18, 40.71, 35.90, 34.65, 28.34, 27.01, 21.90. ESI (*m/z*) 955.45 [M+Na]+.

***Compound 2***: $^1$H NMR (400 MHz, CD$_3$OD) δ 7.88 (bs, 4H, triazole), 7.56-6.57 (bs, 8H), 5.78 (s, 4H, anomeric), 4.66-4.53 (bs, 12H), 4.01-3.94 (bs, 16H), 3.72-3.56 (m, 40H), 3.38-3.31 (m, 8H), 2.82 (bs, 8H), 2.61 (m, 4H), 2.41 (m, 8H), 2.05 (m, 20H), 1.51 (m, 32H), 1.05 (s, 12H). $^{13}$C NMR (101 MHz, CD$_3$OD) δ 176.46, 148.53, 124.13, 98.59, 81.50, 76.91, 74.23, 73.67, 71.53, 70.37, 55.97, 41.28, 35.80, 33.26, 29.95, 26.71, 25.79, 23.83, 14.40.

### Synthesis of 4A4Hex-calix[4]-paromomycin conjugate 3

***Compound 13:*** 430 mg of paromomycin **10** (0.7 mmol) were dissolved in a CH$_3$CN/H$_2$O mixture (2:1 (v/v)), then 196 mg of **11** (0.84 mmol) and 193 mg of K$_2$CO$_3$ (1.4 mmol) were added, and then the reaction mixture was stirred for 48 hrs at r.t. The solvents were removed under reduced pressure and the crude dissolved in 10 mL of dH$_2$O. Next, 567 mg of triethylamine (5.6 mmol) were added to the solution dropwise. Afterwards, 1.2 g of di-tert-butyl dicarbonate (5.6 mmol) were dissolved in 10 mL of DMF, then added to the sol ution dropwise. The solution was next stirred for 24 hrs at r.t. The reaction mixture was then diluted in ethyl acetate and washed with 20 mL of dH$_2$O (3 times) and 20 mL of brine (3 times). The organic layer was separated, dried over Na$_2$SO$_4$ and the solvent removed under reduced pressure. The crude was purified by flash chromatography leading to the compound **13** as a white powder in 43% yield.

***Compound 15***: 390 mg of **14** (0.29 mmol) were dissolved in 10 mL of CH$_3$OH/THF/H$_2$O mixture (6:1.5:1 (v/v/v)). Next, 45 mg of sodium ascorbate (0.23 mmol) and 42 mg of Cu(OAc)$_2$ (0.23 mmol) were added. Then, **7** (0.23 mmol), dissolved in a minimum amount of THF, were added. The mixture was next sonicated until disappearance of the starting material (TLC monitoring), then the mixture was diluted with CH$_2$Cl$_2$, filtered over a celite pad and the solvent was removed under reduced pressure. The crude was purified with flash chromatography (0-10% MeOH in CH$_2$Cl$_2$) leading to the compound **15** as a white solid in 79% yield. *Rf* = 0.52 (CH$_3$Cl:CH$_3$OH 9:1); $^1$H NMR (400 MHz, CD$_3$OD): δ =7.91 (s, 1H), 5.43 (s, 1H), 5.28 (s, 1H), 5.00 (s, 1H), 4.66 (s, 2H), 4.36 (d, J = 8Hz, 2H), 2.99-3.64 (m, 21H), 3.40 (bs, 6H), 3.09 (m, 2H), 2.39 (t, J = 4Hz, 2H), 2.07 (q, J = 6Hz, 3H), 1.53 (bs, 45H). $^{13}$C NMR (101 MHz, CD$_3$OD): δ =173.39, 155.65, 155.63, 155.35, 155.22, 145.57, 143.80, 141.51, 130.63, 121.36, 121.37, 107.40, 97.51, 96.14, 84.69, 80.42, 77.89, 77.61, 72.88, 71,73, 71.51, 70.13, 69.34, 68.77, 68.69, 67.70, 66.39, 60.23, 54.30, 46.83, 46.62, 46.41, 46.19, 45.98, 45.77, 45.56, 43.53, 38.32, 33.48, 33.06, 26.18,26.06, 25.98, 23.97, 23.01. ESI (*m/z*) 1348.4 [M+Na]+.

**Compound 3**: $^1$H NMR (400 MHz, D$_2$O) δ 8.09 (s, 4H), 7.03-6.57 (bs, 8H), 5.89 (s, 4H, anomeric), 5.51 (s, 4H, anomeric), 5.33 (s, 4H, anomeric), 4.73-4.65 (b, 4H), 4.53-4.47 (b, 4H), 4.43-4.37 (b, 8H), 4.36-4.31 (b, 4H), 4.22-4.15 (m, 8H), 4.10-3.97 (m, 24H), 3.93.3.82 (m, 20H), 3.81-3.77 (bs, 8H), 3.76-3.66 (m, 28H), 3.63-3.55 (m, 16H) , 3.48 (d, 4H), 2.88 (bs, 8H), 2.65 (m, 4H), 2.44 (m, 8H), 2.03 (m, 20H), 1.46 (m, 32H), 1.00 (bs, 12H). $^{13}$C NMR (101 MHz, D$_2$O) δ 176.17, 146.04, 124.86, 120.81, 117.91, 115.01, 112.11, 109.67, 96.34, 84.24, 82.52, 77.99, 77.86, 76.67, 75.53, 74.87, 74.25, 74.09, 72.67, 72.42, 69.99, 69.62, 69.10, 68.54, 67.69, 66.44, 60.80, 60.68, 54.07, 52.24, 51.38, 51.11, 49.84, 49.24, 49.11, 44.19, 39.41, 34.99, 32.07, 30.30, 28.24, 26.06, 24.71, 23.58, 22.80, 13.84.

# 3.6 References

1.      Mochizuki, S., Nishina, K., Fujii, S., Sakurai, K. The transfection efficiency of calix[4]arene-based lipids: the role of the alkyl chain length. *Biomater. Sci.* **3,** 317–322 (2015).

2.      Ortiz Mellet, C., Benito, J. M., García Fernández, J.M. Preorganized, Macromolecular, Gene-Delivery Systems. *Chem. A Eur. J.* **16,** 6728–6742 (2010).

3.      Rodik, R. V., Anthony, A.-S., Kalchenko, V. I., Mély, Y., Klymchenko, A. S. Cationic amphiphilic calixarenes to compact DNA into small nanoparticles for gene delivery. *New J. Chem.* **39,** 1654–1664 (2015).

4.      Sansone, F. *et al.* DNA Condensation and Cell Transfection Properties of Guanidinium Calixarenes: Dependence on Macrocycle Lipophilicity, Size, and Conformation. *J. Am. Chem. Soc.* **128,** 14528–14536 (2006).

5.      Bagnacani, V. *et al.* Arginine clustering on calix[4]arene macrocycles for improved cell penetration and DNA delivery. *Nat. Commun.* **4,** 1721-1729 (2013).

6.      Bagnacani, V. *et al.* Lower Rim Guanidinocalix[4]arenes: Macrocyclic Nonviral Vectors for Cell Transfection. *Bioconjugate. Chem.* **23,** 993–1002 (2012).

7.      Bagnacani, V. *et al.* Macrocyclic Nonviral Vectors: High Cell Transfection Efficiency and Low Toxicity in a Lower Rim Guanidinium Calix[4]arene. *Org. Lett.* **10,** 3953–3956 (2008).

8.      Yadav, S. *et al.* Multifunctional self-assembled cationic peptide nanostructures efficiently carry plasmid DNA in vitro and exhibit antimicrobial activity with minimal toxicity. *J. Mater. Chem. B* **2,** 4848–4861 (2014).

9.      Chen, M. *et al.* Multifunctional Hyperbranched Glycoconjugated Polymers Based on Natural Aminoglycosides. *Bioconjugate Chem.* **23,** 1189–1199 (2012).

10.     Huang, Y., Ding, X., Qi, Y., Yu, B., Xu, F.-J. Reduction-responsive multifunctional hyperbranched polyaminoglycosides with excellent antibacterial activity, biocompatibility and gene transfection capability. *Biomaterials* **106,** 134–143 (2016).

11.	Zimmermann, L. *et al.* Tuning the Antibacterial Activity of Amphiphilic Neamine Derivatives and Comparison to Paromamine Homologues. *J. Med. Chem.* **56,** 7691–7705 (2013).

12.	Taylor, P. C., Schoenknecht, F. D., Sherris, J. C., Linner, E. C. Determination of minimum bactericidal concentrations of oxacillin for *Staphylococcus aureus:* influence and significance of technical factors. *Antimicrob. Agents Chemother.* **23,** 142–150 (1983).

13.	Hu, Y., Liu, L., Zhang, X., Feng, Y., Zong, Z. In Vitro Activity of Neomycin, Streptomycin, Paromomycin and Apramycin against Carbapenem-Resistant Enterobacteriaceae Clinical Strains. *Front. Microbiol.* **8,** 2275 (2017).

14.	Bhattacharya, S., Bajaj, A. Advances in gene delivery through molecular design of cationic lipids. *Chem. Commun.* **31,** 4632 (2009).

15.	Ghilardi, A. *et al.* Synthesis of Multifunctional PAMAM–Aminoglycoside Conjugates with Enhanced Transfection Efficiency. *Bioconjugate Chem.* **24,** 1928–1936 (2013).

16.	Wang, H., Tor, Y. Electrostatic interactions in RNA aminoglycosides binding. *J. Am. Chem. Soc.* **119,** 8734–8735 (1997).

17.	Pezzoli, D., Giupponi, E., Mantovani, D., Candiani, G. Size matters for in vitro gene delivery: investigating the relationships among complexation protocol, transfection medium, size and sedimentation. *Sci. Rep.* **7,** 44134 (2017).

18.	Mintzer, M. A., Simanek, E. E. Nonviral Vectors for Gene Delivery. *Chem. Rev.* **109,** 259–302 (2009).

19.	Boussif, O. *et al.* A versatile vector for gene and oligonucleotide transfer into cells in culture and in vivo: polyethylenimine. *Proc. Natl. Acad. Sci. U. S. A.* **92,** 7297–301 (1995).

20.	Van Gaal, E. V. B. *et al.* How to screen non-viral gene delivery systems in vitro? *J. Control. Release* **154,** 218–232 (2011).

21.	Zuhorn, I. S. *et al.* Phase Behavior of Cationic Amphiphiles and Their Mixtures with Helper Lipid Influences Lipoplex Shape, DNA Translocation, and Transfection Efficiency. *Biophys. J.* **83,** 2096–2108 (2002).

22.     Candiani, G., Pezzoli, D., Ciani, L., Chiesa, R., Ristori, S. Bioreducible Liposomes for Gene Delivery: From the Formulation to the Mechanism of Action. *PLoS One* **5,** 13430 (2010).

23.     Zhou, J., Wang, G., Zhang, L.-H. Ye, X.S. Modifications of aminoglycoside antibiotics targeting RNA. *Med. Res. Rev.* **27,** 279–316 (2007).

24.     Nimse, S. B., Kim, T. Biological applications of functionalized calixarenes. *Chem. Soc. Rev.* **42,** 366–386 (2013).

25.     Casnati, A. *et al.* Synthesis, antimicrobial activity and binding properties of calix[4]arene based vancomycin mimics. *Bioorg. Med. Chem. Lett.* **6,** 2699–2704 (1996).

26.     Colston, M. J. *et al.* Antimycobacterial calixarenes enhance innate defense mechanisms in murine macrophages and induce control of Mycobacterium tuberculosis infection in mice. *Infect. Immun.* **72,** 6318–23 (2004).

27.     Kichler, A., Leborgne, C., Marz, J., Danos, O., Bechinger, B. Histidine-rich amphipathic peptide antibiotics promote efficient delivery of DNA into mammalian cells. *Proc. Natl. Acad. Sci.* **100,** 1564–1568 (2003).

28.     Dworkin, R. J. Aminoglycosides for the treatment of gram-negative infections: therapeutic use, resistance and future outlook. *Drug Resist. Updat.* **2,** 173–179 (1999).

29.     Vakulenko, S. B., Mobashery, S. Versatility of Aminoglycosides and Prospects for Their Future. *Clin. Microbiol. Rev.* **16,** 430–450 (2003).

30.     Mingeot-Leclercq, M.P., Glupczynski, Y., Tulkens, M. Aminoglycosides: Activity and Resistance *Antimicrob. Agents Chemother.* **43,** 727–737 (1999).

31.     Carmona-Ribeiro, A., de Melo Carrasco, L., Carmona-Ribeiro, A. M. de Melo Carrasco, L. D. Cationic Antimicrobial Polymers and Their Assemblies. *Int. J. Mol. Sci.* **14,** 9906–9946 (2013).

32.     Goswami, L. N., Houston, Z. H., Sarma, S. J., Jalisatgi, S. S., Hawthorne, M. F. Efficient synthesis of diverse heterobifunctionalized clickable oligo(ethylene glycol) linkers: potential applications in bioconjugation and targeted drug delivery. *Org. Biomol. Chem.* **11,** 1116 (2013).

33.    Sganappa, A. *et al.* Dendrimeric Guanidinoneomycin for Cellular Delivery of Bio-macromolecules. *ChemBioChem* **18,** 119–125 (2017).

34.    Park, W.K.C., Auer, M., Jaksche, H., Wong, C. Rapid Combinatorial Synthesis of Aminoglycoside Antibiotic Mimetics: Use of a Polyethylene Glycol-Linked Amine and a Neamine-Derived Aldehyde in Multiple Component Condensation as a Strategy for the Discovery of New Inhibitors of the HIV RNA Rev Responsive Element. *J. Am. Chem. Soc.* **118,** 10150-10155 (1996).

# Chapter IV: Role of generation on successful DNA delivery of PAMAM-(G)Neo Conjugates

## 4.1 Background

Dendrimers are a class of synthetic and well-structured polymers with excellent monodispersity and symmetrical three-dimensional (3D) branched architecture.[1,2] Due to such structural perfection, along with being highly branched, the presence of multiple peripheral end groups and internal cavities, and the relatively ease of synthesis (overall for low generations), dendrimers have attracted much interest for various applications.[3,4] For instance, they have been used as antibacterial agents[5,6] and antimicrobial surface coatings,[7] nanocarriers for smart drug delivery,[8,9] diagnostic agents,[10,11] and theranostics overall.[12] Above all, dendrimers have attracted great attention as a valid alternative to immunogenic viral vectors for the delivery of NAs.[13] Polyamidoamine (PAMAM) dendrimers have been probably the most explored, due to some unique features such as 1) their inherent ability to condense polyanionic NAs into the so-called dendriplexes, 2) the efficient cellular uptake of PAMAM dendriplexes on different cell lines and their localization into endo-lysosomes, 3) the presence of tertiary amines in the backbone responsible for the "proton sponge" effect favoring endosomal escape, 4) the presence of outer primary amino groups, cationic at physiological pH, and 5) their non-immunogenicity.[14] Although not very effective for siRNA delivery, structurally flexible PAMAMs have been used for gene silencing purposes as well.[15,16] However, some issues have been hampering their applications to a greater extent. Indeed, as gene delivery systems, PAMAM dendrimers have proven to suffer from the transfection efficiency and cytotoxicity paradox. High generation dendrimers are much more efficient transfectants, though they display severe cytotoxicity. Besides, the synthesis of high generation PAMAM dendrimers is unfortunately time-consuming and expensive, which largely limit their biomedical applications.[17] On the other hands, low generation dendrimers are notoriously less toxic, but less effective because of the pDNA complexation/decomplexation ability. In order to make dendrimeric PAMAMs ideal gene delivery vectors, it has been reported the functionalization of high generation PAMAMs with different ligands such as lipids, fluorous compounds, amino acids, polysaccharides, proteins and peptides, other polymers, and some cationic moieties,[13] while low generation PAMAMs have been nanoclustered through covalent and noncovalent bonding.[16] In this context, we have recently designed a new class of multifunctional PAMAM-AG conjugates[18] obtained

by grafting three different AGs, neamine, paromomycin and neomycin B antibiotics on the outer primary amino groups of PAMAM generation 4 (PAMAM G4). Such multifunctional PAMAM G4-AGs displayed high gene delivery efficiency along with negligible cytotoxicity, the PAMAM G4-Neo derivative being the most performing at low N/P.

Herein, we report a step further in the structure-function relationship analysis of such dendrimers, that is the evaluation of the effects of different PAMAM generations, namely G2, G4, and G7, on the efficiency and cytotoxicity of PAMAM-Neo conjugates (PAMAM G2-, G4-, G7-Neo). Starting from PAMAM G2, G4, and G7, we synthetized three polymeric conjugates with Neo using isothiocyanate/amine click chemistry. Moreover, along with PAMAM-Neo conjugates, we have synthetized also PAMAM G4-guanidinoneomycin (PAMAM G4-GNeo) in order to study the influence of guanidinylation on the gene transfection efficiency of these dendrimers.

# 4.2 Materials and methods

## 4.2.1 Materials and reagents

Refers to 2.2.3. Spectra/Por dialysis bags (MWCO = 1 and 8 kDa) were from Spectrum Laboratories (Compton, CA, USA). COS-7 (monkey kidney tissue-derived fibroblast-like, CRL-1651) cell lines were purchased from the American Type Culture Collection (ATCC, Manassas, VA, USA).

## 4.2.2 Synthesis of PAMAM-AG conjugates

General procedure for PAMAM-AG **1-4**. The organic solvent of commercial 10% (w/w) methanolic solution of PAMAM of different generations was evaporated in vacuo and co-evaporated twice with dichloromethane. Neat PAMAM was dissolved in DMSO and a solution of AG-isothiocyanate linker (1.2 equiv. per $NH_2$ group) in a minimal volume of DMSO was added. The solution was stirred at 60°C for 24 hrs. The solution was dialyzed against MeOH (8 hrs, the solvent reservoir was renewed three times, MWCO = 1 and 8 kDa). The solution was evaporated under reduced pressure to give N-Boc-protected PAMAM-AG derivatives. The resulting conjugates were dissolved in TFA and stirred for 30 min at r.t.. The excess of TFA was evaporated under reduced pressure, the crude dissolved in $dH_2O$ and the solution dialyzed overnight against $dH_2O$ (MWCO = 1 kDa). Freeze-drying of the resulting $dH_2O$ solution lead to recover fluffy, white solids. Complete N-Boc deprotection occurred in all cases as evidenced by the NMR spectra.

### 4.2.3 Biological assays

**Preparation of dendrimer solutions:** PAMAM G2, G4 and G7 were diluted in $dH_2O$ to a final concentration of 4.48 mg/mL, 5.0 mg/mL, and 5.0 mg/mL, respectively, corresponding invariably to final nitrogen concentration ([N]) of 22 mM. PAMAM G2-Neo, G4-Neo and G4-GNeo derivatives were diluted in $dH_2O$ to a final concentration of 4.05 mg/mL, 4.12 mg/mL, and 4.57 mg/mL, respectively, corresponding invariably to final nitrogen concentration ([N]) of 22 mM. PAMAM G7-Neo was diluted $dH_2O$ to a final concentration of 2.07 mg/mL, corresponding to final [N] of 6.5 mM, while 25 kDa bPEI was diluted in 10 mM HEPES to a concentration of 0.86 mg/mL and a [N] = 20 mM, considering that there is one nitrogen per repeat PEI unit (-NHCH2CH2-, MW = 43 Da). Dendrimers and bPEI were stored at 4°C until use.
**Preparation of dendriplexes and evaluation of DNA complexation (binding) ability**: Refers to 3.2.3
**Measurement of size ($D_H$) and zeta-potential ($\zeta_P$) of complexes**. Refers to 3.2.3
**In vitro cells transfection experiments.** Cell cultures: refers to 2.2.3
**In vitro cells transfection:** Cells were seeded onto 96-well plates at a density of $2\times10^4$ cells/$cm^2$ and maintained in standard culture conditions for 24 hrs. Next, 160 ng/well of pGL3 were complexed in 10 mM HEPES with PAMAMs and PAMAMs-Neo solutions to yield different N/P (i.e., 1, 2, 3, 5, 15, 30, 45, 60, 75), and cells were incubated with complexes in 100 µL/well of culture medium under standard culture conditions for further 48 hrs. Cells transfected with 25 kDa bPEI/DNA complexes prepared at N/P 10 were used as internal reference.
Following 48-hr transfection, cytotoxicity and transfection efficiency were evaluated as reported in 2.2.
**Statistical analysis**: refers to 3.2.3

## 4.3 Results and discussion

Since their first use in 1993,[19] PAMAM dendrimers have been extensively investigated as non-viral gene delivery vectors. Being dendrimers, PAMAMs possess a well-defined structure, characterized by many functional end groups, responsible for high solubility (especially at low generations) and reactivity, and inner cavities serving as binding sites for drugs. In spite of their fairly good transfection efficiency (especially at high generations), the widespread use of PAMAMs as delivery agents is limited because of their inherent toxicity and high costs. On the other hand, the chemical reactivity of primary amino end-groups of PAMAMs allows for and easy

functionalization with specific moieties to give rise to more and more effective gene vectors.

In this context, we propose the synthesis of an array of PAMAM dendrimers, namely PAMAM G2 (Fig. 46), G4 and G7, decorated with the (G)Neo moiety (Fig. 47). After a thorough chemical characterization to calculate the grafting yield, we have evaluated and compared the performances of PAMAM-(G)Neo dendrimers with those of the parent pristine PAMAMs in transfection, in order to shed light on the role of the dendrimer generation on grafting and thus on their ultimate transfection efficiency in two cell lines, namely HeLa and COS-7 cells.
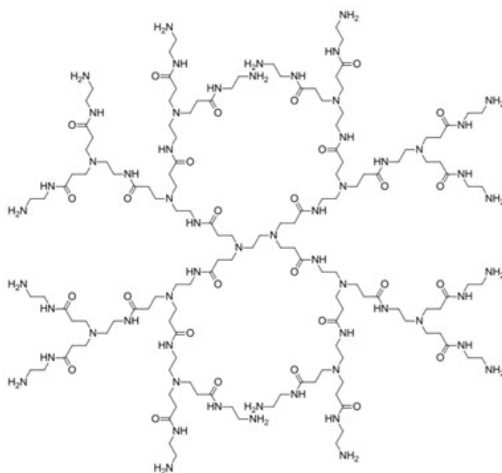
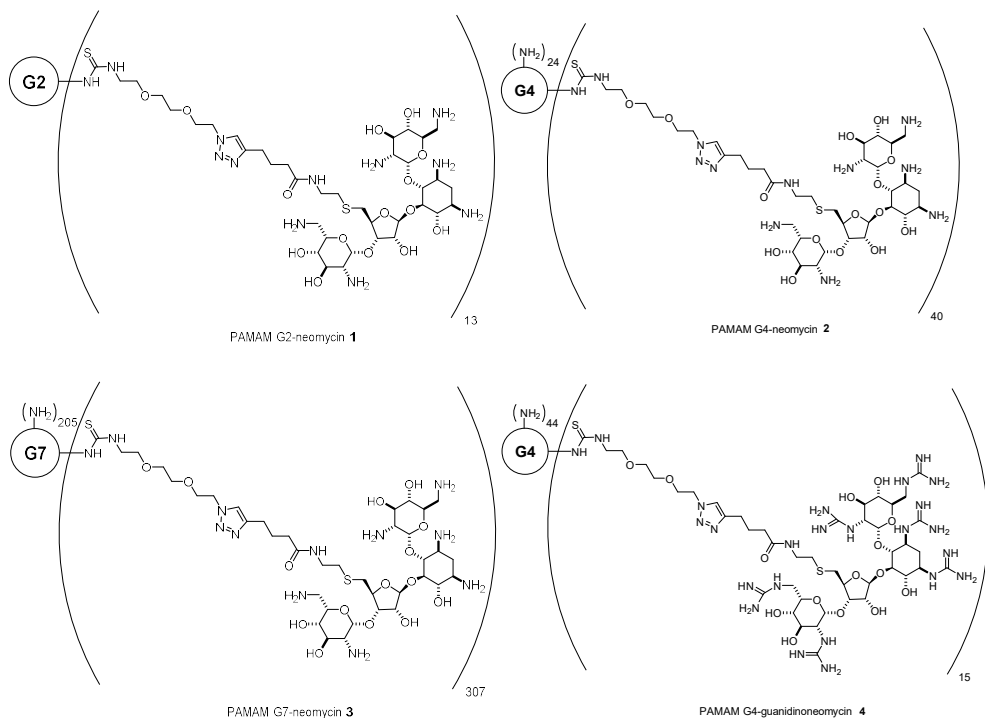

**Fig. 46** *Structure of PAMAM G2*

***Fig. 47 PAMAM-(G)Neo conjugates:*** *schematic representation of PAMAM G2-, G4-, G7-neomycin and PAMAM-G4-guanidinoneomycin conjugates.*

## 4.3.1 Synthesis and characterization of PAMAM G2-, G4-, G7-neomycin and PAMAM G4-guanidinoneomycin conjugates.

AGs are a class of polyaminosugar antibiotics that have been widely used as chemotherapeutic agents in the treatment of bacterial infections and, more recently, as antifungal agents.[20,21] Due to their cationic-bearing moieties, AGs have already been used to build cationic amphiphils[22] and polymers[23,24] for gene delivery. In this context, we have previously developed dendrimeric PAMAM G4-AG conjugates and studied their effectiveness as gene delivery systems in three different cell lines.[25] Considering the high performances obtained with such vectors, especially those of PAMAM G4 tethered with Neo and Paro, we decided to investigate more in depth the influence of the PAMAM generation on their effectiveness in transfection. Moreover, since it has been shown that the conversion of the primary amines of AGs into guanidino groups increases dramatically the ability of AG to deliver high molecular weight cargos into cells,[25–27] we decided to explore the effect of guanidinylation by synthesizing a PAMAM G4-GNeo derivative. Likewise, we exploited the chemistry to anchor AGs and GNeo to the dendrimers, namely reaction between isothiocyanate-functionalized-AGs with the primary amino groups of the PAMAM dendrimers, while

we slightly modified the linker in order to obtain the final conjugates in better yields and in a simpler way. In detail, starting from commercial available Neo **5**, we have synthetized alkyne terminal derivatives **6** and **7** following reported procedures (Fig. 48).[28]

Click reaction with isothiocyanate linker **8** led to the formation of intermediates **9** and **10**, respectively, in good yields, which were next coupled with PAMAM G2, G4, and G7 following the same conditions (DMSO, 40 °C, 12 hrs). After Boc-deprotection with TFA, dialysis in water, and freeze-drying, final PAMAM G2-Neo **1**, PAMAM G4-Neo **2**, PAMAM G7-Neo **3**, and PAMAM G4-GNeo **4** were obtained as fluffy solids.
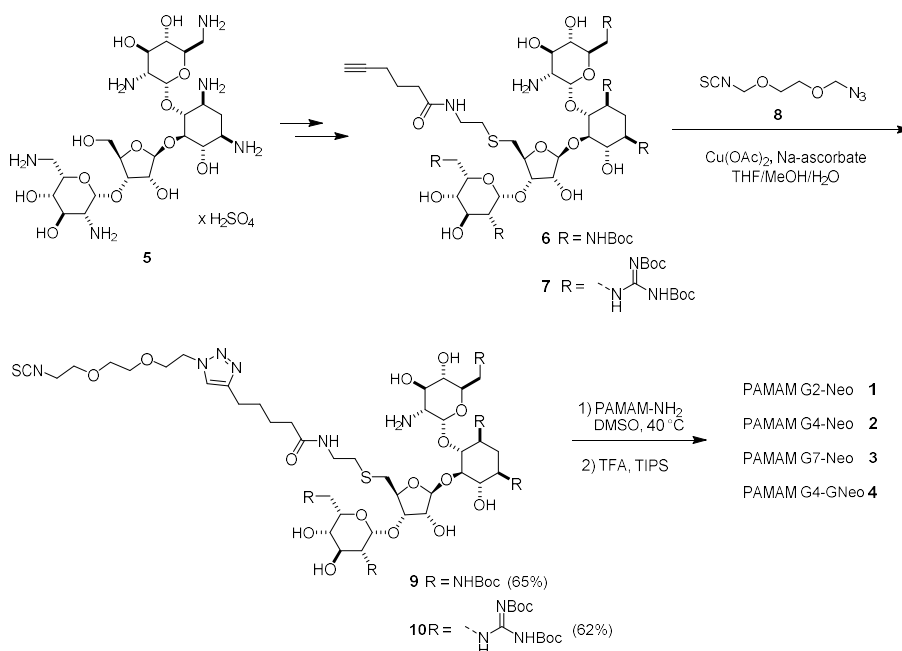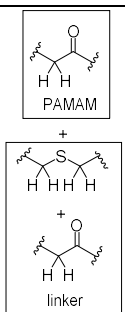


***Fig. 48 Synthesis of PAMAM-(guanidino)neomycin conjugates 1-4:** (G)Neomycin B was modified and equipped with a terminal alkyne (**6-7**). This derivative underwent click reaction with the SCN-PEG-N₃ linker to obtain **9-10**. Coupling with different generation of PAMAM, followed by Boc-deprotection afforded **1-4**.*

According to our previous studies,[25] the degree of grafting was first established by ¹H NMR analysis. Integration of the characteristic signals belonging to the Neo anomeric protons (three singlets resonating between 6.2 and 5.2 ppm), the proton belonging to the triazole ring (which resonates around 8.0 ppm) were compared to the integration of the broad multiplet resonating between 3.1 and 2.7 ppm which correspond to 1) the methylene protons in α position to the carbonyl group of PAMAM dendrimers (56 protons for PAMAM G2, 248 protons for PAMAM G4, and 2,040 protons for PAMAM G7), 2) the two methylene groups in α position to the sulfur atom and 3) the methylene

in α position to the carbonyl group, both belonging to the linker. The relative integrations of these signals revealed that we grafted 13 Neo to PAMAM G2, 40 Neo and 15 GNeo to PAMAM G4, and 307 Neo to PAMAM G7 (Table 1). The lower degree of grafting obtained with GNeo isothiocyanate **10** as compared to the corresponding Neo derivative **9** could be ascribed to the different steric hindrance. Except for PAMAM G7-Neo **3**, the degrees of grafting of **1**, **2**, **4** were also supported by MALDI mass analysis, through which the average molecular mass of the dendrimer derivatives was evaluated and compared to those calculated (Table 1).

**Table 1.** *Degree of grafting calculated by $^1$H NMR integrations and MALDI mass analysis.*

| | $^1$H NMR relative integration | | | | | *m/z value* | |
|---|---|---|---|---|---|---|---|
| | (G)Neo anomeric proton H' | [structure: PAMAM + linker] | Hydrogens belonging to the dendrimer | Calc. hydrogens belonging to the linker[a] | # of (G)Neo grafted[b] | Exp. value | Calc. [M+H$^+$] |
| **1** | 13.0 | 131.5 | 56.0 | 75.5 | 13.0 | 16030.2 | 16034.0 |
| **2** | 40.0 | 486.8 | 248.0 | 338.8 | 40.0 | 39342.7[c] | 39320.0[c] |
| **3** | 307.0 | 3880.8 | 2040.0 | 1804.8 | 307.0 | n.d.[d] | 418274. |
| **4** | 15.0 | 337.8 | 248.0 | 89.8 | 15.0 | 31736.1 | 31776.0 |

*a) The values are calculated subtracting the number of the hydrogens belonging to the PAMAM dendrimers to the hydrogens resonating between 3.1 and 2.7 ppm. b) The degree of grafting was determined dividing the calculated hydrogens belonging to the linker for 6 (number of hydrogens of the linker resonating between 3.1 and 2.7 ppm for the monomeric aminoglycoside) and rounded to the nearest unit. c) It was not possible to detect the MW of the conjugate, but we detected the peak corresponding the MW of the 40 neomycin-linker unit. d)The MW was not detected probably because the dendrimer does not vaporize.*

## 4.3.2 DNA binding ability evaluation and physico-chemical characterization of polyplexes

As for other polycations, such as polylysine (PLL) and polyethylenimine (PEI), PAMAM dendrimers have been shown to self-assemble with NAs through electrostatic interactions to form complexes, named dendriplexes. Indeed, PAMAM dendrimers contains in their backbone both tertiary amines at branching points, as well as protonated primary amino groups at the termini, the latter being responsible

for the binding of the pDNA phosphates. Besides, it has been found that Neo-tethering to dendrimers did enhance the ability of such polymers to pack the DNA.
In this study, PAMAMs at different generations, i.e., G2, G4 and G7, and their (G)Neo conjugates were used to complex and compact pDNA into polyplexes. We thus first evaluated by fluorophore-exclusion assay the ability of these three different arrays of gene delivery vectors (PAMAM G2 and G2-Neo; PAMAM G4, G4-Neo and G4-GNeo; PAMAM G7 and G7-Neo) to bind and condense pDNA as a function of the nitrogen-to-phosphate ratio (N/P). By plotting the fluorescence intensity vs. N/P, all the dendrimers tested displayed typical quasi-sigmoidal curves (PAMAM G2 and G2-Neo: Fig. 49A; PAMAM G4, G4-Neo and G4-GNeo: Fig. 49B; PAMAM G7 and G7-Neo: Fig. 49C).

Overall, any PAMAM derivative showed higher affinity for DNA than PEI, whose maximum pDNA complexation ability (i.e. when DNA is no longer accessible to the SYBR Green I because totally secluded in complexes) was found at N/P ≥ 3 (Fig. 50).[29,30] Of note, PAMAM G2 did displace slightly less SYBR Green I, showing a residual fluorescence signal of ≈ 10% even at high N/Ps (Fig. 49A). This behavior probably rely on the less tight binding of DNA owing to the little surface charge density of this low generation dendrimer.[31,32] Interestingly, the presence of Neo increased the affinity of PAMAM G2 for pDNA, being this AG a well-known NAs binder. Indeed, PAMAM G2-Neo was able to completely condense pDNA at N/P ≥ 1.5.
Besides, unconjugated PAMAM G4 and G7 displayed similar behaviors, because the greatest DNA complexation efficiency was at N/P 1. When tethering such PAMAMs with Neo or GNeo, a displacement of the complexation curve at high N/Ps was observed (maximum complexation ability at N/P 1.5 for PAMAM G4-Neo, and N/P 2 for PAMAM G4-GNeo and G7-Neo derivatives).
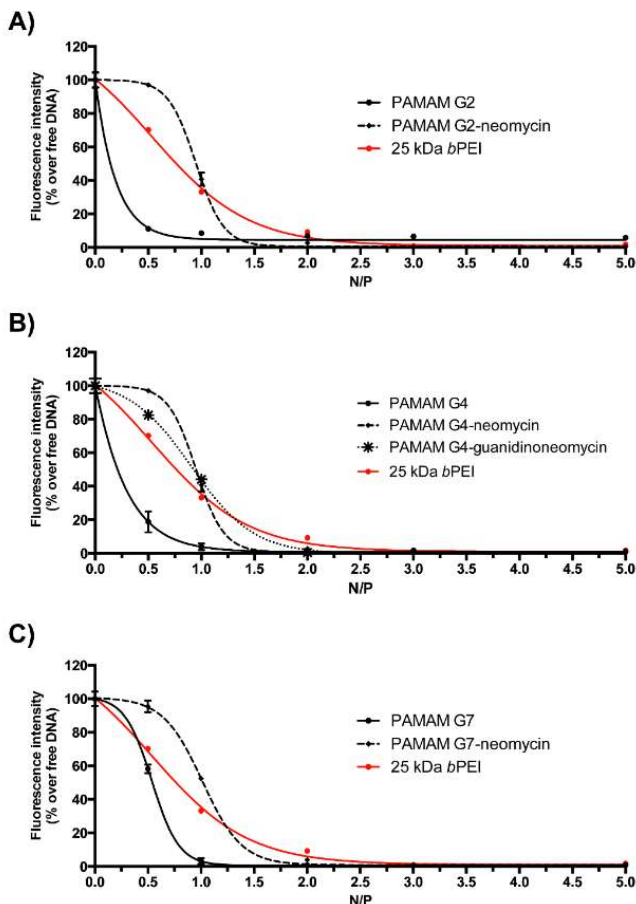
**Fig. 49. DNA complexation abilities of PAMAM G2, G4, G7** *(black circle and solid line) and their relative conjugates (black square (or star) and dotted line) vs. 25 kDa bPEI (red circle and solid line). A) Comparative DNA complexation ability of PAMAMs at different generations: A) G2; B) G4; C) G7. Results are expressed as mean ± SD (n = 3).*

As PAMAM G2, G4 and G7 dendrimers display a well-defined 3D structure and chemistry, such features allow preparing complexes with consistent structure, size and surface charge. Therefore, we investigated by DLS and Electrophoretic Light Scattering (ELS) the $D_H$ and the $\zeta_P$ of every dendriplexes in order to find a possible correlation between the physico-chemical properties of PAMAM- and PAMAM-Neo-based complexes and the transfection behaviors in vitro. In fact, it is well accepted that the size and surface charge are among the key factors affecting the transfection performances of any gene delivery vector, at least in vitro.[29,30]

PAMAM G2, G4 and G7 dendrimers in association with pDNA did form nanometric assemblies at N/P ≥ 2 (i.e., at the same N/P in which the DNA is totally buried within dendriplexes), while the $D_H$ profile of every PAMAM-Neo derivative was fairly

constant at N/P ≥ 5 (Fig. 50). The $\zeta_P$ curves of low generation PAMAMs and PAMAM-Neos as a function of N/P fitted well with an exponential decay equation model, while the best curve fit for PAMAM G7 and G7-Neo was the linear least-squares line with slope 0, so that we found only minor variations in the overall dimensions of dendriplexes as the N/P was increased.

In more detail, complexes of PAMAM G2 and G7 and their corresponding –Neo conjugates, prepared at N/P ≥ 2, showed similar dimensions, ranging over a narrow distribution of ≈ 100-170 nm (Figs 50A and 50C) (p > 0.05 for every series), along with highly positive $\zeta_P$, in good agreement with previously published data.[33] Among them, pDNA/PAMAM G7 complexes displayed the highest $\zeta_P$ of ≈ +35 mV, while PAMAM G2-based dendriplexes exhibited an overall surface charge of +20-25 mV. Such results substantiate the evidence that surface charge is related to dendrimer generation, with PAMAM G2 and G7 showing different $\zeta_P$ behaviors, irrespective of the N/P.

On the other hand, PAMAM G4-based complexes (at N/P ≥ 2) displayed the largest $D_H$, ranging from 200 nm to 450 nm (Fig. 50B), and the lowest $\zeta_P$ of ≈ +10 mV. The conjugation with Neo, whether or not guanidinylated, gave rise to the formation of smaller complexes with $D_H$ < 200 nm (Fig 50B), and higher $\zeta_P$ of ≈ +25 mV (at N/P ≥5). As highlighted by high $D_H$ values and the overall negative surface charge (Figs 50A and 50B), it is also apparent that no stable and fully condensed dendriplexes were found for PAMAM G2 and G4 series at N/P < 2. This was probably because in such conditions residual unshielded DNA was still present.

Taken together, these results led to the conclusion that all PAMAMs effectively condense pDNA into nanoassemblies with positive surface charge, although to different extent. This is a compulsory requirement for gene delivery vectors.
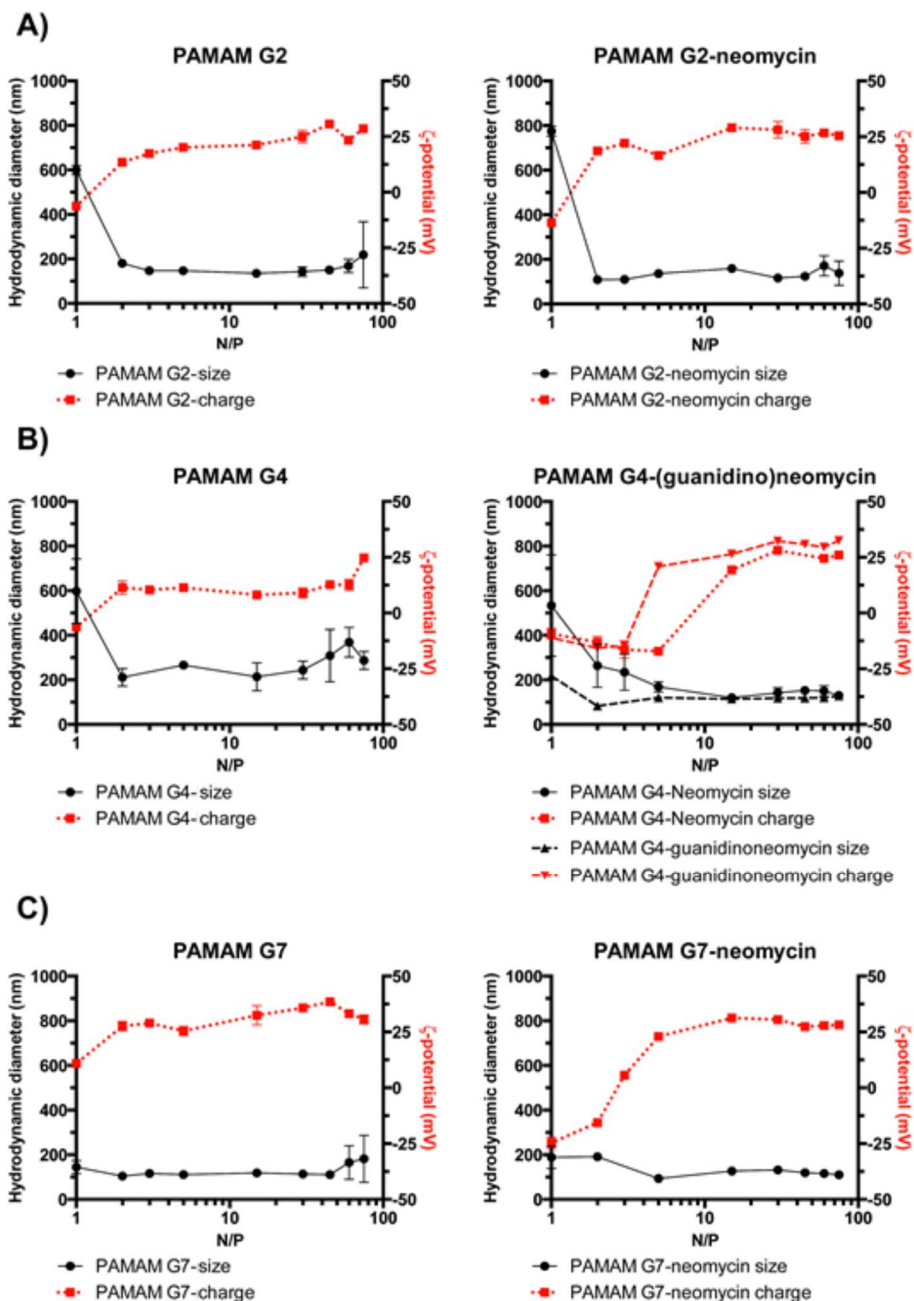
**Fig. 50 Physico-chemical characterization of PAMAMs and PAMAM-AG derivatives**. *Mean hydrodynamic diameter ($D_H$; black circle (triangle) and solid (dashed) line) and overall surface charge ($\zeta_P$; red square (triangle) and dotted (dashed) line), measured by Dynamic Light Scattering (DLS) and Laser Doppler microelectrophoresis, of: A) PAMAM G2 (left panel) and PAMAM G2-Neo (right panel); B) PAMAM G4 (left panel) and PAMAM G4-GNeo (right panel); C) PAMAM G7 (left panel) and PAMAM G7-Neo (right panel). Results are expressed as mean ± SD (n = 3)*

### 4.3.3 In vitro transfection of pDNA/PAMAMs and pDNA/PAMAMs-Neo conjugates.

Transfection efficiency mediated by PAMAM dendrimers has been shown to be dependent on the dendrimer generation. In fact, the higher the generation, the greater the efficiency.[33,34]

In two cell lines, namely HeLa and COS-7 cells, dendriplexes obtained through the mixing of PAMAM G2 (-Neo), G4 (-Neo) and G7 (-Neo) with pDNA at N/P ≥ 3 (i.e., the minimum N/P at which cationic nanoparticles were obtained) exhibited transfection efficiencies similar or even greater than the gold standard 25 kDa bPEI. Of note, pristine PAMAMs displayed different, generation-specific transfection behaviors; pDNA/PAMAM G4 showed the lowest transfection efficiency (Fig. 51), with a plateau at N/P ≥ 5. Such outcome is not surprising if considering the lower $\zeta_P$ displayed by PAMAM G4-based dendriplexes with respect to that of the other PAMAMs. On the other hand, pDNA/PAMAM G7 displayed the highest transfection efficiency at almost all N/Ps tested, with the greatest transgene expression at N/P 75 (Fig. 51C, right panel) and a very low cytotoxicity (Fig. 51C, left panel). Besides, the transfection efficiency of pDNA/PAMAM G2 dendriplexes showed a bell-shape trend, with the maximum centered at N/P 45 (Figure 51A, right panel). Our findings show that high generation dendrimers (PAMAM G7) were more effective in transfecting cells than the less branched counterparts (PAMAM G2 and G4). Similar results were reported by Kukowska-Latallo as well.[34] Although to a different extent, such trends were also found transfecting COS-7 cells (Fig. 52, right panels), but PAMAM G2, G4 and G7 dendriplexes were roughly more toxic to COS-7 than HeLa cells (Fig. 52, left panels), and the cytotoxicity invariably increased as a function of the N/P. Such observations corroborate the fact that the overall surface charge of complexes dramatically affects their ultimate transfection efficiency.

**Fig. 51 Cytotoxicity and transfection efficiency of complexes** *prepared by mixing pGL3 plasmid with PAMAMs at different N/P, evaluated in HeLa cells. A) PAMAM G2 and PAMAM G2-Neo; B) PAMAM G4, PAMAM G4-Neo and PAMAM G4-GNeo; C) PAMAM G7 and PAMAM G7-Neo. Complexes prepared mixing pGL3 and 25 kDa bPEI at N/P 10 were used as internal reference. Results are expressed as mean ± SD (n ≥ 4) (\*p < 0.05 vs. unconjugated PAMAM; #p < 0.05 vs. bPEI).*
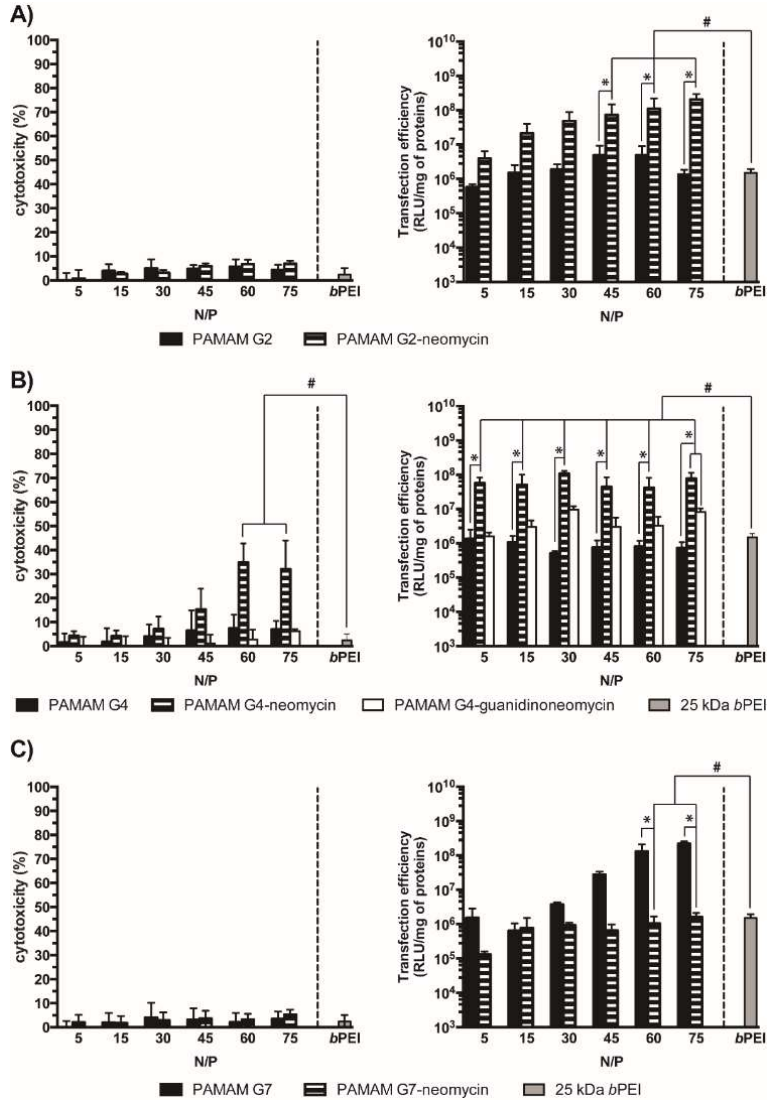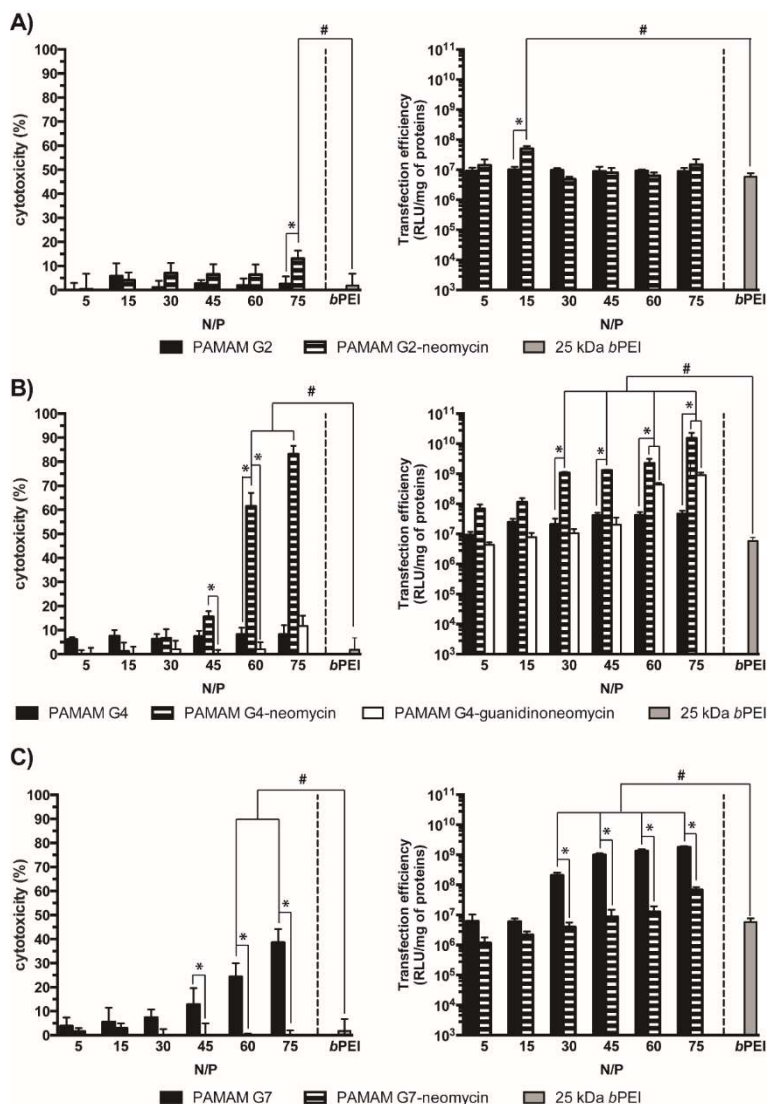
**Fig. 52 Cytotoxicity and transfection efficiency of complexes** *prepared by mixing pGL3 plasmid with PAMAMs at different N/Ps, evaluated in COS-7 cells. A) PAMAM G2 and PAMAM G2-Neo; B) PAMAM G4, PAMAM G4-Neo and PAMAM G4-GNeo; C) PAMAM G7 and PAMAM G7-Neo. Complexes prepared mixing pGL3 and 25 kDa bPEI at N/P 10 were used as internal references. Results are expressed as mean ± SD (n ≥ 4) (\*p < 0.05 vs. unconjugated PAMAM; #p < 0.05 vs. bPEI).*

We have recently shown that the conjugation of PAMAM G4 with AGs, such as Neo, Paro and Nea dramatically enhanced the transfection behavior.[25] In the present study we made another step forward in putting the puzzle together through the investigation of the possible effects of grafting different generations of PAMAM dendrimers with the AG unit Neo.

Interestingly, PAMAM G2-Neo dendriplexes at any N/P tested displayed a ≈ 10-fold increase in transfection efficiency and greater cytotoxicity (Fig. 51A and 52A, respectively) than the pristine PAMAM G2 one in both HeLa (Fig. 51A) (PAMAM G2-Neo vs. PAMAM G2: $p < 0.05$ at N/P ≥ 15) and COS-7 cells (Fig. 52A) (PAMAM G2-Neo vs. PAMAM G2: $p < 0.05$ at N/P 15). Instead, PAMAM G7-Neo displayed an opposite behavior. In fact, from Fig. 51C and Fig. 52C it is apparent that pDNA/PAMAM G7-Neo dendriplexes induced lower luciferase expression in HeLa cells (and COS-7 as well) than pDNA/PAMAM G7 complexes, especially for high N/Ps. It is worthy of note that the physico-chemical features of complexes prepared with PAMAM G2 and G7 (and the corresponding –AG conjugates) were quite different (PAMAM G2(-Neo) at N/P 5-75: $\zeta_P$ ≈ +25 mV vs. PAMAM G7(-Neo) at N/P 5-75: $\zeta_P$ ≈ +35 mV), which means that the differences found in transfection may rely on the PAMAM generation underpinning the specific features of pDNA/PAMAM assemblies. As shown in Fig. 51B, all the pDNA/PAMAM G4-Neo dendriplexes were much more efficient in transfecting HeLa and COS-7 cells than complexes prepared with parent PAMAM G4 (PAMAM G4-Neo vs. PAMAM G4: $p < 0.05$ at NP ≥ 30). In particular, PAMAM G4-Neo was more effective at N/P 30 in both cell lines, especially considering the severe cytotoxic effects displayed at N/P ≥ 45 (Fig. 51B and 51B).

On the other hand, a similar trend was observed once GNeo was tethered to PAMAM G4. As reported in Fig. 51B, the transfection efficiency of pDNA/PAMAM G4-GNeo complexes was higher than that of PAMAM G4 complexes prepared at N/P > 5, and the cytotoxicity they showed was low-to-negligible. As expected, also the transfection profiles of such dendriplexes were strongly dependent on the N/P and the cell line used to carry out transfections; when used to transfect HeLa and COS-7 cells, pDNA/PAMAM G4-GNeo complexes were indeed more effective at N/P 30 and N/P 75, respectively (Fig. 51B, right panel, and 51B, right panel). Besides, pDNA/PAMAM G4-GNeo complexes were less efficient than the –Neo counterparts. Such findings mirrored the results reported by Lehn's group.[35] The reasons for such unfavorable effect remain to be elucidated, though. It is widely accepted that the grafting of guanidino groups to macromolecules favors their cellular uptake.[26,27,36] However, after polyplex uptake, the DNA decomplexation has to occur in a way as efficient as possible in order to enable the release of the transgene and thus its transcription. Some experimental evidence suggests that the presence of guanidinium moieties, in lieu of the primary amines, is likely to strengthen the interaction with the DNA, thus increasing excessively the stability of complexes so that cells are hardly able to disassemble them intracellularly. Besides, we may speculate that the strong basicity of the guanidino group may also affect the buffering capacity of the PAMAM dendrimers, which is one of the reasons of the high transfection activities of several cationic vectors such as PEI.[37]

It is worthy of note that every PAMAM-(G)Neo dendrimer, when tested at the optimum N/P, invariably exhibited greater transfection efficiency than the gold standard 25 kDa bPEI in both HeLa and COS-7 cells.

# 4.4 Conclusions

We have synthesized and characterized four different PAMAM-(G)Neo conjugates, namely PAMAM G2-Neo, PAMAM G4-Neo, PAMAM G7-Neo and PAMAM G4-GNeo. We have tested their cytotoxicity and ability to condense DNA and to transfect two cell lines. Besides PAMAM G7-Neo, all the other conjugates showed greater transfection efficiencies as compared to their corresponding undecorated PAMAM dendrimers. PAMAM G4-GNeo derivative was much less efficient than the corresponding Neo derivative although GNeo (and in general guanidinylation) is known to promote efficient cellular uptake. Of note, PAMAM G4-Neo was the most effective transfectant because very efficient (and much more efficient than gold standard transfectant 25 kDa bPEI) at any N/P, and although its cytotoxicity is not negligible at N/P ≥ 30. Notably, small PAMAM G2-Neo were able to completely condense pDNA, which was not the case for the undecorated PAMAM G2, and, at high N/P (N/P ≥ 45), displayed low cytotoxicity and was more efficient in transfecting HeLa cells than PAMAM G4-Neo. These results are very intriguing because low generation dendrimers are cheaper, safer, and easier to functionalize as compared to the higher generation counterparts. Overall, this study highlights the beneficial effect on transfection of Neo-grafting on low- (G2) to medium- (G4) generation PAMAM dendrimers. Due to high transfection efficiency, low cytotoxicity, and low costs, PAMAM G2-Neo is a very promising gene delivery vehicle.

# 4.5 References

1.      Tomalia, D. A. Birth of a new macromolecular architecture: dendrimers as quantized building blocks for nanoscale synthetic polymer chemistry. *Prog. Polym. Sci.* **30,** 294–324 (2005).

2.      Medina, S. H., El-Sayed, M. E. H. Dendrimers as Carriers for Delivery of Chemotherapeutic Agents. *Chem. Rev.* **109,** 3141–3157 (2009).

3.      Tomalia, D. A. Dendritic effects: dependency of dendritic nano-periodic property patterns on critical nanoscale design parameters (CNDPs). *New J. Chem.* **36,** 264–281 (2012).

4.      Tomalia, D. A. Dendrons/dendrimers: quantized, nano-element like building blocks for soft-soft and soft-hard nano-compound synthesis. *Soft Matter* **6,** 456–474 (2010).

5.      García-Gallego, S. *et al.* Function Oriented Molecular Design: Dendrimers as Novel Antimicrobials. *Molecules* **22,** 1581 (2017).

6.      Scorciapino, M. *et al.* Antimicrobial Dendrimeric Peptides: Structure, Activity and New Therapeutic Applications. *Int. J. Mol. Sci.* **18,** 542 (2017).

7.      Mintzer, M. A., Dane, E. L., O'Toole, G. A., Grinstaff, M. W. Exploiting Dendrimer Multivalency To Combat Emerging and Re-Emerging Infectious Diseases. *Mol. Pharm.* **9,** 342–354 (2012).

8.      Wang, H., Huang, Q., Chang, H., Xiao, J., Cheng, Y. Stimuli-responsive dendrimers in drug delivery. *Biomater. Sci.* **4,** 375–390 (2016).

9.      Nanjwade, B. K., Bechra, H. M., Derkar, G. K., Manvi, F. V., Nanjwade, V. K. Dendrimers: Emerging polymers for drug-delivery systems. *Eur. J. Pharm. Sci.* **38,** 185–196 (2009).

10.     Wolinsky, J. B., Grinstaff, M. W. Therapeutic and diagnostic applications of dendrimers for cancer treatment. *Adv. Drug Deliv. Rev.* **60,** 1037–1055 (2008).

11.     Krause, W., Hackmann-Schlichter, N., Maier, F. K. Müller, R. Dendrimers in Diagnostics. *Dendrimers 210,* 261–308 (2000).

12.    Leiro, V., Garcia, J. P., Tomás, H. Pêgo, A. P. The Present and the Future of Degradable Dendrimers and Derivatives in Theranostics. *Bioconjugate Chem.* **26,** 1182–1197 (2015).

13.    Yang, J., Zhang, Q., Chang, H., Cheng, Y. Surface-Engineered Dendrimers in Gene Delivery. *Chem. Rev.* **115,** 5274–5300 (2015).

14.    Cheng, Y., Zhao, L., Li, Y., Xu, T. Design of biocompatible dendrimers for cancer diagnosis and therapy: current status and future perspectives. *Chem. Soc. Rev.* **40,** 2673-2703 (2011).

15.    Kang, H., DeLong, R., Fisher, M. H., Juliano, R. L. Tat-Conjugated PAMAM Dendrimers as Delivery Agents for Antisense and siRNA Oligonucleotides. *Pharm. Res.* **22,** 2099–2106 (2005).

16.    Cao, Y., Liu, X. Peng, L. Molecular engineering of dendrimer nanovectors for siRNA delivery and gene silencing. *Front. Chem. Sci. Eng.* **11,** 663–675 (2017).

17.    Duncan, R., Izzo, L. Dendrimer biocompatibility and toxicity. *Adv. Drug Deliv. Rev.* **57,** 2215–2237 (2005).

18.    Ghilardi, A. *et al.* Synthesis of multifunctional PAMAM-aminoglycoside conjugates with enhanced transfection efficiency. *Bioconjugate Chem.* **24,** 1928–1936 (2013).

19.    Haensler, J., Szoka, F. C. Polyamidoamine cascade polymers mediate efficient transfection of cells in culture. *Bioconjugate Chem.* **4,** 372–379 (1993).

20.    Houghton , J. L., Green, K. D., Chen , W. Garneau-Tsodikova, S. The Future of Aminoglycosides: The End or Renaissance? *ChemBioChem* **11,** 880–902 (2010).

21.    Fosso, M. Y., Li, Y., Garneau-Tsodikova, S. New trends in the use of aminoglycosides. *Med. Chem. Commun.* **5,** 1075–1091 (2014).

22.    Desigaux, L. *et al.* Self-assembled lamellar complexes of siRNA with lipidic aminoglycoside derivatives promote efficient siRNA delivery and interference. *Proc. Natl. Acad. Sci.* **104,** 16534–16539 (2007).

23.    Lee, M. M., French, J. M., Disney, M. D. Influencing uptake and localization of aminoglycoside-functionalized peptoids. *Mol. BioSyst.* **7,** 2441-2451 (2011).

24.    Chen, M. *et al.* Multifunctional Hyperbranched Glycoconjugated Polymers Based on Natural Aminoglycosides. *Bioconjugate Chem.* **23,** 1189–1199 (2012).

25.    Ghilardi, A. *et al.* Synthesis of Multifunctional PAMAM–Aminoglycoside Conjugates with Enhanced Transfection Efficiency. *Bioconjugate Chem.* **24,** 1928–1936 (2013).

26.    Elson-Schwab, L. *et al.* Guanidinylated neomycin delivers large, bioactive cargo into cells through a heparan sulfate-dependent pathway. *J. Biol. Chem.* **282,** 13585–13591 (2007).

27.    Sarrazin, S., Wilson, B., Sly, W. S., Tor, Y. Esko, J. D. Guanidinylated neomycin mediates heparan sulfate-dependent transport of active enzymes to lysosomes. *Mol. Ther.* **18,** 1268–1274 (2010).

28.    Dix, A. V. *et al.* Cooperative, Heparan Sulfate-Dependent Cellular Uptake of Dimeric Guanidinoglycosides. *ChemBioChem* **11,** 2302–2310 (2010).

29.    Mintzer, M. A. Simanek, E. E. Nonviral Vectors for Gene Delivery. *Chem. Rev.* **109,** 259–302 (2009).

30.    van Gaal, E. V. B. *et al.* How to screen non-viral gene delivery systems in vitro? *J. Control. Release* **154,** 218–232 (2011).

31.    Navarro, G., Tros de ILarduya, C. Activated and non-activated PAMAM dendrimers for gene delivery in vitro and in vivo. *Nanomedicine: NBM* **5,** 287–297 (2009).

32.    Chen, W., Turro, N.J.,  Tomalia, D. A. Using Ethidium Bromide To Probe the Interactions between DNA and Dendrimers, *Langmuir,* **16**, 15-19 (2000).

33.    Braun, C. S. *et al.* Structure/Function Relationships of Polyamidoamine/DNA Dendrimers as Gene Delivery Vehicles. *J. Pharm. Sci.* **94,** 423–436 (2005).

34.    Kukowska-Latallo, J. F. *et al.* Efficient transfer of genetic material into mammalian cells using Starburst polyamidoamine dendrimers. *Proc. Natl. Acad. Sci. U. S. A.* **93,** 4897–902 (1996).

35.    Martin, B. *et al.* The Design of Cationic Lipids for Gene Delivery. *Curr. Pharm. Des.* **11,** 375–394 (2005).

36.    Luedtke, N. W., Carmichael, P., Tor, Y. Cellular uptake of aminoglycosides, guanidinoglycosides, and poly-arginine. *J. Am. Chem. Soc.* **125,** 12374–12375 (2003).

37.    Vermeulen, H., Westerbos, S. J., Ubbink, D. T. Benefit and harm of iodine in wound care: a systematic review. *J. Hosp. Infect.* **76,** 191–199 (2010).

38.    Malloggi, C. *et al.* Comparative evaluation and optimization of off-the-shelf cationic polymers for gene delivery purposes. *Polym. Chem.* **6,** 6325–6339 (2015).

39.    Goswami, L. N., Houston, Z. H., Sarma, S. J., Jalisatgi, S. S. Hawthorne, M. F. Efficient synthesis of diverse heterobifunctionalized clickable oligo(ethylene glycol) linkers: potential applications in bioconjugation and targeted drug delivery. *Org. Biomol. Chem.* **11,** 1116 (2013).

Part III

Enhancing Aminoglycoside

Antibacterial activity

# Chapter V: Introduction to the use of AGs in synergy with other antibiotics

The discovery of antibiotics initiated a new era in medicine revolutionizing the management of bacterial infectious diseases. Together with the changing in the outcome of infections, they became crucial for advances in medicine in chemotherapy treatments and in surgery, thus allowing invasive operations as organ transplants.[1] Bacteria naturally evolve and develop resistance mechanisms; however, this natural process has been accelerated by human overuse of antibiotics in medical treatments and agriculture.[2] Nowadays, the development of resistance mechanisms[3] together with the lack of new discoveries due to economic and regulatory obstacles favored the occurrence of the present antibiotic crisis.[2,4] The World Health Organization (WHO), in fact, considers antibiotic resistance as a global health security threat.[5] In 2017 the European Antimicrobial Resistance Surveillance Network reported an increase in the percentage of *E. coli* resistant to the commonly used antibiotics with more than a half of the isolates resistant to at least one of the antibiotic groups under surveillance.[6] The dramatic increase in resistance to third-generation cephalosporins[7] and combined resistance to third-generation cephalosporins, fluoroquinolones and aminoglycosides[8] is particularly concerning.

In this scenario, it is clear that an effort toward the discovery of new antibiotics or the improvement of the activity of the already established ones is neccessary.

AGs' antibacterial activity depends upon their concentration in the cells. This means that their potency as antibacterial agents can be increased by increasing the concentration of the antibiotic within the bacteria. AGs are usually administered parentally,[9] however, if provided with drug delivery systems,[10] it is possible to increase the antibiotic concentration locally to the infection site. Moreover, an improved delivery of the AG to the bacteria would lower the dose of antibiotic needed to achieve a therapeutic effect, thus reducing the side effects. This is particularly relevant when prolonged treatment are needed.

A way to improve the effect of existing AGs is to provide them with an effective means of delivery to the bacteria. In this context, special formulations of AGs have been developed. Herein two examples are reported:

- TOBI is an inhalation solution with tobramycin as an active principle contained in a nebulizer or an inhaler device. Its function is to deliver high concentration of tobramycin in the lungs, where it is used to fight *P. aeruginosa* infections in cystic fibrosis patients.[10] Cystic fibrosis is a genetic

disease that predisposes to recurrent, and sometimes fatal, lung infections.[11] Inhaled tobramycin has been shown to be more effective than intravenous tobramycin in these patients.[12]

– ARIKACE is a form of amikacin enclosed in liposomal nanocapsules and is administered using a nebulizer system. Inhaled liposomal amikacin showed activity against respiratory infection with no acquired resistance.[13]

A great advantage of AGs is their ability to act in synergy if administered with other antimicrobial agents, such as azlocillin and penicillin.[14–17]
When combined with antibiotics that inhibit cell wall biosynthesis, such as β-lactams, AGs display a better cellular uptake due to the permeabilization of the bacteria membrane.[18] It was reported that a combination of ampicillin-amikacin was active against enterococcal infection despite the intrinsic resistance of this strain to both these antibiotics.[19]

A growing attention is being paid to studies on the combined effects of AGs and cationic AntiMicrobial Peptides (AMPs). The AMP family includes a wide range of peptides with antibacterial activity that share common features.[21] They are in fact short peptides (10-50 AAs), positively charged (+2, +9) owing to the presence of arginine, lysine and histidine, with a consistent part of hydrophobic AAs. Their amphiphilic structures fold creating a separation between the positively charged hydrophilic domain(s) and the hydrophobic domain(s), thus making such a molecule well suited to interact with membranes. AMPs are produced by every organism (including bacteria, plants, insects, birds and mammals) as part of the non-specific defense against infections.[21,22] Different AMPs have different target sites and mechanisms of action.[23] After interacting and crossing the outer membrane of Gram-negative bacteria, they interact and insert within the cytoplasmatic membrane. Their insertion is due to the formation of ion channels, transmembrane pores or the extensive membrane rupture. Besides these lytic mechanisms, AMPs can translocate across the membranes and, once inside the cytoplasm, they can inhibit cell-wall synthesis, NAs synthesis, protein synthesis or enzymatic activity.[21–24] AMPs have been already successfully used in synergy[25,26] with AGs. Recently, it was found that plectasin, a small cysteine-rich AMP, can be successfully used in synergy with neomycin and gentamicin showing improved antibacterial activity.[25] Bolosov *et al.* found that a synergystic effect can be achieved by using gentamicin in combination with another AMP, arecinin-1 against *S. Aureus*.[26] Moreover, it was recently demonstrated that the synergysitc effect can be achieved by covalent AGs-AMPs conjugates. They display an improved activity against both AGs-sensitive and AGs-resistant pathogens[27,28] if compared with a mixture of the AMP with the antibiotics.[29,30]

The effective synergy between AGs and AMPs covalently bonded give us the idea of synthesizing and exploring the antimicrobial properties of AG-AMP conjugates, as it will be discussed in the next chapter.

## 5.2 References

1.      Garrod, L. P., O'Grady, F. Antibiotic and chemotherapy. (1971).

2.      Fair, R. J., Tor, Y. Antibiotics and bacterial resistance in the 21st century. *Perspect. Medicin. Chem.* **6,** 25–64 (2014).

3.      Blair, J. M. A., Webber, M. A., Baylay, A. J., Ogbolu, D. O. Piddock, L. J. V. Molecular mechanisms of antibiotic resistance. *Nat. Rev. Microbiol.* **13,** 42–51 (2015).

4.      Ventola, C. L. The antibiotic resistance crisis: part 1: causes and threats. *J. Formul. Manag.* **40,** 277–83 (2015).

5.      *ANTIMICROBIAL RESISTANCE Global Report on Surveillance*.

6.      European Centre for Disease Prevention and Control. Surveillance of antimicrobial resistance in Europe. (2017).

7.      Tenover, F. C. Mechanisms of antimicrobial resistance in bacteria. *Am. J. Infect. Control* **34,** 64-73 (2006).

8.      Alekshun, M. N., Levy, S. B. Molecular Mechanisms of Antibacterial Multidrug Resistance. *Cell* **128,** 1037–1050 (2007).

9.      Kumana, C. R., Yuen, K. Y. Parenteral Aminoglycoside Therapy. *Drugs* **47,** 902–913 (1994).

10.     Takahashi, Y., Igarashi, M. Destination of aminoglycoside antibiotics in the 'post-antibiotic era'. *J. Antibiot. (Tokyo).* **71,** 4–14 (2018).

11.     Lyczak, J. B., Cannon, C. L., Pier, G. B. Lung infections associated with cystic fibrosis. *Clin. Microbiol. Rev.* **15,** 194–222 (2002).

12.     Cheer, S. M., Waugh, J., Noble, S. Inhaled Tobramycin (TOBI). *Drugs* **63,** 2501–2520 (2003).

13.     Rose, S. J., Neville, M. E., Gupta, R., Bermudez, L. E. Delivery of Aerosolized Liposomal Amikacin as a Novel Approach for the Treatment of Nontuberculous Mycobacteria in an Experimental Model of Pulmonary Infection. *PLoS One* **9,** 108703 (2014).

14.     Giamarellou, H., Zissis, N. P., Tagari, G., Bouzos, J. In Vitro Synergistic Activities of Aminoglycosides and New β-Lactams Against Multiresistant Pseudomonas aeruginosa. *Antimicrob. Agents Chemother.* **25,** 534-536 (1984).

15.     Anantharaman, A., Rizvi, M. S., Sahal, D. Synergy with Rifampin and Kanamycin Enhances Potency, Kill Kinetics, and Selectivity of De Novo-Designed Antimicrobial Peptides. *Antimicrob. Agents Chemother.* **54,** 1693–1699 (2010).

16.     Neu, H. C., Fu, K. P. Synergy of azlocillin and mezlocillin combined with aminoglycoside antibiotics and cephalosporins. *Antimicrob. Agents Chemother.* **13,** 813–819 (1978).

17.     Sande, M. A., Irvin, R. G. Penicillin-Aminoglycoside Synergy in Experimental Streptococcus viridans Endocarditis. *J. Infect. Dis.* **129,** 572–576 (1974).

18.     Moellering, R. C., Weinberg, A. N., Weinberg, A. N. Studies on antibiotic syngerism against enterococci. II. Effect of various antibiotics on the uptake of 14 C-labeled streptomycin by enterococci. *J. Clin. Invest.* **50,** 2580–2584 (1971).

19.     Iannini, P. B., Ehret, J., Eickhoff, T. C. Effects of ampicillin-amikacin and ampicillin-rifampin on enterococci. *Antimicrob. Agents Chemother.* **9,** 448–51 (1976).

20.     Hancock, R. E. W. Aminoglycoside uptake and mode of action-with special reference to streptomycin and gentamicin II. Effects of aminoglycosides on cell*s. of Antimicrob. Chemother* **8,** 428-445 (1981).

21.     Hancock, R. E. Cationic peptides: effectors in innate immunity and novel antimicrobials. *Lancet Infect. Dis.* **1,** 156–164 (2001).

22.     Hancock, R. E. Diamond, G. The role of cationic antimicrobial peptides in innate host defences. *Trends Microbiol.* **8,** 402–410 (2000).

23.     Brogden, K. A. Antimicrobial peptides: pore formers or metabolic inhibitors in bacteria? *Nat. Rev. Microbiol.* **3,** 238–250 (2005).

24.     Zasloff, M. Antimicrobial peptides of multicellular organisms. *Nature* **415,** 389–395 (2002).

25.     Hu, Y. *et al.* Combinations of β-lactam or aminoglycoside antibiotics with plectasin are synergistic against methicillin-sensitive and methicillin-resistant Staphylococcus aureus. *PLoS One* **10,** 1–15 (2015).

26.     Bolosov, I. A., Kalashnikov, A. A., Panteleev, P. V., Ovchinnikova, T. V. Analysis of synergistic effects of antimicrobial peptide arenicin-1 and conventional antibiotics. *Bull. Exp. Biol. Med.* **162,** 765–768 (2017).

27.     Mohamed, M. F., Brezden, A., Mohammad, H., Chmielewski, J. Seleem, M. N. Targeting biofilms and persisters of ESKAPE pathogens with P14KanS, a kanamycin peptide conjugate. *Biochim. Biophys. Acta Gen. Subj.* **1861,** 848–859 (2017).

28.     Bera, S., Zhanel, G. G., Schweizer, F. Evaluation of amphiphilic aminoglycoside–peptide triazole conjugates as antibacterial agents. *Bioorg. Med. Chem. Lett.* **20,** 3031–3035 (2010).

29.     Brezden, A. *et al.* Dual Targeting of Intracellular Pathogenic Bacteria with a Cleavable Conjugate of Kanamycin and an Antibacterial Cell-Penetrating Peptide. *J. Am. Chem. Soc.* **138,** 10945–10949 (2016).

30.     Deshayes, S. *et al.* Designing Hybrid Antibiotic Peptide Conjugates To Cross Bacterial Membranes. *Bioconjugate Chem.* **28,** 793–804 (2017).

# Chapter VI: Synthesis and study of the antibacterial properties of AGs-AMP conjugates

## 6.1 Background

Covalent combination of two antibiotics could be problematic due to a possible mutual interference. However, some attempts have been made with encouraging results. Schmidt *et al.* developed a new multifunctional antibiotic that combines two different antibacterial agents in a single molecule (pentobra): tobramycin and an AMP derived from penetratin.[1] Pentobra (Fig. 53) was proven to be efficient against *E. coli* and *S. aureus* persisters.[2] This approach was further explored by considering variations in the composition and the sequence of the peptide.[3] The activity of this multivalent antibiotic was applied against a wide range of *P. acne* isolates while being non-toxic for human cells.[4]
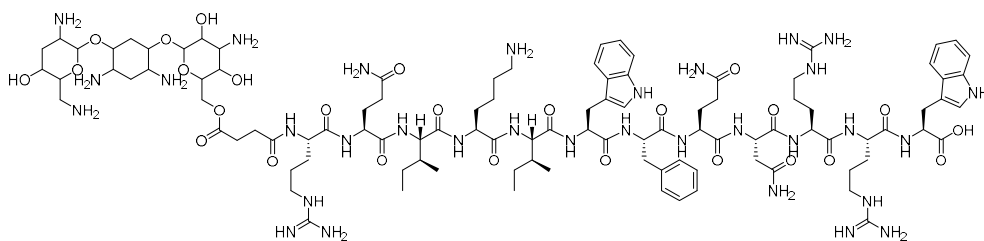


**Fig. 53 Pentobra**: *a multifunctional antibiotic that combines the effect of tobramycin and an antimicrobial peptide.*

Therefore, we hypothesize that the use of AGs conjugated to an AMP could be exploited against antibiotic resistance. Herein, we propose the synthesis and the evaluation of the antimicrobial activity of a library of 10 compounds based on two different AGs, namely neomycin and tobramycin, covalently tethered by means of linkers of different length to an AMP.

## 6.2 Materials and methods

### 6.2.1 Materials and reagents

Starting materials and solvents were purchased from commercial suppliers (ABCR GmbH, Alfa Aesar, AppliChem, CHEMsolute, Fluka, Iris Biotech, LabScan, Merck, Sigma Aldrich and VWR and used without further purification. Deionized water was

filtered (0.22 µm) in-house by use of a Milli-Q plus system (Millipore, Billerica, MA). For peptides preparative reversed-phase high pressure liquid chromatography (RP-HPLC) was performed by using a Phenomenex Luna C18(2) column (250 × 21.2 mm, 5 µm particle size) on a Shimadzu system consisting of a CBM-20A Prominence communication bus module, an LC-20AP Prominence pump, an SPD-M20A Prominence diode array detector, and an SIL-20A HT Prominence autosampler. Elution was performed by using an aqueous MeCN gradient with 0.1% TFA (eluent A: 5:95 MeCN–H2O + 0.1% TFA, eluent B: 95:5 MeCN–H2O + 0.1% TFA). Analytical RP-HPLC was performed on a Shimadzu system consisting of an SCL-10A VP controller, a SIL-10AD VP autosampler, an LC-10AT VP pump, an SPD-M10A VP diode array detector, and a CTO-10AC VP column oven, using a Phenomenex Luna C18(2) column (150 × 4.6 mm, 3 µm particle size) by using same eluents as for preparative RP-HPLC. MALDI-TOF: Acquisition of MS spectra was performed on MALDI-TOF or Bruker Autoflex (Bruker Daltonik GmbH, Bremen, Germany).

## 6.2.2 Synthesis of the conjugates

**Peptide synthesis:** oncocin-Cys (VDKPPYLPRPRPPRRIYNRC) (or Cys-oncocin) was synthesized on a CEM LibertyTM microwave peptide synthesizer by using microwave-assisted Fmoc-based solid-phase peptide synthesis (SPPS) on an H-Rink-Amide ChemMatrix® resin (loading 0.52 mmol/g, 0.1 mmol). After a 3x3 mins wash in DMF, MeOH and CH2Cl2, the peptide was cleaved with a TFA:H2O:TIS (4.75:0.125:0.125) mixture and purified by HPLC (Eluent B 0 to 30%).
**Maleimido-aminoglycoside derivatives synthesis (compounds 50-57) :** The AG(Boc)$_n$-NH2 (compounds **45,46, 48, 49** see 6.5) (1 eq) was dissolved in 6 mL of 1:1 mixture of ACN-H2O, then the NHS-linker (3-(Maleimido)propionic acid N-succinimidyl ester or 3-[2-[2-[[3-(2,5-Dihydro-2,5-dioxo-1H-pyrrol-1-yl)-1-oxopropyl]amino]ethoxy]etho -xy]propanoic acid ) (1.2eq) was added, the reaction was monitored with MALDI-TOF. After completion the solvents were removed under reduced pressure. The crude was treated with a 1:1 TFA/CH2Cl2 mixture for 2 hrs. After removing the solvents under reduced pressure the residue was diluted with milli-Q water and freeze-dried. HPLC (Eluent B 0-15% in 20 min) led to fluffy powders that where characterized throuh MALDI-TOF.
**AG-oncocin conjugates synthesis:** To a solution of oncocin-Cys (or Cys-oncocin) were added (1eq) compounds **50-57** (1.2eq) dissolved in few drops of milli-Q water. The solution was shaken until completion, detected by MALDI-TOF. The crude was purified with HPLC (Eluent B 0-25%). After freeze drying the final conjugates were obtained as white fluffy solids that were characterized though HR-MALDI.

### 6.2.3 Antimicrobial activity of Aminoglycoside-peptide conjugates:

The minimun inhibitory concentrations (MICs) were evaluated by the modified Hancock lab protocol in non-binding polystyrene microtitre plates, using bacterial suspensions of ~2 × $10^5$ CFU/mL in Mueller-Hinton broth (Difco, Sparks MD, USA), with $Mg^{2+}$ and $Ca^{2+}$ concentrations of 4 mg/L each. The compounds were dissolved in $H_2O$ and diluted in 0.01% acetic acid, 0.2% BSA (final concentration), and aliquots of 11 µL of 10× test compounds were transferred to the appropriate wells with bacterial suspensions. To prepare the compounds, low-binding sterile tubes and tips (Axygen, Union City CA, USA) were used. The MICs were read after 20 h incubation of covered plates at 35 °C (± 2 °C) with circular shaking 220 rpm.

## 6.3 Results and discussion

The development of new antibiotic alternatives is of paramount importance to fight the increasing prevalence of resistant strains. The synergistic activity of conventional antibiotics, such as AGs, together with AMPs show enhanced bactericidal effects.[5–7] The combination of two different mechanisms of action, i.e. permeabilization of bacterial membrane (by AMPs) and inhibition of protein synthesis (by AGs), can be efficient against peristers[2] and resistant strains.[4] Oncocin is a synthetic prolin-rich AMP that do not kills bacteria by a purely lytic mechanism. It is also able to interact with the 70S rRNA, thus inhibiting bacterial protein translation.[8,9] Amongst AMPs, oncocin demonstrated good antibacterial activity against Gram-negative pathogens and a low cytotoxicity against mammalian cells.[10]

### 6.3.1 Synthesis of the conjugates

**Modification of the AGs:** AGs are cheap and easily avaiable, thus being optimal starting materials. Two AGs were selected to build this library of compounds: tobramycin (Fig. 54A) as representative of the 4-5 disubstituted DOS and neomycin (Fig. 54B) as example of the 4-6 disubstituted DOS.
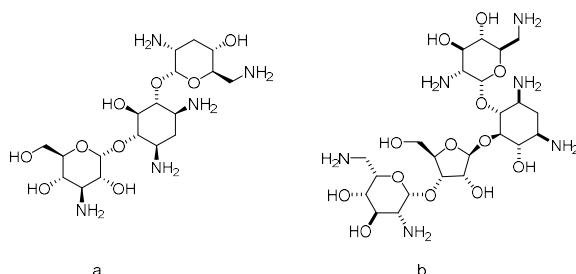
**Fig. 54 Structures of the two aminoglycosides chosen as starting materials**: a) *tobramycin as representative of the 4-5 disubstituted DOS and b) neomycin as example of the 4-6 disubstituted DOS.*

The two AGs were properly modified prior to conjugation with the peptide (for the complete synthetic pathway refer to 6.5), exploiting the less hindered primary hydroxyl group as reactive site. Briefly, the Boc-protected AG was allowed to react with the steric hindered 2,4,6-triisopropyl benzenesulfonyl chloride that selectively functionalized the primary hydroxyl group. This group is then displaced with an azide by using $Bu_4NN_3$ to obtain derivative **44** (**47** for neo) (Fig. 55). At this point, two strategies were adopted to obtain two different AG(Boc)$_n$-NH$_2$ derivatives for each AG: on one hand the azide was reduced to an amine through a Staudinger reaction in the presence of PMe$_3$ leading to compound **45** (**48** for neo) (Fig. 55), whilst on the other an acetylene-PEG-NH$_2$ linker was introduced by means of click chemistry producing compound **46** (**49** for neo) (Fig. 55).
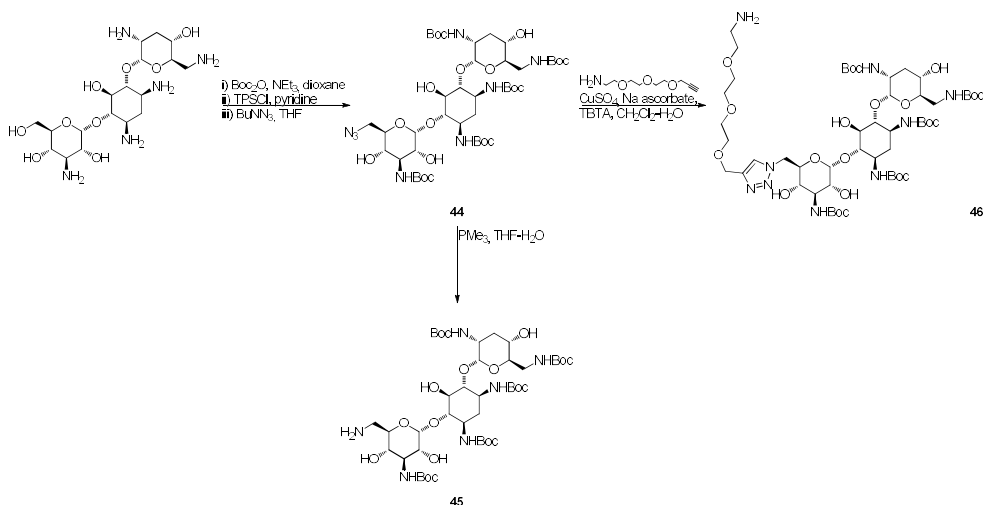


**Fig. 55. Syntetic pathway to obtain the AGs-NH₂:** *Boc-protected AG reacts with 2,4,6-triisopropyl benzenesulfonyl chloride that selectively functionalized the primary hydroxyl group. This group is then displaced with an azide by using Bu₄NN₃ to obtain derivative **44** .Then the product were either treated with PMe₃ leading to **45** or 'clicked' with a NH₂-PEG-N₃ producing **46**.*

At this point the AG(Boc)$_n$-NH$_2$ derivatives were treated with two different maleimido-NHS linkers (Fig. 56), a short one and a longer maleimido-PEG-NHS to obtain four different AG-maleimido derivatives for each AG.
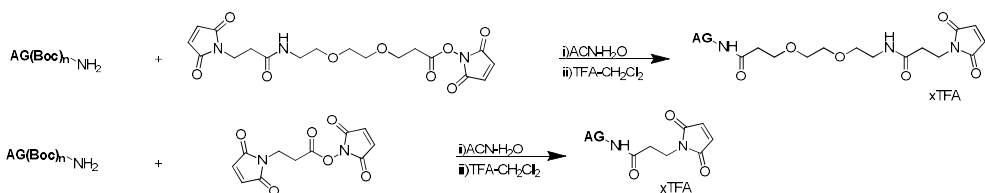


**Fig. 56 Syntetic pathway to obtain the AGs-Maleimido derivatives:** *AG-NH$_2$ was reacted with two different NHS-linker*

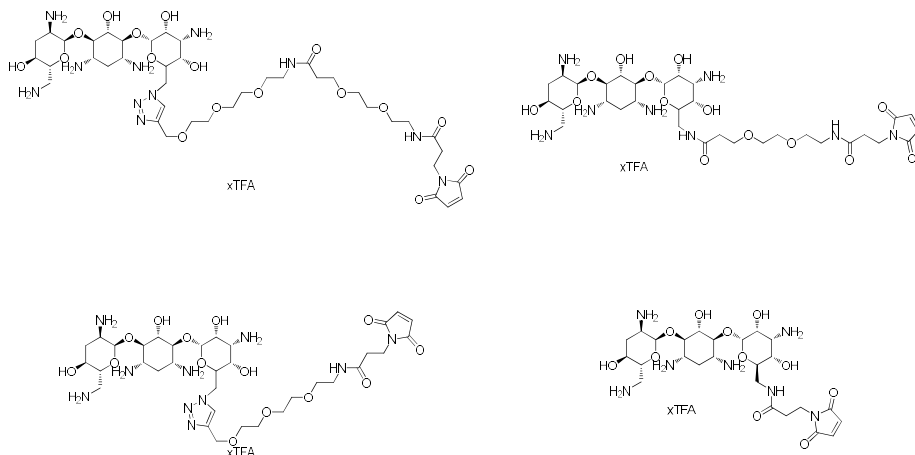Final Boc deprotection with TFA and purification through HPLC led to the final products ready to be coupled to the peptide (Fig. 57).



**Fig. 57** *Tobramycin-maleimido derivatives*

**Solid phase strategy:** In the first attempt to conjugate the AGs-maleimido derivatives to the peptide a solid phase strategy was used, this means that the peptide was still bound to the resin prior to the coupling with the AG. A solid support synthesis is useful to minimize the purification steps. In order to verify the feasibility of this approach we choose a small cell penetrating peptide (CPP), the (KFF)$_3$K. This peptide on one hand can be easily synthesized in few hours, and on the other is a CPP already known to permeabilize the membrane of bacteria as in *K. pneumoniae*[11] or *S. aureus.*[12] Therefore, we hypothesize that it could also boost the uptake of AGs enhancing their antibacterial activity. A cysteine was introduced within the peptide at the N-terminal to allow a 1,4 addition with the AGs-maleimido derivatives. The coupling with compound [Mal-(CH$_2$)$_2$(C=O)]-NH-tobra was carried both in DMF and in a THF-DMF mixture, but unfortunately, no conversion into the desired product was

observed after 24 hrs in both cases. We hypothesize that the reaction did not occurred due to either steric factors or solvent incompatibility.

**In-solution strategy: synthesis of eight oncocin-Cys-AGs derivatives:** In order to overcome steric hinderance, we switch the coupling reaction between the peptide and the AGs-maleimido derivatives to take place in solution. In this case the coupling was carried out by using oncocin as peptide. This is a well explored, small proline-rich peptide effective against 37 isolates such as *E.coli*, *K. pneumoniae* and *P. aeruginosa*.[10] Moreover, oncocin has been already proven as effective vehicle for bacterial delivery.[13]

The AGs-maleimido were mixed with the oncocin-Cys (Fig. 58) in minimum amount of milliQ water. The reaction proceeded instantaneously as it was detected by analytical HPLC.
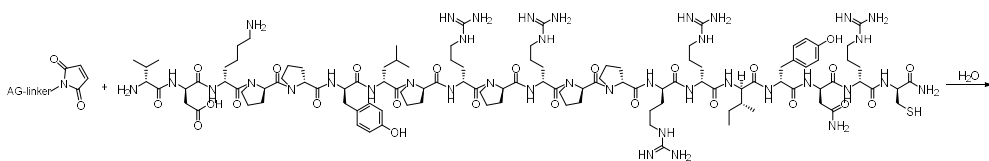


**Fig. 58 Synthesis of the final derivatives:** *oncocin-Cys was reacted with the AG-linker*

 A wide library of compound can be obtained by exploiting the in-solution strategy. Once obtained a batch of the peptide and a batch of AG-maleimide, in fact, many combinations of AG-maleimido-peptide can be quickly arranged. The reaction was also successfully performed in DMF, excluding any solvent incompatibility. A library of eight compounds (Fig. 59) was synthesized in milliQ water by coupling the two selected AGs, neomycin and tobramycin, equipped with linkers of different length with oncocin obtaining derivatives **58** to **65**.
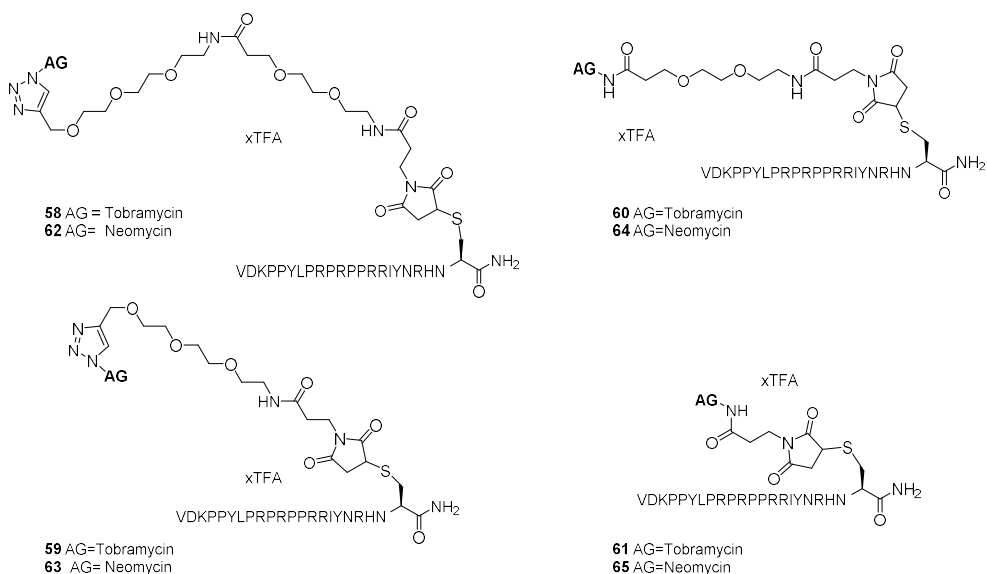
**58** AG = Tobramycin
**62** AG= Neomycin

**60** AG=Tobramycin
**64** AG=Neomycin

**59** AG=Tobramycin
**63** AG= Neomycin

**61** AG=Tobramycin
**65** AG=Neomycin

**Fig. 59**. *AG-oncocin conjugates where AG can be tobramycin or neomycin*

## 6.3.2 Antibacterial activity

The MIC of the neomycin and tobramycin conjugated **58** to **65** was determined *in vitro* against five different Gram-negative strains. Colistin was used as positive control while the oncocin was used as reference peptide.

*P. aeruginosa, A. baumannii* an *K. pneumoniae* are highly troublesome pathogens that have been included in the ESKAPE[14] class. They are, in fact, the most common multidrug-resistance (MDR) bacteria responsible for nosocomial infections.

Some AGs, such as tobramycin, still retain activity against *P. aeruginosa*[15] and *A. baumannii.*[16] However, since the rate of antimicrobial resistance development is increasing, they are frequently used in combination with other antimicrobials[17,18] to achieve a synergistic effect.[15] Resistance is also due to the failure of antibiotics to accumulate in the cytoplasm of these strains[19,20], owing to a combination of restricted permeability of the outer membrane and the removal of those antibiotic molecules that manage to successfully penetrate inside the bacterial cell by the action of efflux pumps. We hypothesized that AGs-oncocin derivatives could overcome antibiotic resistance by combining their mechanisms of action. However, none of the derivatives obtained displayed a significant MIC against both *P. aeruginosa* and *A. baumannii.* The MIC against *K. pneumoniae* range between 1-4 µg/mL. The conjugates equipped with shorter linkers both in neomycin (**65**) and tobramycin (**61**), displayed an improved activity if compared to our reference peptide, oncocin. Moreover, a higher MIC was found in comparison with colistin, that is the last resort treatment against this strain and with the unconjugated AG.

The MICs against *E. coli* were 2-8 µg/mL, with derivatives **59** (H-Oncocin-Cys-[Mal-(CH$_2$)$_2$(C=O)]-NH-(PEG$_3$-triazol)-tobra) and **60** (H-Oncocin-Cys-[Mal-peg]- NH-tobra) showing an improved activity with respect to the peptide alone. Interesting results were obtained if considering the sbmA dependence in *E. coli*. The *sbmA* gene encodes a membrane protein included in ABC transport-systems that mediate the uptake of a wide range of substances across the cell membranes. It is possible to identify orthologues of this gene in numerous Gram-negative bacteria; however, *sbmA* and its orthologue genes are totally absent in Gram-positive pathogens. *SbmA* and analogues mediate the susceptibility of bacteria against antibacterial peptides with intracellular target; in fact, their products are involved in the mechanism of internalization of Pro-rich peptides.[21,22] The four derivatives (obtained by click chemistry) with longer linkers (**58**, **59**, **62**, **63**) and the triazole show an sbmA-indipendent activity. The presence of the AG may provide an alternative transporter system, bypassing the SbmA transporter system thus overcoming a potential bacterial resistance mechanism.

Overall, our results depict two scenarios: when compared to the activity of oncocin alone, our compounds showed little improvement in the bactericidal activity; on the other hand, when compared to the activity of antibiotics alone, the coupling of the AG with the AMP was proved to be counterproductive: the MIC spiked from 0.5 to > 64 such as in the case of *P. aeruginosa* (as shown in Table 1). Nevertheless, the combination of antibiotic and AMP could be useful against biofilm-producing species and persisters, as noted by Mohamed M. *et al.*[5] Further tests are still ongoing.

However, the sbmA-independent activity is an interesting property that may be further explored. Mutation of the *sbmA* gene, in fact, could readily lead to development of resistance to the antibiotic. As far as the length of the linker was concerned, for *E. coli* a longer linker and the presence of the triazole ring seemed to favor a sbmA-independent activity. On the other hand, in the case of *K. pneumoniae* we observed MIC improvement in compounds where tobramycin and neomycin were conjugated to oncocin with a shorter linker. Therefore, it is not possible to highlight a trend in the effect of the linker on the antimicrobial activity of the compound stratified according to linker length.

**Table 1. MIC values of AGs-oncocin-Cys derivatives tested on 5 different Gram-negative bacteria strains.** *Violet: improved activity as compared to that of unmodified oncocin*
*Blue: retained activity as compared to that of unmodified oncocin*
*Grey: activity independent of SbmA Orange: SbmA-dependent activity (~ 4-fold higher MIC as compared to that in WT strain)*

| No. | | E. coli WT ATCC 25922 | E. coli. ΔsbmA | K. pneumoniae WT ATCC 13883 | P. aeruginosa PAO1 | A. baumannii WT ATCC 19606 |
|---|---|---|---|---|---|---|
| | Tobramycin (wild tipe eucast.org) | 0.25-2 | 0.25-2 | 0.25-2 | 0.125-2 | 0.25-4 |
| | Colistin | 0.125-0.5 | 0.25-1 | 0.125 | 0.5 | 0.5 |
| | H-Oncocin-NH$_2$ | 4 | - | 2-4 | >64 | 16-32 |
| 61 | H-Oncocin-Cys-[Mal-(CH$_2$)$_2$(C=O)]-NH-tobra | 2-4 | 16 | 1 | 64 | 8-16 |
| 65 | H-Oncocin-Cys-[Mal-(CH$_2$)$_2$(C=O)]-NH-neo | 4-8 | 16 | 1 | >64 | 16-32 |
| 64 | H-Oncocin-Cys-[Mal-peg1-NH-neo | 4 | 32 | 2 | >64 | 32 |
| 60 | H-Oncocin-Cys-[Mal-peg]-NH-tobra | 2 | 16 | 1 | >64 | 16 |
| 59 | H-Oncocin-Cys-[Mal-(CH$_2$)$_2$(C=O)]-NH-(PEG3-triazol)- tobra | 2 | 4-8 | 2 | >64 | 8 |
| 63 | H-Oncocin-Cys-[Mal-(CH$_2$)$_2$(C=O)]-NH-(PEG3-triazol)-neo | 4 | 8 | 4 | >64 | 32 |
| 58 | H-Oncocin-Cys-[Mal-eg1]-NH(PEG3-triazol)- tobra | 4 | 4-8 | 2-4 | >64 | 8 |
| 62 | H-Oncocin-Cys-[Mal-eg1]-NH(PEG3-triazol)-neo | 4-8 | 8 | 4 | >64 | 32 |

### 6.3.3 Synthesis and antibacterial activity of two Cys-oncocin-AGs derivatives

To check whether the antibacterial properties can be influenced by the position of the AG in the peptide, two derivatives were synthesized by coupling the AG-maleimido derivatives to an oncocin, where the Cys was at the N-terminus position, obtaining derivatives **66** and **67** (Fig. 60).
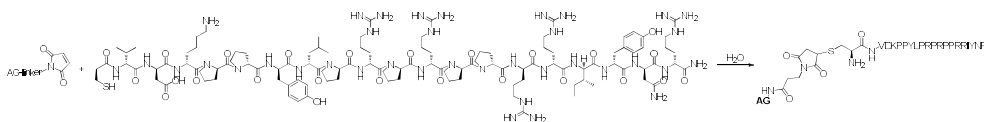


***Fig. 60*** *AG-oncocin derivatives obtained by using Cys-oncocin. AG= tobramycin or neomycin.*

These derivatives underwent *in vitro* testing against the same bacteria of their C-terminus counterpart. The results reported in Table 2 highlight that there is not a significant difference in the antibacterial activity if the AG is conjugated to the C-terminus. This conclusion is in agreement with a previous stuby by Deshayes *et al*.[23] It was showed, in fact, that the terminus of conjugation did not greatly impact the antibacterial activity.

**Table 2. MIC values of AGs-Cys-oncocin derivatives tested on 5 different Gram-negative bacteria strains**. *Violet: improved activity as compared to that of unmodified oncocin Blue:retained activity as compared to that of unmodified oncocin Grey:activity independent of Sbma Orange:SbmA-dependent activity (∼ 4-fold higher MIC as compared to that in WT strain.*

| No | | *E. coli* WT ATCC 25922 | *E. coli.* Δ*sbmA* | *K. pneumoniae* WT ATCC 13883 | *P. aeruginosa* PAO1 | *A. baumannii* WT ATCC 19606 |
|---|---|---|---|---|---|---|
| 66 | Tobra-NH$_2$-[(C=O)-(CH$_2$)$_2$Mal]-Cys-Oncocin-NH$_2$ | 4 | 16 | 1 | >64 | 16 |
| 62 | H-Oncocin-Cys-[Mal-(CH$_2$)$_2$(C=O)]-NH-tobra | 2-4 | 16 | 1 | 64 | 8-16 |
| 67 | Neo-NH$_2$-[(C=O)-(CH$_2$)$_2$Mal]-Cys-Oncocin-NH$_2$ | 4-8 | 16 | 2 | 64 | >64 |
| 65 | H-Oncocin-Cys-[ Mal-(CH$_2$)$_2$(C=O)]-NH-neo | 4-8 | 16 | 1 | >64 | 16-32 |

## 6.4. Conclusions

The increase of antibiotic resistance is an inevitable consequence of continuous antibiotic usage all over the world that poses a great clinical concern and needs to be urgently addressed. Herein, the synthesis of a library AGs-AMP conjugates is reported. Eight conjugates constituted by tobramycin or neomycin covalently bonded to oncocin-Cys were synthesized by means of an in-solution strategy. A solid phase approach was found to be unsuitable, probably due to steric factors. Four different spacers between the AG and the AMP were used in order to establish whether the length of the linker could affect the compounds' biological properties. The antimicrobial activity of the derivatives was evaluated against different Gram-negative strains. Some compounds showed improved activity with respect to unconjugated oncocin, however, lower activity was observed in comparison with the AG itself. It worth of note that the derivatives of both neomycin and tobramycin equipped with a longer linker and presenting a triazole showed a *sbmA*-independent activity. We also found out that the antibacterial activity of the derivatives is not influenced by the position of the AG; in fact, the two derivatives obtained by coupling the AG to the N-terminus of the peptide did not show significant differences in the bactericidal activity compared with those where the AGs was at the C-terminus.

It may be interesting to further investigate the antibacterial activity of these derivatives against AGs resistance strains, were a beneficial effect due to synergy could be detected.

# 6.5 Supporting Information
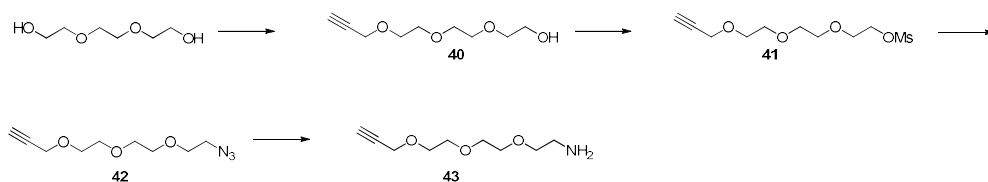


**Compound 40:** To a solution of triethylene glycole (3g, 20 mmol) in THF (15 mL) an aqueous solution of NaOH 4M (10 mL) was added. The reaction was stirred 0.5 hrs before adding propargyl bromide (2.2 mL, 20 mmol) dropwise, the mixture was stirred overnight at rt. The solution was diluted with water and extracted with EtOAc. The combined organic layer was dried over $Na_2SO_4$ and concentrated under reduced pressure. Vacuum liquid chromatography (VLC) (50% EtOAc in n-heptane) led to the product as yellow oil in 40% yield. The NMR spectra were in accord with literature data.

**Compound 41:** To a solution of **40** (1.45 g, 7.7 mmol) in $CH_2Cl_2$ (20 mL), DMAP (cat) and $Et_3N$ (2.2 mL, 15 mmol) were added. Then MsCl (1.2 mL, 15 mmol) was added dropwise. The solution was stirred 4 hrs at rt, and then washed with brine. The crude was used for the next reaction with no further purification.

**Compound 42:** To a solution of **41** (7.7 mmol) in THF (18 mL) $Bu_4NN_3$ (3.3 g, 11.5 mmol) was added and the solution was stirred overnight at 50°C. After cooling the solvent was removed under reduced pressure and the crude was dissolved in $CH_2Cl_2$, washed with a 1M aqueous solution of HCl and brine, dried over $Na_2SO_4$. A short VLC (30% EtOAc in n-heptane) led to the desired product as pale yellow oil in 60% yield. The NMR spectra were in accord with literature data.

**Compound 43:** To a solution of **42** (1.2 g, 5.6 mmol) in THF (25 mL) and $H_2O$ (2 mL) a solution of $PPh_3$ (2.2g, 8.4 mmol) in $CH_2Cl_2$ (25 mL) was added. The reaction mixture was stirred overnight. The volatiles were removed under reduced pressure and the water containing residue was diluted with HCl 2N (50 mL), washed with $CH_2Cl_2$. The aqueous portion was treated with NaOH pellets until basic pH was reached. The basic layer was extracted with $CH_2Cl_2$, dried over $Na_2SO_4$ and concentrated. The product was obtained as a colorless oil in 44% yield. The NMR spectra were in accord with literature data.
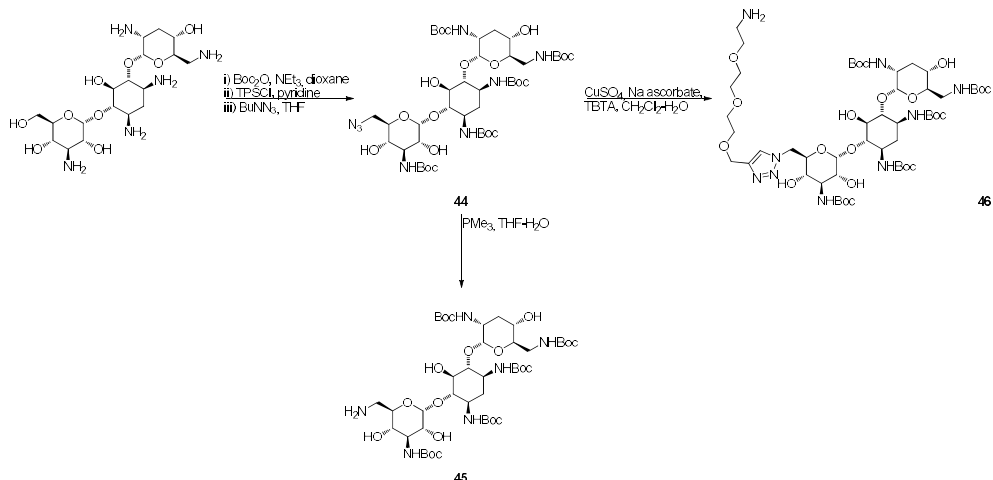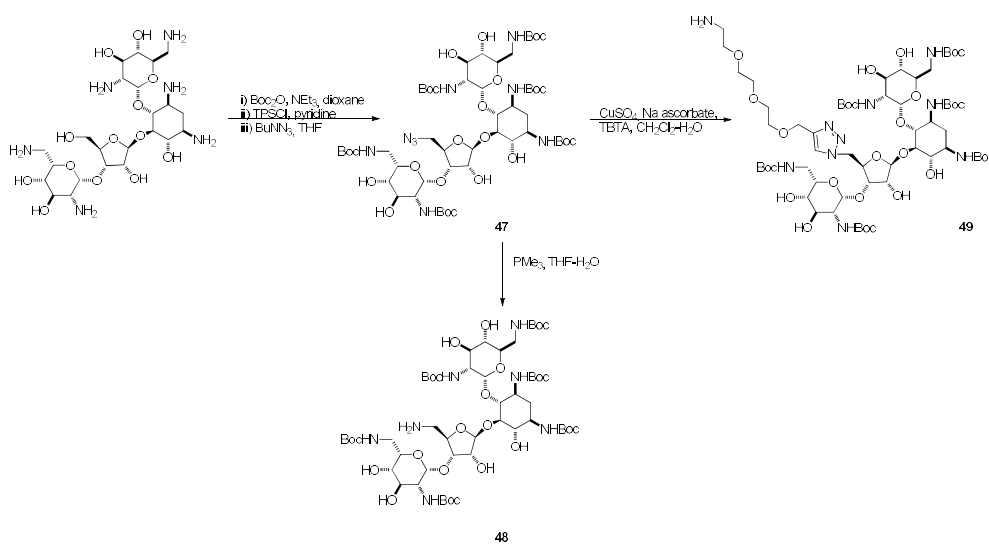
**Compound 44:** i) To a solution of tobramycin (5 g, 10 mmol) and Et$_3$N (10 mL) in 7 mL of H$_2$O a solution of Di-tert-butyl dicarbonate (14 g, 64 mmol) in dioxane (50 mL) was added dropwise. The solution was stirred 4 hrs at 60° C and then allowed to cool at rt. The solvents were evaporated under reduced pressure and the solid was washed with water and n-heptane. After drying a white solid was obtained in 90% yield. The NMR spectra and mass spectral analyses were in accord with literature data.

ii)The product (3 g, 3.1 mmol) was dissolved in pyridine (15 mL) and a solution of 2,4,6-triisopropylbenzenesulfonyl chloride (6.5 g, 22 mmol) in pyridine (15 mL) was added. The solution was stirred overnight at rt and then neutralized by adding HCl 1N and portioned between water and EtOAc. The aqueous layer was extracted with EtOAc. The combined organic layer was washed with brine, dried over Na$_2$SO$_4$ and concentrated under reduced pressure. VLC (0-3% MeOH in CH$_2$Cl$_2$) led to the desired product as a white solid in 70% yield. The NMR spectra and mass spectral analyses were in accord with literature data.

iii)The pure compound (1.8 g, 1.4 mmol) was dissolved in THF (15 mL) and Bu$_4$NN$_3$ was added (0.82 g, 2.9 mmol). The reaction mixture was stirred overnight at 70°C. After cooling to rt the solvent was evaporated under reduced pressure. The crude was dissolved in EtOAc and washed with HCl 1N and brine, dried over Na$_2$SO$_4$ and concentrated. VLC (0-5% MeOH in CH$_2$Cl$_2$) afforded the desired product as white solid in 65% yield. The NMR spectra and mass spectral analyses were in accord with literature data.

**Compound 45:** To a solution of **44** (2g, 2 mmol) dissolved in 20 mL of THF and several drops of H$_2$O, PMe$_3$ (12 mmol) was added. The solution was stirred 1hr at 50°C, then it was allowed to reach rt. The volatiles were removed under reduced pressure. VLC afforded a white solid in 40% yield. The NMR spectra were in accord with literature data.

**Compound 46:** To a solution of **44** (1.4 g, 1.4 mmol) in $CH_2Cl_2$ (15 mL) and $H_2O$ (0.5 mL) **43** (0.37 g, 1.8 mmol) and a catalytic amount of $CuSO_4$, sodium ascorbate and TBTA were added. The reaction was stirred overnight. The solvents were removed under reduced pressure. The crude was dissolved in EtOAc and washed with EDTA 5%. The organic layer was dried over $Na_2SO_4$. A short VLC (MeOH in $CH_2Cl_2$ 0-25%) afforded the product as a yellow powder in 25% yield. $^1H$ NMR (600 MHz, $CD_3OD$) δ 8.04 (s, 1H), 5.11(s, 1H), 5.08 (s, 1H), 4.65 (s, 2H), 4.43 (s, 1H) 3.86-3.32 (m, 26H), 3.14 (t, J 5.04Hz, 1H), 3.00 (m, 1H), 2.04 (b, 2H), 1.66 (q, 1H), 1.55-1.32 (m, 45H). $^{13}C$ NMR (151 MHz, $CD_3OD$) δ 179.74, 159.45, 157.74, 145.46, 126.56, 99.68, 98.98, 82.92, 80.76, 80.51, 80.41, 80.26, 76.64, 73.56, 71.98, 71.51, 71.36, 71.20, 70.59, 67.94, 66.50, 64.85, 57.10, 40.68, 28.87. MALDI-TOF *m/z* [M+H$^+$]$^+$ 1180.4.



**Compound 47:** i) To a solution of neomycin (5 g, 5.5 mmol) and $Et_3N$ (10 mL) in 6 mL of $H_2O$ a solution of Di-tert-butyl dicarbonate (7.2 g, 33 mmol) in dioxane (20 mL) was added dropwise. The solution was stirred overnight at rt. The solvents were evaporated under reduced pressure. The crude was dissolved in EtOAc and washed with brine. Dry over $Na_2SO_4$. VLC (0-5% MeOH in $CH_2Cl_2$) afforded the product as a white solid in 70% yield. The NMR spectra and mass spectral analyses were in accord with literature data.

ii)The product (2.7 g, 2.2 mmol) was dissolved in pyridine (15 mL) and a solution of 2-4-6-triisopropylbenzenesulfonyl chloride (21.5 g, 71 mmol) in pyridine (15 mL) was added. The solution was stirred overnight at rt and then neutralized by adding HCl 1N and portioned between water and EtOAc. The aqueous layer was extracted with EtOAc. The combined organic layer was washed with brine, dried over $Na_2SO_4$ and

concentrated under reduced pressure. VLC (0-3%MeOH in $CH_2Cl_2$) led to the desired product as a white solid in 65% yield. The NMR spectra and mass spectral analyses were in accord with literature data.

iii)The pure compound (1.8 g, 1.2 mmol) was dissolved in THF (20 mL) and $Bu_4NN_3$ was added (0.69 g, 2.4 mmol). The reaction was stirred overnight at 70°C. After cooling the solvent was evaporated under reduced pressure. The crude was dissolved in EtOAc and washed with HCl 1N and brine, dried over $Na_2SO_4$ and concentrated. VLC (0-5% MeOH in $CH_2Cl_2$) afforded the desired product as white solid in 67% yield. The NMR spectra and mass spectral analyses were in accord with literature data.

**Compound 48:** To a solution of **47** (2 g, 1.6 mmol) in 20 mL of THF and several drops of $dH_2O$, $PMe_3$ (9.6 mmol) was added. The solution was stirred 1 hr at 50°C then it was allowed to reach rt. The solvents were removed under reduced pressure. VLC afforded a white solid in 27% yield. The NMR spectra were in accord with literature data.

**Compound 49:** To a solution of **47** (0.7 g, 0.56 mmol) in $CH_2Cl_2$ (6 mL) and $H_2O$ (0.2 mL) **43** (0.15 g, 0.73 mmol), a catalytic amount of $CuSO_4$, sodium ascorbate and TBTA were added. The reaction was stirred overnight. The solvents were removed under reduced pressure. The crude was dissolved in EtOAc and washed with EDTA 5%. The organic layer was dried over $Na_2SO_4$. VLC afforded a yellow powder in 26% yield. ^{1}H NMR (400 MHz, $CD_3OD$) δ 8.17 (s, 1H), 5.40 (s, 1H), 5.16 (s, 1H), 4.95 (s, 1H), 4.69 (b, 2H), 4.33 (b, 2H), 4.18 (b, 1H), 3.95 (m, 2H), 3.77-3.35 (m, 25H), 3.23 (t, 2H), 3.15 (t, 2H), 1.93 (b, 1H), 1.55-1.30 (m, 55H). MALDI-TOF $[M+H^+]^+$ 1428.0
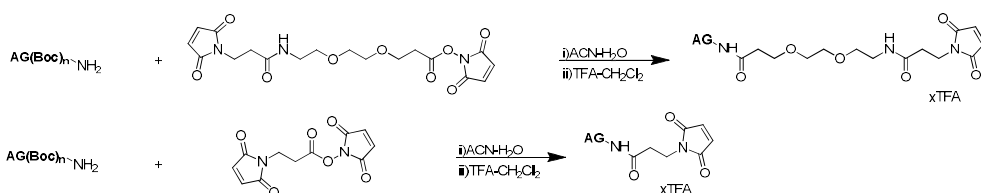


**General procedure**: The **AG-NH$_2$** (compounds 45, 46, 48, 49) (1 eq) was dissolved in 6 mL of 1:1 mixture of $ACN-H_2O$, then the **NHS-linker** (3-(Maleimido)propionic acid N-succinimidyl ester or 3-[2-[2-[[3-(2,5-Dihydro-2,5-dioxo-1*H*-pyrrol-1-yl)-1-oxopropyl]amino]ethoxy]ethoxy]propanoic acid ) (1.2eq) was added, the reaction was monitored with MALDI-TOF. After completion the solvents were removed under reduced pressure. The crude was treated with a 1:1 TFA $CH_2Cl_2$ mixture for 2 hrs. After removing the solvents under reduced pressure, the residue was diluted with $H_2O$ and freeze-dried. HPLC (B 0-15% in 20 min) led to fluffy powders.
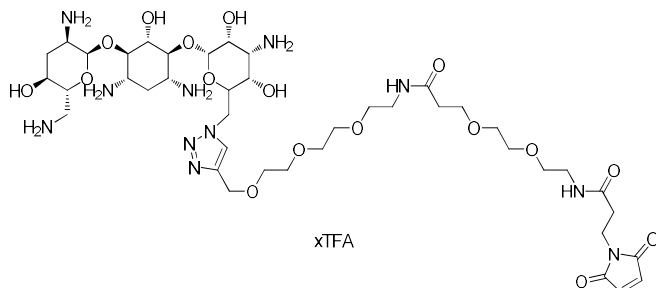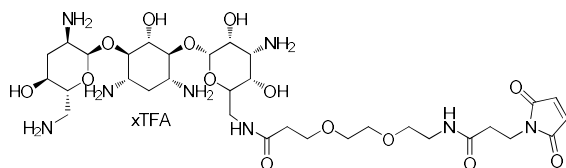
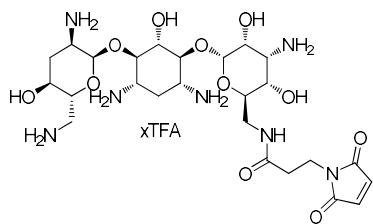**Compound 50:** yellow solid, 15% yield. MALDI-TOF *m/z* [M+Na$^+$]$^+$ 1014.1.
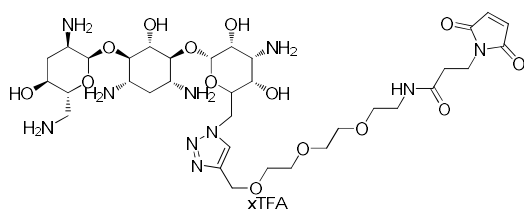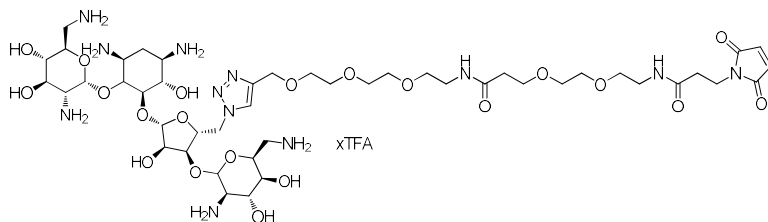


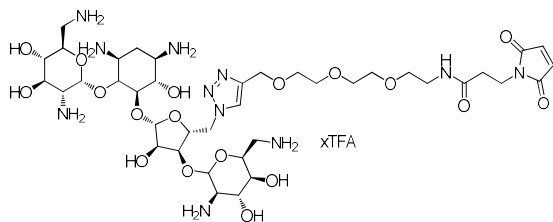**Compound 51:** yellow solid, 15% yield. MALDI-TOF *m/z* [M+H$^+$]$^+$ 831.1.



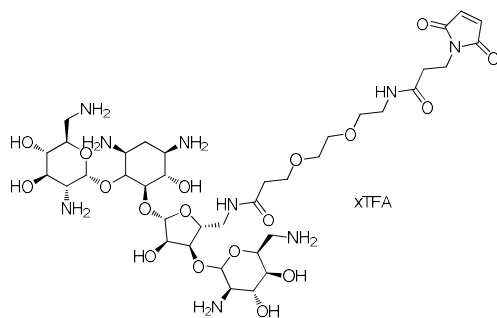**Compound 52:** white solid, 45% yield. MALDI-TOF *m/z* [M+H$^+$]$^+$ 777.8.



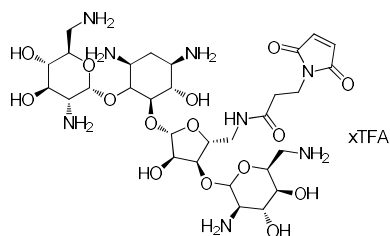**Compound 53:** white solid, 45% yield. MALDI-TOF *m/z* [M+H$^+$]$^+$ 618.1.

**Compound 54:** yellow solid, 15% yield. MALDI-TOF *m/z* [M+H$^+$]$^+$ 1137.7.



**Compound 55:** yellow solid, 15% yield. MALDI-TOF *m/z* [M+H$^+$]$^+$ 979.2



**Compound 56:** white solid, 36% yield. MALDI-TOF *m/z* [M+H$^+$]$^+$ 925.3



**Compound 57:** white solid, 20% yield. MALDI-TOF *m/z* [M+H$^+$]$^+$ 765.2
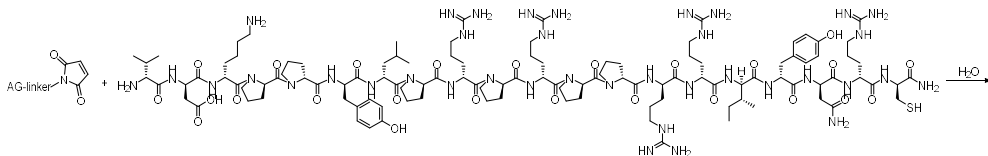
**General procedure:** To a solution of **oncocin-Cys** (or Cys-oncocin) (1eq) compounds **50**-**57** (1.2eq) dissolved in few drops of milli-Q water were added. The solution was shaken until completion, detected by MALDI-TOF. The crude was purified with HPLC (0-25% B). After freeze drying the final conjugates are obtained as white fluffy solids.
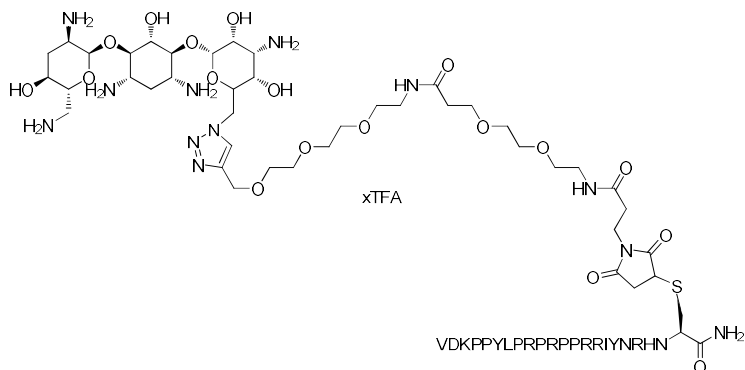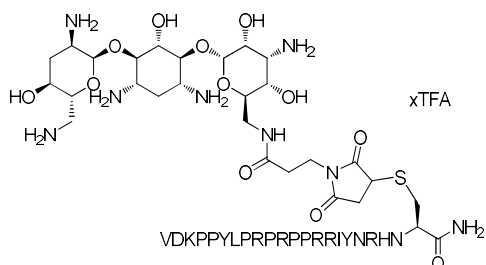


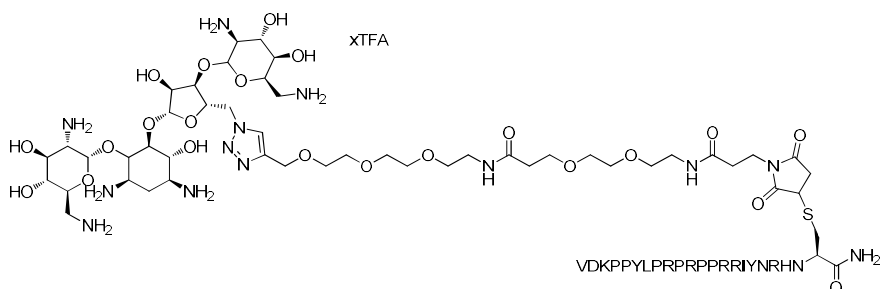**Compound 58:** 30% yield. HR-MALDI calc for $C_{153}H_{253}N_{49}O_{42}S$ 3480,89 found m/z [M+H$^+$]$^+$: 3483.8902
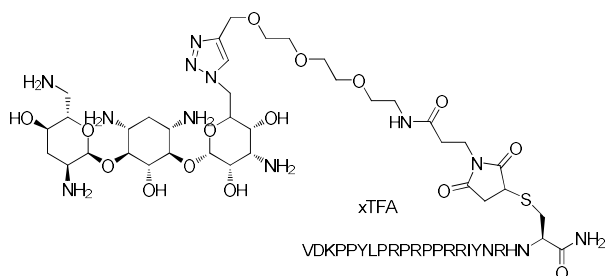


**Compound 59:** 30% yield. HR-MALDI calc for $C_{146}H_{240}N_{48}O_{39}S$ 3321,80 found m/z [M+H$^+$]$^+$: 3323.7936
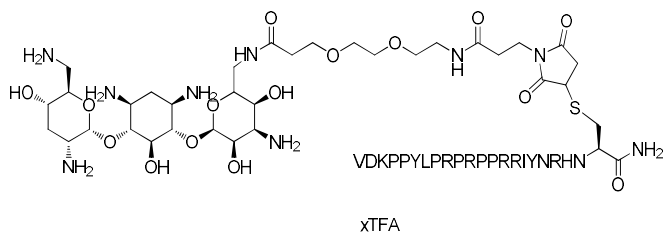
**Compound 60:** 33% yield. HR-MALDI calc for $C_{144}H_{238}N_{46}O_{39}S$ 3267,78 found m/z [M+H$^+$]$^+$: 3269.7837
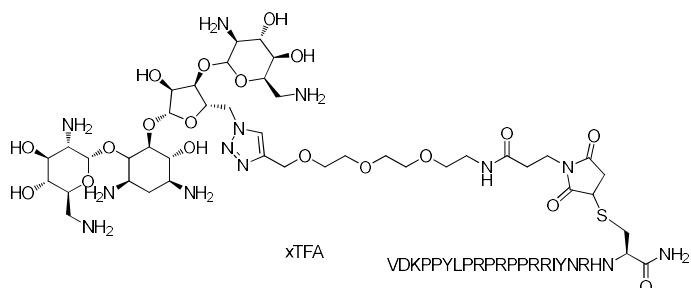


**Compound 61:** 60% yield. HR-MALDI calc for $C_{137}H_{225}N_{45}O_{36}S$ 3108,69 found m/z [M+H$^+$]$^+$: 3110.6863



**Compound 62:** 30% yield. HR-MALDI calc for $C_{158}H_{262}N_{50}O_{46}S$ 3627,94 found  m/z [M+H$^+$]$^+$: 3629.9471

**Compound 63:** 50% yield. HR-MALDI calc for $C_{151}H_{249}N_{49}O_{43}S$ 3468,85 found m/z [M+H$^+$]$^+$: 3470, 8524



**Compound 64:** 30% yield. HR-MALDI calc for $C_{149}H_{247}N_{47}O_{43}S$ 3414,83 found m/z [M+H$^+$]$^+$: 3416.8397



**Compound 65:** 60% yield. HR-MALDI calc for $C_{142}H_{234}N_{46}O_{40}S$ 3255,74 found m/z [M+H$^+$]$^+$: 3257.7471

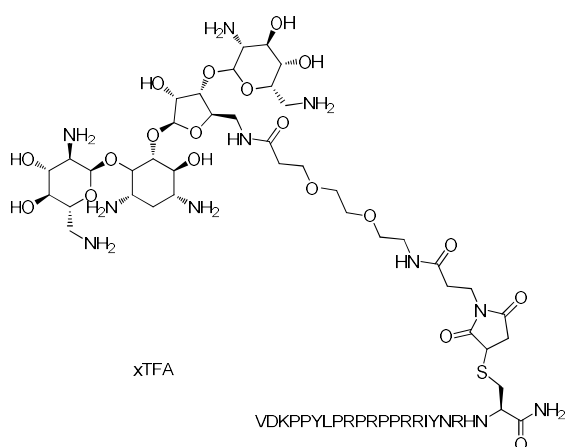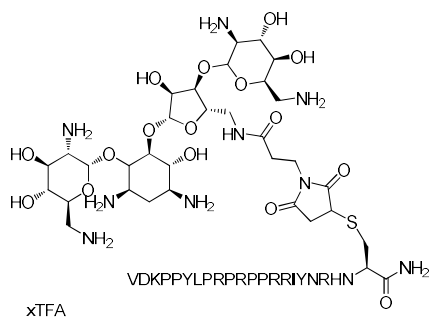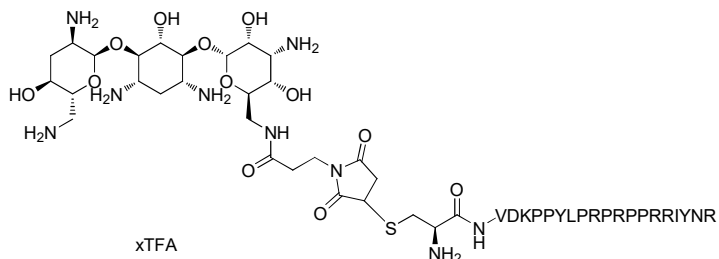**Compound 66**: 30% yield. HR-MALDI calc for $C_{137}H_{225}N_{45}O_{36}S$ 3108,69 found m/z $[M+H^+]^+$ 3110.69581
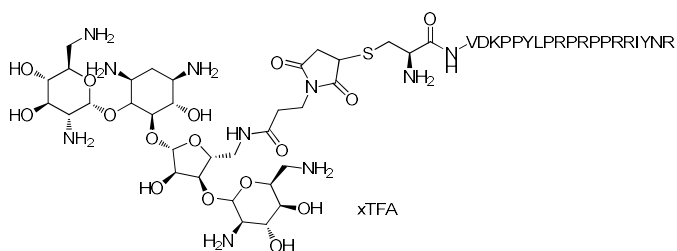


**Compound 67**: 40% yield. HR-MALDI calc for $C_{142}H_{234}N_{46}O_{40}S$ 3255,74 found m/z $[M+H^+]^+$ 3257.74252

# 6.6 References

1.    Dupont, E., Prochiantz, A., Joliot, A. Penetratin Story: An Overview. *Methods Mol Biol.* **683,** 21–29 (2011).

2.    Schmidt, N. W. *et al.* Engineering Persister-Specific Antibiotics with Synergistic Antimicrobial Functions. *ACS Nano* **8,** 8786–8793 (2014).

3.    Deshayes, S. *et al.* Designing Hybrid Antibiotic Peptide Conjugates To Cross Bacterial Membranes. *Bioconjugate Chem.* **28,** 793–804 (2017).

4.    Schmidt, N. W. *et al.* Pentobra: A Potent Antibiotic with Multiple Layers of Selective Antimicrobial Mechanisms against Propionibacterium Acnes. *J. Invest. Dermatol.* **135,** 1581–1589 (2015).

5.    Mohamed, M. F., Brezden, A., Mohammad, H., Chmielewski, J., Seleem, M. N. Targeting biofilms and persisters of ESKAPE pathogens with P14KanS, a kanamycin peptide conjugate. *Biochim. Biophys. Acta - Gen. Subj.* **1861,** 848–859 (2017).

6.    Brezden, A. *et al.* Dual Targeting of Intracellular Pathogenic Bacteria with a Cleavable Conjugate of Kanamycin and an Antibacterial Cell-Penetrating Peptide. *J. Am. Chem. Soc.* **138,** 10945–10949 (2016).

7.    Bera, S., Zhanel, G. G., Schweizer, F. Evaluation of amphiphilic aminoglycoside–peptide triazole conjugates as antibacterial agents. *Bioorg. Med. Chem. Lett.* **20,** 3031–3035 (2010).

8.    Krizsan, A. *et al.* Insect-Derived Proline-Rich Antimicrobial Peptides Kill Bacteria by Inhibiting Bacterial Protein Translation at the 70 S Ribosome. *Angew. Chemie Int. Ed.* **53,** 12236–12239 (2014).

9.    Gagnon, M. G. *et al.* Structures of proline-rich peptides bound to the ribosome reveal a common mechanism of protein synthesis inhibition. *Nucleic Acids Res.* **44,** 2439–2450 (2016).

10.   Knappe, D. *et al.* Oncocin (VDKPPYLPRPRPPRRIYNR-NH2): A novel antibacterial peptide optimized against gram-negative human pathogens. *J. Med. Chem.* **53,** 5240–5247 (2010).

11.   Kurupati, P., Tan, K. S. W., Kumarasinghe, G.,, Poh, C. L. Inhibition of gene expression and growth by antisense peptide nucleic acids in a multiresistant β-lactamase-producing Klebsiella pneumoniae strain. *Antimicrob. Agents Chemother.* **51,** 805–811 (2007).

12.   Nekhotiaeva, N., Awasthi, S. K., Nielsen, P. E., Good, L. Inhibition of Staphylococcus aureus gene expression and growth using antisense peptide nucleic acids. *Mol. Ther.* **10,** 652–659 (2004).

13. Hansen, A. M. *et al.* Antibacterial Peptide Nucleic Acid–Antimicrobial Peptide (PNA–AMP) Conjugates: Antisense Targeting of Fatty Acid Biosynthesis. *Bioconjugate Chem.* **27,** 863–867 (2016).

14. Rice, L. B. Federal Funding for the Study of Antimicrobial Resistance in Nosocomial Pathogens: No ESKAPE. *J. Infect. Dis.* **197,** 1079–1081 (2008).

15. Ratjen, F., Brockhaus, F., Angyalosi, G. Aminoglycoside therapy against Pseudomonas aeruginosa in cystic fibrosis: A review. *J. Cyst. Fibros.* **8,** 361–369 (2009).

16. Fishbain, J., Peleg, A. Y. Treatment of *Acinetobacter* Infections. *Clin. Infect. Dis.* **51,** 79–84 (2010).

17. Nakamura, A. *et al.* Combined effects of meropenem and aminoglycosides on Pseudomonas aeruginosa in vitro. *J. Antimicrob. Chemother.* **46,** 901–904 (2000).

18. Giamarellou, H., Zissis, N. P., Tagari, G., Bouzos, J. In Vitro Synergistic Activities of Aminoglycosides and New β-Lactams Against Multiresistant Pseudomonas aeruginosa. *Antimicrob. Agents Chemother.* **25,** 534-536 (1984).

19. Bonomo, R. A., Szabo, D. Mechanisms of Multidrug Resistance in Acinetobacter Species and Pseudomonas aeruginosa. *Clin. Infect. Dis.* **43,** 49–56 (2006).

20. Zavascki, A. P., Carvalhaes, C. G., Picão, R. C., Gales, A. C. Multidrug-resistant *Pseudomonas aeruginosa* and *Acinetobacter baumannii* : resistance mechanisms and implications for therapy. *Exp. Rev. Anti. Infect. Ther.* **8,** 71–93 (2010).

21. Mattiuzzo, M. *et al.* Role of the Escherichia coli SbmA in the antimicrobial activity of proline-rich peptides. *Mol. Microbiol.* **66,** 151–163 (2007).

22. Krizsan, A., Knappe, D., Hoffmann, R. Influence of the *yjiL-mdtM* Gene Cluster on the Antibacterial Activity of Proline-Rich Antimicrobial Peptides Overcoming Escherichia coli Resistance Induced by the Missing SbmA Transporter System. *Antimicrob. Agents Chemother.* **59,** 5992–5998 (2015).

23. Deshayes, S. *et al.* Designing Hybrid Antibiotic Peptide Conjugates To Cross Bacterial Membranes. *Bioconjug. Chem.* **28,** 793-804 (2017).

# Conclusive remarks

The research carried out during my PhD project addressed two relevant issues: gene delivery and antibiotic resistance.

The main topic of the work was the use of aminoglycosides for two different purposes; the synthesis of novel classes of gene delivery vectors and the synthesis of conjugated with improved antibacterial activity.

The insertion of exogenous NAs into cells for therapeutic purposes is a promising strategy for treatment of inheritable or acquired diseases. In the last decade, many strides have been made in this field. However, the ideal vector has not been developed yet.

Recent efforts have been made in the development of non-viral vectors as safer alternatives to the viral one. Synthetic carriers comprise many different structures including cationic lipids and polymers.

The goal of this PhD thesis was to develop novel classes of gene delivery vectors exploiting various aminoglycosides in combination with lipidic chains (Chapter II), calix[4]arenes (Chapter III) and PAMAM (Chapter IV). The carriers were synthesized and characterized. Biological validation was carried out in *Biocell* laboratories in collaboration with the group of Prof. Candiani (Politecnico di Milano).

Cationic lipids structures have been explored (Chapter II) by using a triazine scaffold that offers a functionalization with a virtually unlimited variety of moieties. From preliminary biological assays emerged that single-tailed derivatives demonstrated low cytotoxicity in conjunction with low value of transfection efficiency. Nevertheless, the transfection efficiency of AGs-triazine lipids could be enhanced by modification of the lipidic part of the CL.

Amphiphilic molecules were also synthesized by combining AGs with calix[4]arenes, the project (chapter III) was carried out in collaboration with Prof. Sansone (Università di Parma). This scaffold has already proven to be effective in transfecting cells. The conjugates displayed high transfection efficiency together with low cytotoxicity. Moreover, the derivatives displayed inherent antimicrobial activity. Such combination of gene delivery and antibacterial activity is interesting in the prospective of the treatment of some diseases where immune suppression occurs.

In chapter IV AG-PAMAM derivatives were synthesized and validates as gene carriers. The derivatives were able to condense DNA and transfect two different cell

lines. Interestingly, PAMAM G2, when conjugated with Neo, displayed good values of transfection efficiency. These results are interesting as low generation dendrimers are cheaper, safer and easily to synthesize if compared to higher generation dendrimers.

During my six months as a guest of Prof. Henrik Franzyk's laboratories, I explored and tried to enhance AG's antibacterial properties. The antibiotics were conjugated to oncocin, an antimicrobial peptide, and their antibacterial activity were evaluated (chapter VI). Despite the antibacterial activity was lower than the free aminoglycoside, some interesting results have emerged. The combination of AG and AMP can lead to a sbmA-indipendent antimicrobial activity. This finding is interesting as mutation of the *sbmA* gene may be responsible of antibiotic resistance.

# Acknowledgment

I would like to express my sincere gratitude to my advisor, Prof. Alessandro Volonterio, who gave me trust and continuous support during these years.

I would like to extend my gratitude to Dr. Rossi, Dr. Sani, Dr. Viani and Massimo for the always interesting discussions and helpful suggestions.

My sincere thanks go also to Prof. Candiani, who gave me access to *BioCell*, for the inspiring discussions and advice on the biological aspects.

A special gratitude goes to Dr. Bono, whose scientific and personal help has been essential for the realization of this project.

A special thanks to Walter Panzeri for his kindly assistance on the Mass Spectroscopy analysis.

I would like to thank Prof. Galimberti, who welcomed me in his group.

I wish to thank Prof. Henrik Franzyk, who welcomed me in his group at the University of Copenhagen and introduced me to the new intriguing world of the peptides.

I would also like to thank Dr. Hansen, Wan and Brigitte for their enormous scientific and personal help during my staying in Copenhagen. A special thanks to Marianne, you made me feel like home.

Finally, I would like to thank my Thesis Committee Prof. Sansone and Prof. Franzyk.

!!! Ma soprattutto !!!

Grazie ad Alessandro, Bianca, Daniele, Fiorenza, Massimo e Monica per tutti i piacevoli momenti di svago e lunghe chiacchiere!

Grazie a Gabriele per il tempo dedicatomi e i preziosi consigli al di là delle questioni professionali.

Grazie a Nina, per la tua amicizia, nata tra una mascazzulata e neologismi vari, per esserci stata, sempre.

Ai miei nuovi compagni di ufficio: Daniele, Fatima, Gea, Jiemeng, Lucia, Sophia.

E siccome dico sempre che gli amici sono la famiglia che scegliamo, grazie ai miei compagni di avventure: Alice, Alessandro, Angelo, Elettra ed Enza. Per avermi fatto sentire a casa in questa città.

Il ringraziamento più importante va alla mia super tribù.
Ai miei genitori per avermi supportato nella scelta di questo interminabile percorso di studi (è finito, lo prometto!), ma soprattutto per avermi permesso di affrontare la vita in maniera serena e libera.
A Sandra, Paolo, Francesca, Antonio, Carlo, Antonietta, Francesco e Stefania: nonostante i disparati caratteri, ho sempre potuto, e so che sempre potrò, trovare in voi appoggio e supporto.
Ad Alessandro, Giacomo, Antonio, Alessandro e Iole per il tempo passato a giocare ed allargare la mia scatola della fantasia.
A Francesco per la cura che hai di me.